2019

UNDERSTANDING STRUCTURE-ACTIVITY RELATIONSHIP OF SYNTHETIC CATHINONES (BATH SALTS) UTILIZING METHYLPHENIDATE

Barkha J. Yadav
Virginia Commonwealth University

UNDERSTANDING STRUCTURE-ACTIVITY RELATIONSHIP OF SYNTHETIC CATHINONES (BATH SALTS) UTILIZING METHYLPHENIDATE

A Dissertation submitted in partial fulfillment of the requirements for the degree of Doctor of Philosophy at Virginia Commonwealth University.

by

BARKHA JITENDRA YADAV
Masters in Pharmaceutical Analysis, University of Strathclyde, Glasgow, UK, 2014
Bachelor of Pharmacy, Mumbai University, India, 2013

Director: DR. RICHARD A. GLENNON
PROFESSOR
DEPARTMENT OF MEDICINAL CHEMISTRY

Virginia Commonwealth University
Richmond, Virginia
May, 2019

Acknowledgement

I would like express my deepest gratitude to my advisor, Dr. Richard A. Glennon for having been a wonderful mentor during the course of my graduate school. Dr. Glennon has been a constant support in my professional and personal life. All the group meetings and discussions have taught me to think critically and to question everything. Thank you for being tough on me which has made me the person I am today, and dealing with a difficult person like me. Joining Dr. Glennon's group was one of the best decisions of my life, as I also had constant support of Dr. Małgorzata Dukat. In the last four years, Dr. Dukat has been my go-to person and she has given me countless advice for my professional and personal life. Thank you Dr. Dukat for making the laboratory a family and thank you for all the parties and coffee, I will surely miss those!

I am extremely grateful to Dr. Jose M. Eltit, for taking time and teaching me the in vitro assays. Without his help this work would have been incomplete. Thank you Dr. Eltit for being so patient with me and teaching every aspect of the assays and also reminding me to take some me-time. I would also like to thank my advisory committee members Dr. Laura Sim-Selley, Dr. Youzhong Guo, Dr. Richard Young, and Dr. Jose Eltit for the time they have invested in my training. I wish to express my sincere thanks to Dr. Aron Lichtman and Dr. Hilda Meth for bestowing me with the Lowenthal Award and thank you for always believing in me.

I very much appreciate the help of all the past and present members of Dukat-Glennon laboratory. Thank you, Dr. Umberto Battisti for helping me set up my very first reaction. A very special thanks to Dr. Malaika Argade, who showed me how fun chemistry is and eventually made me fall in love with it. Thanks should also go to Dr. Urjita Shah,

Dr. Kavita Iyer, Dr. Abdelrahman Shalabi, Ahmed Abdelkhalek, Rachel Davies, Pallavi Nistala, and Prithvi Hemanth for making the laboratory a wonderful place to be. I would also like to thank Rachel Davies specially who has been my continuous support and thank you for making me believe in myself.

Pallavi Nistala and Shravan Morla, I am short of words to describe what you both mean to me. You both have made Richmond my second home. I am sure that I will be leaving Richmond with two friends for life. Thank you for always being there during my happy and most importantly my sad times. Thank you Pallavi for being the perfect roommate and a sister and thank you Shravan for being the only person I can watch horror movies with. I would also like to thank Claudio, Heather, Connor, Prithivi, and Tamim for all the Friday night outings, discussions, arguments, and wonderful memories. I cannot begin to express my thanks to Aaditi, Jayesh, and Dixit who were always by my side and always motivated me to achieve my dreams.

I am deeply indebted to my Mom, Dad, Yash, and Aryan. Mom and Dad, you have played a crucial role in my success. Thank you, Mom, for being my role model and keeping me focused, and thank you Dad for raising me like a princess. You both have kept me grounded and at the same time taught me how to fly. Yash, you have been my perfect partner in crime and I could not have asked for a better brother. I would also like to thank my dog, Chico, who can make me smile even during my toughest time. Thanks to my mother and father-in-law who have always treated me as their daughter. Last but not the least, I would like to express my deepest gratitude to my husband, Sravan Kumar Samudrala, who has been my biggest cheerleader and believes in me more than myself. This journey would have been impossible without you. I am forever in your debt.

Table of Contents

List of Tables

Page

List of Figures

Page

List of Schemes

Page

List of Abbreviations

5-HT	Serotonin
α	alpha
μM	Micromolar
Å	Angstrom
α-PVP	α-Pyrrolidinovalerophenone
AcOH	Acetic acid
Ala	Alanine
$AlCl_3$	Aluminum chloride
AMPH	Amphetamine
APP^+	4-(4-dimethylamino)phenyl-1-methylpyridinium
Asp	Aspartate
AUC	Area under curve
βC	Beta-carbon
Boc	tert-Butyloxycarbonyl
BOP	(benzotriazol-1-yloxy)tris(dimethylamino)phosphonium hexafluorophosphate
CCl_4	Carbon tetrachloride
CES1A1	Carboxyesterase 1A1
CES2	Carboxyesterase 2
CES3	Carboxyesterase 3
Cl_e	Oral clearance

C_{max}	Peak concentration
DA	Dopamine
DAT	Dopamine transporter
dDAT	Drosophila melanogaster dopamine transporter
DMEM	Dulbecco's modified Eagle's medium
DMF	Dimethylformamide
EC	Extended release capsules
EDG	Electron-donating group
EGFP	Enhanced green fluorescent protein
EMCDDA	European Monitoring Centre for Drugs and Drug Addiction
eMP	*erythro* Methylphenidate
ER	Extended release
ES	Extended release suspension
ET	Extended release tablets
EWG	Electron-withdrawing group
FDA	Food and drug administration
FT	Fourier-transform
f.u.	Fluorescence units
h	hour/s
$HClO_4$	Perchloric acid
hDAT	Human dopamine transporter
HEK	Human embryonic kidney

HINT	Hydropathic INTeraction
hSERT	Human serotonin transporter
Hz	Hertz
i.p.	Intraperitoneal
i.v.	Intravenous
IR	Immediate release
IR	Infrared
IS	Imaging solution
K	Elimination constant
MCAT	Methcathinone
MDMC	Methylone
MDPV	Methylenedioxypyrovalerone
MEPH	Mephedrone
METH	Methamphetamine
MHz	Megahertz
MP	Methylphenidate
mp	Melting point
MS	Mass spectrometry
N_2	Nitrogen
NCX	Na^+/ Ca^{2+} exchanger
NE	Norepinephrine
NET	Norepinephrine transporter

NMR	Nuclear magnetic resonance
nM	Nanomolar
nm	Nanometer
NPS	New Psychoactive Substance
P	Transdermal patch
PBD	Protein Data Bank
PCl_3	Phosphorous trichloride
PCl_5	Phosphorous pentachloride
PET	Positron emission tomography
Phe	Phenylalanine
PIA	Phenylisopropylamine
PMCA	Plasma membrane Ca^{2+} ATPase
PPA	Phenylalkylamine
ppm	Parts per million
Pt	Platinum
RA	Ritalinic acid
RMSD	Root mean square deviation
S	Solutions
s.c.	Subcutaneous
Ser	Serine
SERT	Serotonin transporter
SLC6	Solute carrier 6

$SOCl_2$	Thionyl chloride
T	Tablets
$t_{1/2}$	Half life
TEA	Triethylamine
TLC	Thin-layer chromatography
T_{max}	Time of peak concentration
*t*MP	*threo* Methylphenidate
TMS	Tetramethylsilane
TQD	Tandem quadrupole
Tyr	Tyrosine
UK	United Kingdom
UniProt	Universal Protein Resource
UNODC	United Nations Office on Drug and Crime
Val	Valine
VMAT2	Vesicular monoamine transporter 2
WHO	World Health Organization

Abstract

UNDERSTANDING STRUCTURE-ACTIVITY RELATIONSHIP OF SYNTHETIC CATHINONES (BATH SALTS) UTILIZING METHYLPHENIDATE

By Barkha Jitendra Yadav, Ph.D.

A Dissertation submitted in partial fulfillment of the requirements for the degree of Doctor of Philosophy at Virginia Commonwealth University.

Virginia Commonwealth University, 2019

Major Director: Dr. Richard A. Glennon
Professor
Department of Medicinal Chemistry

Synthetic cathinones are stimulant drugs of abuse that act at monoamine transporters e.g. the dopamine transporter (DAT) as releasing agents or as reuptake inhibitors. More than >150 new synthetic cathinones have emerged on the clandestine market and have attracted considerable attention from the medical and law enforcement communities.

threo-Methylphenidate (*t*MP) is an FDA approved drug for the treatment of ADHD and narcolepsy, which also acts as a DAT reuptake inhibitor and is widely abused. *t*MP and synthetic cathinones share some structural similarities and extensive structure-activity relationship (SAR) studies on *t*MP have been conducted. However, much less is known about the SAR of synthetic cathinones, and the available MP literature might assist in understanding it. The main focus of this research was to compare SAR between methylphenidate-cathinone hybrids and available methylphenidate SAR in order to identify some guiding principles that might allow us to predict their abuse potential and to identify which cathinones should be targeted for more extensive evaluation.

In the present study, we evaluated eight 2-benzoylpiperidine analogs and a descarbonyl analog to determine if *t*MP SAR can be applied to cathinone SAR. We conducted molecular modeling and docking studies and predicted the order of potency to be *t*MP > 2-benzoylpiperidine > 2-benzylpiperidine based on the number of hydrogen bonds. The synthesized analogs were evaluated in a competition assay using live-cell imaging against APP^+ in HEK293 cells stably expressing hDAT. All compounds were found to be DAT reuptake inhibitors and, as the modeling studies predicted, the order of potency in our functional studies was also found to be *t*MP > 2-benzoylpiperidine > 2-benzylpiperidine. A significant correlation was obtained between the potency of the benzoylpiperidines and *t*MP binding data ($r = 0.91$) suggesting that the SAR of *t*MP analogs might be applicable to the synthetic cathinones as DAT reuptake inhibitors.

I. Introduction

Synthetic cathinones represent a novel class of drugs of abuse which are stimulants in nature.[1] They first appeared on the clandestine market in 2008 and, since then, >150 synthetic cathinone analogs have been identified and they have drawn worldwide attention.[1,2] Synthetic cathinones are chemically related to cathinone (**1**), which is a naturally occurring stimulant of *Catha edulis* (khat plant) identified in the 19th century.[3] Due to their stimulant effects, synthetic cathinones are used as an alternative to widely abused substances such as amphetamine (**2**) and cocaine (**4**). Although they are known to act at the monoamine transporters as releasers or reuptake inhibitors, very little is known about their pharmacokinetic and pharmacodynamic profiles.[1] Early cathinones were found to act as releasing agents at the monoamine transporters, however, cathinone analogs bearing a tertiary amine or a bulky secondary amine and/or extended α-side chain (e.g. α-PVP) act as reuptake inhibitors at the dopamine transporter (DAT) and norepinephrine transporter (NET).[2]

Methylphenidate (MP) is an FDA-approved drug commonly prescribed to treat attention deficit hyperactivity disorder (ADHD) in children and narcolepsy in adults.[4] MP is a recognized stimulant and has a mechanism of action similar to that of cocaine (**4**). Due

to the presence of two chiral centers, MP has four isomers and it was identified that *threo*-methylphenidate (*t*MP) is the active isomer.[5] *t*MP acts as a reuptake inhibitor at DAT and NET, however, similar to cocaine (**4**), it does not have any effect at the serotonin transporter (SERT).[6,7] The structure-activity relationships (SARs) of MP (**70**) as a DAT reuptake inhibitor have been widely studied.[8,9] With respect to the ester group at the β-position, it was found that the methyl ester can be replaced with other β-substituents such as hydroxylamine, amide, and methoxymethyl, however the methyl ester was found to be optimal for the DAT binding affinity.[8]

For the current study, we designed a novel cathinone analog (hybrid between MP and cathinone), where the α-side chain of α-PVP is ligated to the terminal amine to resemble the piperidine ring of methylphenidate, and replacing the methyl ester of MP with a carbonyl group to resemble cathinone. In preliminary studies, previously done in our laboratory, the hybrid analog was found to act as a DAT reuptake inhibitor and this prompted our current study. We designed and synthesized eight hybrid analogs with different aryl substituents and a descarbonyl analog to determine the importance of the carbonyl oxygen atom. We evaluated the analogs for their functional activity in APP^+ uptake and intracellular Ca^{2+} determination assays.

Much is known about the SAR of MP and very little is known about the SAR of synthetic cathinones. Therefore, the current study focuses on conducting parallel SAR studies between MP and hybrid analogs and would help answering whether or not MP SAR can be applied to synthetic cathinones. If so, it would help understand the SAR of synthetic

cathinones by synthesizing a minimum number of analogs, which would save us time and resources. It would also help us predict and assist in the identification and potential scheduling of novel synthetic cathinones that are yet to be prepared or that might eventually find their way on the “street”.

II. Background

A. The Worldwide Drug Abuse Problem

According to the recent World Drug Report in 2016, approximately 275 million people worldwide aged 15 to 64 years (5.6% of the global population) used licit and/or illicit drugs at least once.[10] There has been a steady rise in the number of people using drugs and it has increased by 20 million people from 2015 to 2016. The concerning fact is that one in nine people who use drugs have a drug-use problem or are dependent on drugs and/or require treatment. This accounts for 30.5 million people worldwide (0.62% of global population).[10]

New psychoactive substances (NPS) are a complex class of drugs, most of which are not currently covered under international drug controls. They consist of a broad range of drug classes including synthetic cannabinoids, synthetic cathinones, opioids, stimulants and benzodiazepines.[11] Every year, NPS have been added to the illicit drug market. From 2009 to 2017 a total of 803 NPS have been reported by 111 countries and territories.[12] The number of NPS available on the market are on a steady rise and they are marketed in many different ways and their pattern of emergence differs from countries and regions.[13] NPS pose a significant threat as their effects on the human body and their

toxicological data are often unavailable. This results in additional challenges for identification, treatment, and scheduling purposes.[13]

By the end of 2017, among all the NPS reported to the United Nations Office of Drug and Crime (UNODC), synthetic cannabinoids form the largest class (251 substances), which is followed by "other substances" (155 substances), synthetic cathinones (148 substances) and phenethylamines (136 substances).[12,13] Not all the NPS reported stay on the market for a long time. Seventy two NPS were reported for the first time in 2016 which is fewer compared to NPS reported in 2015 (137 substances).[13] About 70 of the 130 NPS which were reported by the UNODC in 2009 have continued to appear on the market every year and many of them are now placed under international control.[13] On the contrary, 200 NPS reported between 2009 and 2014 disappeared from the reports of 2015 and 2016.[13]

B. Synthetic Cathinones

Synthetic cathinones represent a novel class of drugs of abuse that have drawn worldwide attention over the last decade. The first emergence of synthetic cathinones in Europe was in 2008 and has since become a new class of stimulants.[1] Synthetic cathinones are chemically related to cathinone (**1**, Figure 1), which is a naturally occurring stimulant of the khat plant identified in the 19th century.[3] Cathinones belong to the phenylalkylamine (PAA) class of compounds and are the β-keto analogs of amphetamine (AMPH; **2**, Figure 1).

Synthetic cathinones are often used as an alternative to widely abused and controlled drugs such as MDMA (**3**), AMPH (**2**), and cocaine (**4**) because of their stimulant effects (Figure 1). Very little is known about the pharmacokinetic and pharmacodynamic profiles of synthetic cathinones, although they are known to act at the monoamine transporters, as releasers or reuptake inhibitors, like AMPH and cocaine.[1]

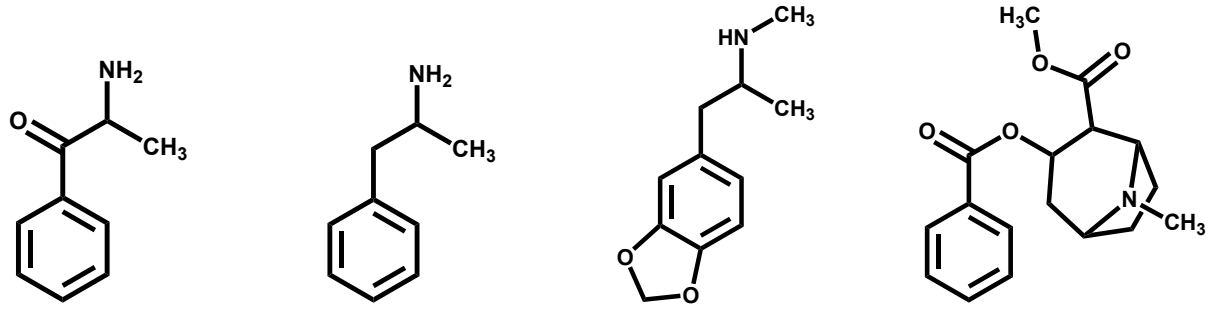

Cathinone (**1**) AMPH (**2**) MDMA (**3**) Cocaine (**4**)

Figure 1. Structures of cathinone (**1**) and the widely abused drugs amphetamine (AMPH, **2**), MDMA (**3**) and cocaine (**4**).

According to the EMCDDA, the majority of the synthetic cathinones appearing in Europe are reported to be synthesized mainly in China and, to a lesser extent, India.[1] In the last decade there has been a shift in the pattern of distribution, sale, and marketing strategies of these illicit drugs from street-level drug dealers to a more widespread and readily available virtual markets on the Internet.[14] Online retailers use the Internet to advertise synthetic cathinones and other NPS by giving them catchy names such as “meow meow”, “ivory wavy”, “vanilla sky”. They also provide ambiguous descriptions and are commonly sold as research chemicals, plant food or bath salts with a warning stating “not for human

consumption".[14] The so-called "darknet" also plays an important role in anonymous online markets for the purchase of synthetic cathinones and other NPS.[11,14]

According to the EMCDDA, synthetic cathinones are the second largest group of new substances monitored. Of the synthetic cathinones, 12 were detected for the first time in 2017.[11] In 2016, synthetic cathinones were the second most frequently seized NPS. They accounted for one-third of the total number of seizures, with over 23,000 seizures (Figure 2). Synthetic cathinones were the most seized NPS by quantity in 2016, amounting to nearly 1.9 tons.[11]

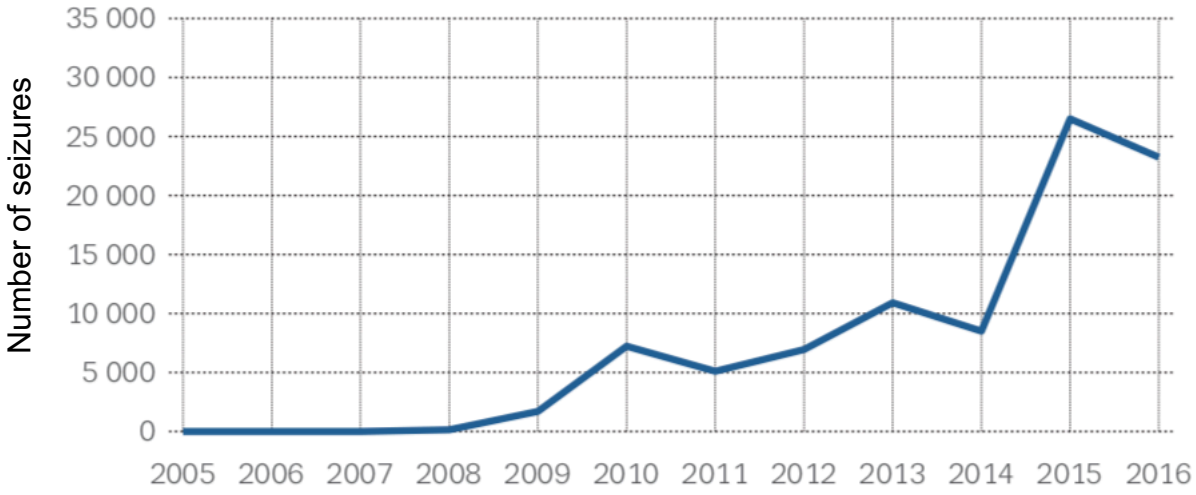

Figure 2. Number of seizures of synthetic cathinones over the years.[11]

C. Cathinone

1. Origins and History

Cathinone is a naturally occurring compound present in the shrub *Catha edulis.*[3,15] The general name used for the shrub is khat (also spelled as qat, kat, cat or qhat), although it has different names in different regions where it is cultivated.[15] It is called '*tchat*' by Amharas, '*Jimma*' by Gallas, and in Kenya, it is known as '*miraa*'.[16] Other names include "African salad", "Abyssinian Tea", "Bushman's tea" and "Flower of Paradise".[15,16] Khat is majorly cultivated in Ethiopia and Yemen for a very long time and its cultivation has spread to East Africa, South Africa, and Madagascar.[15,16] There have been reports of khat growing in the far west in Turkistan, Afghanistan and northern Hejaz (Saudi Arabia).[15,17]

The origin of the khat plant is under debate. The most ancient mention of a drug, which might have been khat, comes from Egypt.[18] From the available linguistic evidence, Cotterville-Gorandet theorized that the plant which was forbidden in the Temple of Philae was khat as reported by Kennedy.[18] More factual evidence of the origins of khat are the Arabic sources which suggest that khat was used as a medicinal plant in Turkestan and Afghanistan in the 11th century.[18] However, there is no mention of khat being used for pleasure or as a recreational drug.[18]

The most debated issue about khat is whether it originated in Yemen and spread to Ethiopia or vice versa. The first evidence of khat being used as a recreational drug and its origin is in the chronicle "wonder and deeds" of the Christian Ethiopian King, Amda Seyon I, reigning from 1314-1344, who fought against the Muslim King, Sabr al-Din who

boastfully said ‘As for Mardi its capital, I will make it mine and I will plant khat there because the Muslims like it.’[16,18] Most historians believe khat to be of Ethiopian origin and imported into Yemen but some still have an opposing view.[18] The cultivation and use of khat in Ethiopia and South-Western Arabia is thought to be earlier than that of coffee.[16]

Khat belongs to the Celastraceae family which includes 60-70 genera and 850-900 species.[16] It was first described by the Swedish botanist Peter Forskal in 1762 who gave khat the name *Catha edulis*. [15,16] The “*edulis*” in its name signifies that the plant is edible.[19] It is an evergreen tree and has a slender bole with white bark and has serrated leaves. In Yemen, the khat tree grows from 1 to 10 m in height, whereas in Ethiopian highlands, due to an abundance of rain, it can reach up to 20 m.[15,18,20] There are many different types of khat identified based on the area and ecology they grow in. In Yemen alone, 44 different types of khat exist and differ in the proportion of active ingredient and alkaloids.[18,19] It is rarely affected by diseases and if taken care, it can live up to 100 years.[15,18] Khat is a high-income crop and is a major source of income for Ethiopia’s export revenues.[15]

2. Khat chewing habit

Legends in Ethiopia have it that the first use of khat was by a Yemeni herder named Awzulkernayien.[20] He noticed the effects of the khat leaves on his goats and then tried it himself.[15,20] The leaves were chewed by farmers, laborers, and students to reduce fatigue and keep alert.[15] It is usually used in social gatherings in Yemen, called *majlis al-qat,* the *matka* or the *maqayyal.*[18] The guest usually consumes 100-200 g of leaves.[15] The effects

of khat experienced by the chewers are divided into desirable (experienced during the first few hours) and non-desirable (experienced at the end of khat-chewing session).[15,18]

The desirable effects are associated with euphoria, alertness, increased ability to concentrate, friendliness, and this state is referred to as *kayf*.[15] This is followed by the phase of *sulimania*, in which the chewers detach from the surroundings and often engage in deep thinking.[15,21] Men are the main consumer of khat and it is considered to be a male habit, but over 50% of women in Yemen chew khat on a regular basis.[18] Women have an elaborate form of khat-chewing session called *tafrita*, which is held less frequently.[18] However, khat chewing is only limited to old and married women and it is unacceptable for young and unmarried women to chew khat. [22]

3. Active constituents of khat

It was thought that, as its sister plant coffee, khat also contained caffeine.[18] However, this theory was debunked in 1887 when Flückiger and Gerock found no traces of caffeine in their studies as reported by Kennedy.[18] Early investigations found an active stimulant alkaloid and named it *katine* and later changed it to cathine.[18] Mosso in 1891 separated a basic extract and named it 'celastrina' as reported by Alles[16] and Kennedy.[18] He found that injecting celastrina into isolated frog hearts had a stimulant action. He also found injecting it directly in frogs resulted in dilation of the pupil, increased motor and respiratory activity followed by loss of coordination and tremors, convulsions, and finally respiratory arrest as reported by Alles et al.[16] In 1901, Beitter isolated the basic extract that he was able to crystallize,[23] however it was not for next 20 years that Wolfes (1930) extracted

and characterized the active compound as (+)norpseudoephedrine and was identified as 'cathine' (**5**, Figure 3).[24]

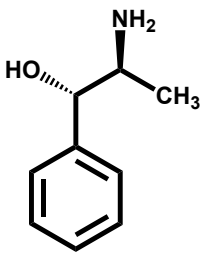

Cathine (**5**)

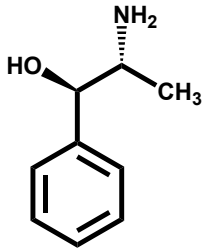

Norephedrine (**6**)

Figure 3. Structure of 1S,2S (+)norpseudoephedrine (cathine, **5**) and its isomer 1R, 2S (-)norephedrine (**6**).

Another investigator, Von Brucke, was not convinced that cathine (**5**) in such a small amount would be responsible for the effect it has on khat chewers, which made investigators believe that there might be other stimulant components in the plant as reported by Kennedy.[18] This suspicion was cleared in 1958 when Paris and Moyse showed that removal of cathine (**5**) from the khat tincture was still as active.[25] Friebel and Brilla in 1963 isolated the other alkaloid as an oxalate salt from the fresh plant and found that it had locomotor effects on mice greater than that of cathine (**5**).[26] Cais and co-workers[27] in 1964 isolated a substance and called it *cathedine D* and with further analysis they were able to determine the complete structures of cathedine A, B, C and D. The work of another team at the United Nations Narcotics Laboratory analyzed the data further and identified a phenylalkylamine, *S*(-)α-aminopropiophenone, and was named *cathinone* (**1**)[28] and its configuration was confirmed by comparing it with synthetic cathinone.[29] (-) Cathinone (*S*(-)**1**, Figure 4) was found to be the most active stimulant component of khat.

Only the *S*(-) enantiomer of cathinone is found in the khat plant and it has the same absolute configuration as (+)AMPH (*S*(+)**2**, Figure 4).[30] The (-)cathinone (*S*(-)**1**) was found in young leaves which accounted for 70% of the phenylalkylamines present.[28] This study also concluded that (-)cathinone (*S*(-)**1**) is a biosynthetic precursor which converts to cathine (**5**) via enzymatic reduction as the leaves age.[28]

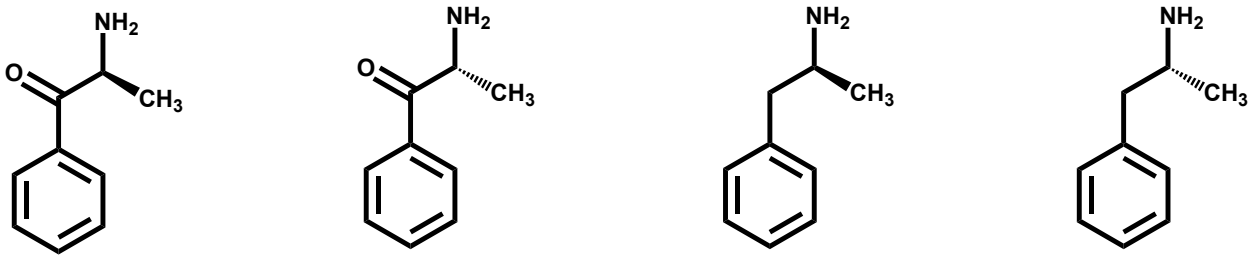

S(-)**1** *R*(+)**1** *S*(+)**2** *R*(-)**2**

Figure 4. Structures of the optical isomers of cathinone (**1**) and AMPH (**2**).

Apart from alkaloids (phenylalkylamine and cathedulins), flavonoids, sterols, terpenes, volatile aromatic compounds, and vitamins such as ascorbic acid, niacin, riboflavin and thiamine are also found in leaves and roots of khat plant.[19,31]

4. Neuropharmacological effects of khat

Due to its structural similarity to AMPH (**2**), it was thought that cathinone (**1**) might have AMPH-like effects and this has been reviewed by Kalix 1985.[21]

a. Somatic effects

Cardiovascular effects of (-)cathinone (*S*(-)**1**) were examined in isolated guinea pig atria and it showed to have positive inotropic and chronotropic effects.[32] The effect of (-)cathinone (*S*(-)**1**) was found to be twice that of (+)cathine (**5**) and (+)AMPH (*S*(+)**2**).[32] In another study conducted by Kohli et al.,[33] it was found that both (-)cathinone (*S*(-)**1**) and AMPH (**2**) produce an identical dose-related increase in heart rate, blood pressure in anaesthetized dogs.

A number of studies were carried out in order to investigate the analgesic properties of (-)cathinone (*S*(-)**1**) since AMPH (**2**) demonstrates analgesic effects.[21] The analgesic properties of (-)cathinone *S*(-) **1** were tested in three models.[34] In a tail-flick test, a single intraperitoneal (i.p.) administration of 2.5 mg/kg of (-)cathinone (S(-)**1**) in rats resulted in an increase in reaction time which lasted for 48 h. This increase in the reaction time was dose-dependent and with a dose of 10 mg/kg, the latency of tail-flick was more than the control values until six days after the administration of (-)cathinone (*S*(-)**1**).[34] The antinociceptive property of (-)cathinone (*S*(-)**1**) was tested in mice using a hot-plate test. With doses of 10, 20 and 40 mg/kg the antinociceptive effect was maximal at 15 min and lasted for approximately 30 min.[34] Lastly, a dose-dependent analgesia was also seen in a writhing test, where 10 mg/kg of (-)cathinone (*S*(-)**1**) reduced the number of writhings induced by i.p. administration of acetic acid and was completely blocked with 20 mg/kg of (-)cathinone (*S*(-)**1**) administration.[34]

b. Behavioral Effects

i. Locomotor stimulation

An early investigation by Yanagita et al.[32] showed that subcutaneous (s.c.) administration of (-)cathinone (*S*(-)**1**) significantly increased the locomotor activity of rats. Both (-)cathinone (*S*(-)**1**) and AMPH (**2**) were found to be equipotent in their stimulatory activities. In a study conducted by Glennon and Showalter,[35] in mice (-)cathinone (*S*(-)**1**) was found to be slightly more potent than (+)cathinone (*R*(+)**1**) and twice as potent as racemic cathinone (**1**) in stimulating locomotor activity. However, it was found to be 7-fold less potent compared to (+)AMPH (*S*(+)**2**).[35] Another study in 1982 also showed similar results where (-)cathinone (*S*(-)**1**) was found to be 4-fold less potent than (+)AMPH (*S*(+)**2**) in locomotor stimulation.[36]

In order to examine whether (-)cathinone (*S*(-)**1**) produces locomotor stimulation through the activation of dopamine (DA) receptors, like AMPH (**2**), its effect was tested in mice pretreated with DA antagonists such as haloperidol, spiroperidol, and pimozide.[36] It was found that at the concentration appropriate for DA antagonism, the above mentioned DA antagonists completely blocked the locomotor effects of (-)cathinone (*S*(-)**1**) similar to (+)AMPH (*S*(+)**2**). These studies indicated that the locomotor effects of (-)cathinone (*S*(-)**1**) and (+)AMPH (*S*(+)**2**) were comparable and involved the activation of postsynaptic DA receptors.[36]

ii. Stereotyped behavior

The general profile of the stereotyped behavior produced by cathinone (**1**) was found to be very similar to AMPH (**2**). Valterio and Kalix[36] found that i.p. administration of 11 mg/kg of (-)cathinone (*S*(-)**1**) induced stereotyped behavior in mice, this effect was also seen in rabbits after intravenous (i.v.) administration of 24 mg/kg of (-)cathinone (*S*(-)**1**).[37] The behavior produced by injection of the DA agonist apomorphine (5 mg/kg) was different from that induced by cathinone (**1**), cathine (**5**), and AMPH (**2**) with less verticalization and rapid head movements.[38] As seen with (+)AMPH (*S*(+)**2**), pretreatment of animals with the catecholamine synthesis blocker α-methylparatyrosine or the DA receptor antagonist haloperidol either completely abolished or significantly reduced the induction of stereotyped behavior by (-)cathinone (*S*(-)**1**) and (+)cathine (**5**).[38]

iii. Anorectic effects

Khat leaves are often chewed to suppress hunger and this anorectic effect has been demonstrated in several animal models such as rhesus monkeys,[39] rats[40] and pregnant guinea pigs.[41] It has been reported that intracerebroventricular injection of (-)cathinone (*S*(-)**1**) or (+)cathine (**5**) in rats significantly inhibited food intake to a greater extent than (+)AMPH (*S*(+)**2**).[42] Zelger and Carlini[40] reported that, i.p. administration of racemic cathinone (**1**) in rats resulted in decreased food intake and chronic administration led to loss in body weight. The order of potency in this study was found to be (+)AMPH (*S*(+)**2**) > cathinone (**1**) > (+)cathine (**5**). The anorexic effect of cathinone was much shorter, and tolerance was developed within a week and the weight reducing effect disappeared in 4

weeks, in contrast to AMPH (**2**) where tolerance developed in 2 weeks and its effect was seen for 7 weeks.[40]

iv. Drug discrimination studies

Drug discrimination studies not only help investigate the effects of the training drug, but also its mechanism of action.[43] A study conducted by Glennon et al.,[44] in rats trained to discriminate racemic cathinone from vehicle, (-)cathinone (*S*(-)**1**) was found to be 3-fold more potent than (+)cathinone (*R*(+)**1**), and 7-fold more potent than cathine (**5**). In another study, cathinone (**1**) trained rats showed generalization when they were given stimulants such as AMPH (**2**), cocaine (**4**), and methamphetamine[45] but did not show generalization with non-stimulants such as opioids, benzodiazepines, fenfluramine, and haloperidol.[46] Also, in a two-lever operant procedures where animals were trained to discriminate either (+)AMPH (*S*(+)**2**) or DOM (**7**, Figure 5), cathinone (**1**) did not show any DOM-like hallucinogenic effects, which indicated that cathinone (**1**) is not a hallucinogen.[47]

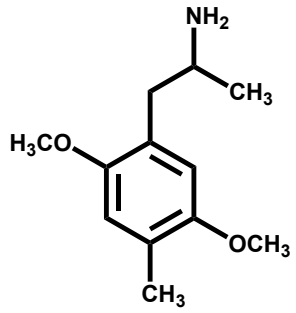

DOM (**7**)

Figure 5. Structure of the hallucinogen DOM (**7**).

v. Self administration

In a study on rhesus monkeys that were previously trained to lever-press for cocaine (**4**) injection, the monkeys continued to press the lever even when the training drug was replaced with (-)cathinone (*S*(-)**1**). The reinforcing effects of (-)cathinone (*S*(-)**1**) were found to be greater than (+)AMPH.[48] In another study, where the monkeys were given a drug-drug choice by lever pressing, the reinforcing effects of racemic cathinone (**1**) and cocaine (**4**) were found to be equal.[49] A similar pattern was observed in rhesus monkeys trained to self-administer cocaine intravenously in a progressive ratio test.[50] In this test, a breaking point of the animal is obtained and the fixed-ratio requirement for the next dose is increased i.e., the animal has to work more for the drug. The final ratio obtained was similar for (-)cathinone (*S*(-)**1**) and AMPH (**2**) and roughly half for cocaine (**4**) in monkeys.[32]

vi. Conditioned place preference

Conditioned place preference is used to assess the rewarding and motivating nature of drugs of abuse.[43] Calcagnetti et al.[51] showed that intracerebroventricular injection of 16 or 32 μg of racemic cathinone (**1**) in rats, when confined to the non-preferred side of the place-preference apparatus, significantly increased the time they spent in the non-preferred side. Same results were not obtained with a lower dose (8 μg).[51] This suggested that dopamine played a significant role in this reward behavior and was supported by a previous study where rats when pre-treated with the DA release inhibitor CGS 10746B (15 μg/rat) failed to show conditioned place preference with cathinone (**1**).[52]

c. Cellular effects

i. Dopaminergic effects

Since cathinone closely resembled (+)AMPH (*S*(+)**2**) in its somatic and behavioral effects, it was of interest to determine whether its effects were due to the release of DA similar to (+)AMPH, or if it acted as a dopamine transporter (DAT) reuptake blocker such as cocaine (**4**).

The effect of (-)cathinone (*S*(-)**1**) on the increase in radioactivity from isolated rabbit caudate nucleus prelabeled with [^{3}H]DA was examined.[53] It was found that superfusion of the tissue with (-)cathinone (*S*(-)**1**) caused a rapid increase in radioactivity and the amplitude was comparable to that produced by the same concentration of (+)AMPH (*S*(+)**2**), however (+)cathine (**5**) had no effect.[53] A similar study was conducted later by Zelger and Carlini,[54] where they showed that in rat striatal slices prelabeled with [^{3}H]DA, racemic cathinone (**1**) was about two-thirds as effective as (+)AMPH (*S*(+)**2**) in increasing radioactivity at 5 μM concentration, whereas at 50 μM both racemic cathinone (**1**) and (+)AMPH (*S*(+)**2**) were found to be equipotent.

ii. Serotonergic effects

AMPH (**2**) has been known to cause release of serotonin (5-HT) in a dose dependent manner and therefore it was thought that cathinone might also have a similar effect.[55] (-)Cathinone (*S*(-)**1**) was examined for its ability to release radioactivity from rat striatal tissue prelabeled with [^{3}H]5-HT. It was observed that in order to produce an effect similar to (+)AMPH (*S*(+)**2**), a three times higher concentration of (-)cathinone (*S*(-)**1**) was

required.[56] In another study conducted by Glennon and Liebowitz,[57] it was found that (-)cathinone (*S*(-)**1**) had 4-fold greater affinity for 5-HT receptors than (+)AMPH (*S*(+)**2**).

iii. Adrenergic effects

Since cathinone causes a number of sympathomimetic effects, especially cardiovascular, investigations were made to determine if these effects were due to the release of norepinephrine (NE) from synaptic nerve terminals. In an experiment with slices of rabbit heart tissue prelabeled with [^{3}H]NE, it was found that (-)cathinone (*S*(-)**1**) was able to increase the radioactivity and its potency was found to be half of (+)AMPH (*S*(+)**2**).[58] This NE release due to cathinone was blocked when the tissue was pretreated with desipramine and cocaine. Hence, it was concluded that like (+)AMPH (*S*(+)**2**), (-)cathinone (*S*(-)**1**) also had a releasing effect on peripheral NE storage sites.[58] It was also found that, (+)cathine (**5**) and (-)cathinone (*S*(-)**1**) were equipotent in increasing the radioactivity in [^{3}H]NE-prelabeled rabbit atrium slices.[59] These results were supported by previously conducted in vivo experiments by Kawaguchi et al.[60] where they showed that, in anaesthetized rats, (+)cathine (**5**) and (-)cathinone (*S*(-)**1**) had the same potencies in increasing heart rate and blood pressure.

5. Early structure-activity relationship (SAR) studies

a. In vivo studies

Drug discrimination studies were conducted by Glennon et al.[44] on both the isomers of cathinone (**1**), (+)cathine (**5**), α-desmethylcathinone (**8**) and a few 4-substituted cathinones (Table 1).[44] All the compounds were tested in rats previously trained to

discriminate between 0.6 mg/kg of racemic cathinone (**1**) from vehicle in a two-lever operant task. It was found that the naturally occurring (-)cathinone (*S*(-)**1**) (ED_{50} = 0.22 mg/kg) was 3-fold more potent than (+)cathinone (*R*(+)**1**) (ED_{50} = 0.72 mg/kg) and almost equipotent to (+)AMPH (*S*(+)**2**) (ED_{50} = 0.20 mg/kg).[44] α-Desmethylcathinone (**8**) was found to be inactive even at twice the concentration (1.2 mg/kg) of the training drug. This suggested that the α-methyl group contributes to the activity/potency of cathinone (**1**). (+)Cathine (**5**) (ED_{50} = 1.61 mg/kg) was found to be 7-fold less potent than (-)cathinone (*S*(-)**1**), whereas all the 4-substituted cathinones were found to be inactive.[44]

Table 1. Cathinone analogs examined in early drug discrimination studies.[44]

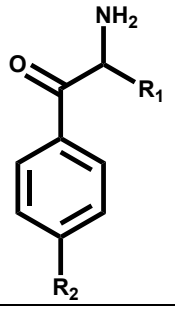

Agent	R_1	R_2	ED_{50} (mg/kg)
Racemic cathinone (**1**)	$-CH_3$	-H	0.24
(-)Cathinone (*S*(-)**1**)	$-CH_3$	-H	0.22
(+)Cathinone (*R*(+)**1**)	$-CH_3$	-H	0.72
α-Desmethylcathinone (**8**)	-H	-H	Inactive
(±)-4-Hydroxycathinone (**9**)	$-CH_3$	-OH	Inactive
(±)-4-Methoxycathinone (**10**)	$-CH_3$	$-OCH_3$	Inactive
(±)-4-Chlorocathinone (**11**)	$-CH_3$	-Cl	Inactive

In another drug discrimination study, (-)cathinone (*S*(-)**1**), 2-amino-1-tetralone (**12**, Figure 6), and *N,N*-dimethylaminopropiophenone (**13**, Figure 6) were tested for their ability to substitute for (+)AMPH (*S*(+)**2**) in rats trained to discriminate between (+)AMPH (*S*(+)**2**) and saline.[61] It was found that 2-amino-1-tetralone (**12**) produced saline-like responses at two and four times the generalization dose of (-)cathinone (*S*(-)**1**) (0.8 mg/kg) and caused disruption in behavior at higher doses. *N,N*-Dimethylaminopropiophenone (**13**) was also found to produce saline-like responses at doses up to 2.5 mg/kg. This suggested that constraining or extending the chain diminished the ability of the compound to produce AMPH-like responses.[61]

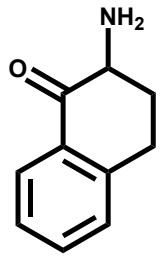

2-Amino-1-tetralone ("ringcathinone") (**12**)

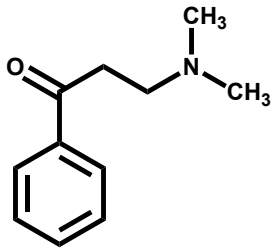

N,N-Dimethylaminopropiophenone (**13**)

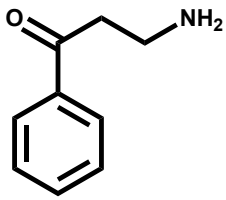

β-Aminopropiophenone (**14**)

Figure 6. Structures of 2-amino-1-tetralone (**12**), *N,N*-dimethylaminopropiophenone (**13**), and β-aminopropiophenone (**14**).

b. In vitro studies

(-)Cathinone (*S*(-)**1**), α-desmethylcathinone (**8**), 2-amino-1-tetralone (**12**), β-aminopropiophenone (**14**, Figure 6), and *N,N*-dimethylaminopropiophenone (**13**) were examined by Kalix and Glennon[61] for their in vitro ability to release [^{3}H]DA from rat caudate nucleus. In this study, (-)cathinone (*S*(-)**1**) was found to be the most potent

compound, and among the four analogs only α-desmethylcathinone (**8**) had an effect of similar magnitude as (-)cathinone (*S*(-)**1**).[61] These results suggested that (-)cathinone (*S*(-)**1**), like (+)AMPH (*S*(+)**2**) exerts its effects via a dopaminergic system.[61]

D. Synthetic cathinones

1. Methcathinone

a. History

Because *N*-monomethylation of AMPH (**2**), methamphetamine (METH, **15**), results in increased stimulant potency,[62] the same was thought for cathinones. The N-monomethylated cathinone was coined by Glennon et al.[63] as 'methcathinone' (MCAT, **16**) by the analogy to amphetamine-methamphetamine.[63] MCAT (**16**, Figure 7) might be considered as the first synthetic cathinone.[63] Compound **16** was first synthesized in 1915[64] and again in 1920[65] by Eberhard. It was synthesized as an intermediate in the preparation of ephedrine (**19**) and norephedrine (**6**) as reported by Glennon.[66] However, the most acknowledged synthesis of MCAT (**20**) was by Roger Adams and his students in 1928 where they used Eberhard's synthetic scheme (Scheme 1).[67]

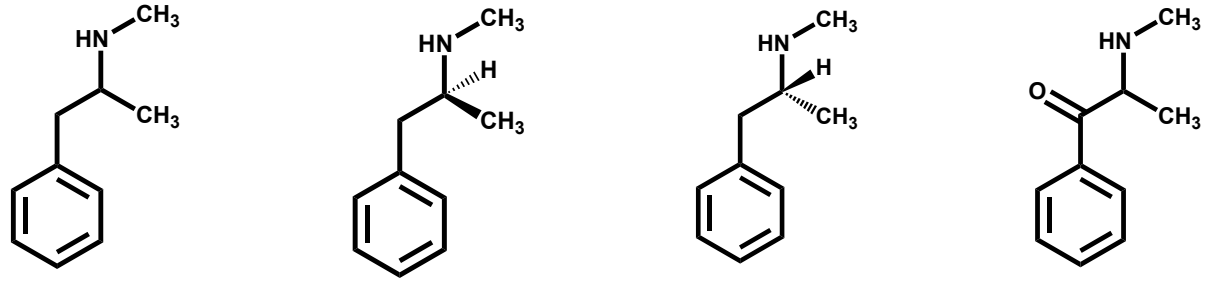

METH (**15**) *S*(+)**15** *R*(-)**15** MCAT (**16**)

Figure 7. Structures of METH (**15**), its optical isomers *S*(+)**15**, *R*(-)**15** and MCAT (**16**).

Scheme 1.[a] Eberhard's synthetic scheme for ephedrine with MCAT as an intermediate.[67]

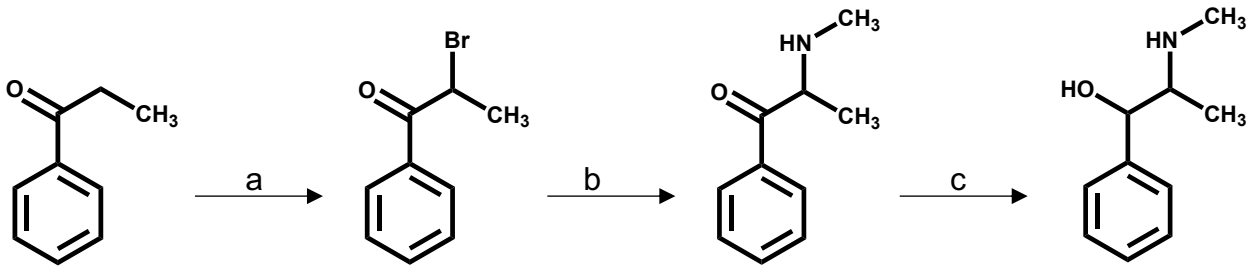

17 **18** MCAT (**16**) **19**

[a]Reagents: a. Bromination; b. CH_3NH_2 (condensation); c. reduction.

Although MCAT (**16**) has been around for over a century, it was only synthesized as a precursor for the synthesis of ephedrine (**19**) as reported by Glennon.[66] The optical isomers of MCAT (**16**) (Figure 8) were first synthesized and patented in Germany in 1936 as intermediate for ephedrine (**19**) synthesis.[68] It was again patented in 1957 as an analeptic agent by Parke-Davis.[69] Serendipitously, it was also found to have locomotor stimulation in mice when a number of phenylisopropylamine (PIA)-related analogs were tested[70] but not much attention was paid during the time.

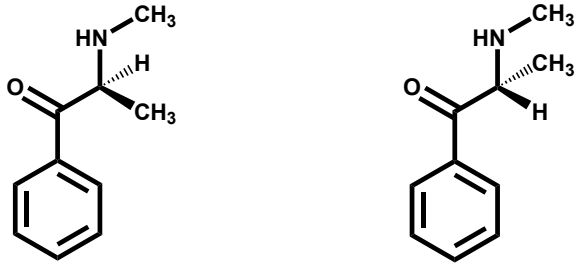

S(-)**16** *R*(+)**16**

Figure 8. Structures of optical isomers of MCAT (**16**).

As reported by Glennon,[66] in a document from the then USSR Interior Ministry in 1989, it was found that MCAT (**16**) was widely abused in the former Soviet Union under the name of *Ephedrone* (other street names include “jeff”, “Jee cocktail” and “cosmos”) and had surfaced for the first time in 1982.[66] However the reports of its abuse only came to light in the United States in the early 1990s which resulted in its placement in the Schedule I controlled substances.[2,66,71]

b. Early studies on MCAT (16)

In a study conducted by Glennon et al.[63] it was found that MCAT (**16**) had AMPH-like stimulus effects and was able to increase the release of radioactivity from rat striatal tissues prelabeled with [^{3}H]DA. In the same study, it was also found that MCAT (**16**) was several times more potent than racemic cathinone (**1**) in producing locomotor stimulation in mice.[63]

Stimulus generalization studies with rats trained to discriminate 8 mg/kg cocaine from saline were conducted.[72] The rank order of potency was found to be MCAT (**16**) (ED_{50} = 0.39 mg/kg) > cathinone (**1**) (ED_{50} = 0.69 mg/kg) > cocaine (**4**) (ED_{50} = 2.6 mg/kg).[72] Racemic MCAT (**16**) was found to be approximately 2- and 7-fold more potent than cathinone (**1**) and cocaine (**4**), respectively.[72] It was thought that like cathinone (**1**), (-)MCAT (*S*(-)**16**) would be more potent than (+)MCAT (*R*(+)**16**) and the first enantiomeric comparison study was conducted in 1995 by Glennon et al.[73] In a mouse locomotor stimulation study, (-)MCAT (*S*(-)**16**) was found to be several times more potent than (+)MCAT (*R*(+)**16**).[73] It was also found to be 3.5- and 6-fold more potent than (+)AMPH

(*S*(+)**2**) and (-)AMPH (*R*(-)**2**), respectively as a locomotor stimulant.[73] In a drug discrimination study using rats trained to discriminate cocaine (**4**) from saline the rank order of potency was found to be (-)MCAT (*S*(-)**16**) (ED_{50} = 0.18 mg/kg) > racemic MCAT (16) (ED_{50} = 0.39 mg/kg) > (+)MCAT (*R*(+)**16**) (ED_{50} = 0.51 mg/kg).[73]

A few years later another study was conducted by Young and Glennon[74] where (-)MCAT (*S*(-)**16**) was used as a training drug in rats. It was found that (-)MCAT (*S*(-)**16**) had a rapid onset of action i.e. within 5 min, and its effects lasted for approximately 60-90 min.[74] In this stimulus generalization study the order of potency was found to be (-)MCAT (*S*(-)**16**) (ED_{50} = 0.11 mg/kg) > (+)METH (*S*(+)**15**) (ED_{50} = 0.17 mg/kg) > (-)cathinone (*S*(-)**1**) (ED_{50} = 0.19 mg/kg) > (+)AMPH (*S*(+)**2**) (ED_{50} = 0.23 mg/kg) > racemic MCAT (**16**) (ED_{50} = 0.25 mg/kg) > racemic cathinone (**1**) (ED_{50} = 0.41 mg/kg) > (+)MCAT (*R*(+)**16**) (ED_{50} = 0.43 mg/kg) > cocaine (ED_{50} = 1.47 mg/kg).[74] It was also found that the DA receptor antagonist, haloperidol antagonized (-)MCAT (*S*(-)**16**) effects.[74] This concluded that (-)MCAT (*S*(-)**16**) is a very potent CNS stimulant drug of abuse and had AMPH-like stimulus effects.[74]

c. Transporter studies

MCAT (**16**) had been shown to act as a DAT releaser[63] and its effects on the norepinephrine transporter (NET) and serotonin transporter (SERT) were examined. Rothman[75] showed that (-)MCAT (*S*(-)**16**) had the ability to act as a releasing agent at DAT, NET and SERT and had potency similar to (+)METH (*S*(+)**15**) (Table 2). (-)MCAT (*S*(-)**16**) was found to be a potent releasing agent at DAT and NET but was weak at SERT.[75] In another study Cozzi et al.[76] evaluated the ability of MCAT (**16**) to release

monoamines at DAT, NET, SERT and vesicular monoamine transporter 2 (VMAT2). From these studies it was concluded that MCAT (**16**) exerts its effects primarily through DAT and NET and not SERT nor VMAT2.[76]

Table 2. Releasing potencies of METH (**15**) and MCAT (**16**) at the transporters.[75]

Test agents	**DA Release** $[EC_{50}$ **(nM ± S.D)]**	**NE release** $[EC_{50}$ **(nM ± S.D)]**	**5-HT Release** $[EC_{50}$ **(nM ± S.D)]**
(+)METH (*S*(+)**15**)	24.5 ± 2.1	12.3 ± 0.7	736 ± 45
(-)MCAT (*S*(-)**16**)	14.8 ± 0.4	13.1 ± 0.6	1772 ± 160

d. Subsequent SAR studies on MCAT (16)

Early SAR studies on MCAT (**16**) were focused on the terminal amine.[77] Increasing the chain length of the terminal amine to ethyl (ethcathinone, *N*-EtCAT, **20**, Figure 9) or to n-propyl (n-propylcathinone, *N*-PrCAT, **21**, Figure 9) resulted in a slight decrease in their potencies but resulted in stimulus generalization in drug discrimination studies in rats trained to discriminate (+)AMPH (*S*(+)**2**) from vehicle (Table 3).[77] *N,N*-Dimethylcathinone ((±)Di MeCAT, **22**, Figure 9) was found to be 1.6-fold less potent than racemic MCAT (**16**), and its isomer (-)*N,N*-dimethylcathinone ((-)Di MeCAT, **23**, Figure 9) was also found to be only 1.6-fold less potent than (-)MCAT (S(-)**16**) and equipotent to (-)cathinone (*S*(-)**1**).[77]

Table 3. Stimulus generalization studies in rats trained to discriminate (+)AMPH (*S*(+)**2**) from vehicle.[47,73,77]

Test agent	ED_{50} (mg/kg)
(-)Cathinone (*S*(-)**1**)	0.42
(+)AMPH (*S*(+)**2**)	0.33
(±)MCAT (**16**)	0.37
(-)MCAT (S(-)**16**)	0.25
N-EtCAT, **20**	0.77
N-PrCAT, **21**	2.03
(±)Di MeCAT, **22**	0.61
(-)Di MeCAT, **23**	0.44

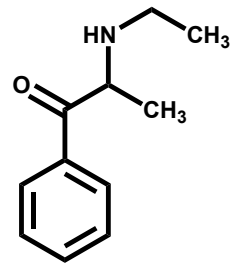

N-EtCAT (**20**)

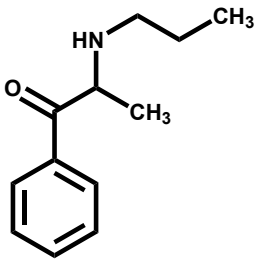

N-PrCAT (**21**)

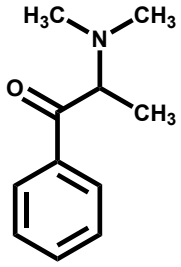

(±)Di MeCAT (**22**)

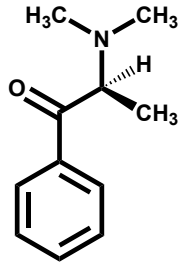

(-)Di MeCAT (**23**)

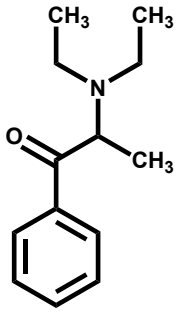

Di EtCAT (**24**)

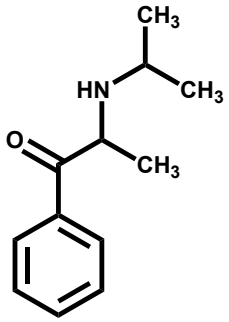

N-*i*PrCAT (**25**)

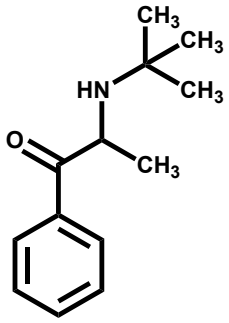

N-*t*BuCAT (**26**)

Figure 9. Structures of compounds studied in the early SAR studies with changes at the terminal amine.

In a rat brain synaptosome study conducted by Yu et al.[78] *N,N*-diethylcathinone (Di EtCAT, **24**, Figure 9) was found to be inactive in both release and uptake assay at DAT, NET and SERT. *N,N*-Diethylcathinone (**24**), also known as Tenuate®, was found to be a prodrug and its metabolite, *N*-EtCAT (**20**), was found to act as a substrate (releaser) at NET (IC_{50} = 99.3 nM) and as a reuptake inhibitor at DAT (IC_{50} = 1014 nM).[78] Interestingly, at SERT *N,N*-diethylcathinone (**24**) was found to act as a weak substrate, stimulating [^{3}H]5-HT release (IC_{50} = 2118 nM) and had similar potency as a SERT reuptake inhibitor (IC_{50} = 3840 nM).[78] In another study, *N*-isopropylcathinone (*N*-*i*PrCAT, **25**, Figure 9) and *N*-tert-butylcathinone (*N*-*t*BuCAT, **26**, Figure 9) were able to produce hyperlocomotion in rats at doses of 7.5 mg/kg and 10 mg/kg, respectively, which was approximately half of the effect produced by MCAT (**16**) at 5 mg/kg suggesting that increasing the bulk at the terminal amine reduces its AMPH-like locomotor stimulant activity.[79]

2. Bath Salts

a. Background

Iverson[80] in 2010, submitted a report to the British Home Office on the novel synthetic cathinones emerging on the European clandestine market at an alarming rate. One of the popular drug combination in 2010 was called 'bath salts' but also had several other names.[66] Bath salts mainly comprised of methylone (MDMC, **27**, Figure 10), mephedrone (MEPH, **28**, Figure 10), and methylenedioxypyrovalerone (MDPV, **29**, Figure 10).[66] It can also consist of a combination of one, two or more of these and/or other agents.[66]

It was reported that there was an increase in the number of compounds with simple β-keto modification of well-known amphetamines.[80] The presence of the ketone functionality was enough to circumvent the control measures which were already in place for their amphetamine counterparts.[80] The most common synthetic cathinone encountered by UK forensic providers was MEPH (**28**) and it accounted for 89% of all the cathinone seizures.[80] MEPH (**28**) and other cathinones were predominantly sold over the internet and in '*head shops*' and often had a disclaimer saying 'not for human consumption'.[80] They were sold as research chemicals, 'novelty bath salts' or as plant food/plant growth regulators as reported by Iverson.[80]

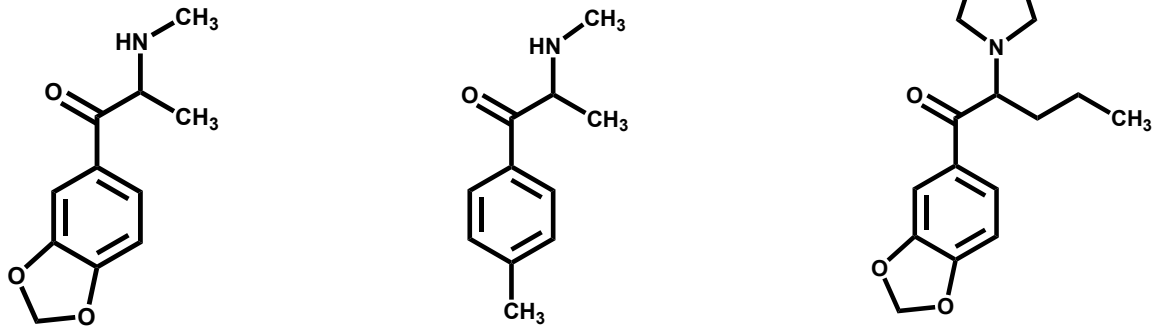

MDMC (**27**) MEPH (**28**) MDPV (**29**)

Figure 10. Structures of methylone (MDMC, **27**), mephedrone (MEPH, **28**), and methylenedioxypyrovalerone (MDPV, **29**), the three initial components of bath salts.

It was suggested that this tremendous escalation in the use of MEPH and other cathinones was due to the unavailability and low purity of cocaine (**4**) and MDMA in 2009.[80] As reported by Iverson,[80] a number of cathinone-related deaths had also been reported in the UK and other European countries. Due to this sudden rise and a number of cases of cathinone abuse, MDMC (**27**), MEPH (**28**) and MDPV (**29**) were temporarily

placed under U.S Schedule I category in 2011[81] and eventually led to their permanent placement in U.S Schedule I class.[82,83]

b. Mode of action

Rothman et al.[84] showed that MEPH (**28**) produced (+)AMPH-like responses, but little was known about MDMC (**27**) and MDPV (**29**). In a study conducted by Cameron et al.[85] using a frog oocyte preparation transfected with human dopamine transporter (hDAT), MEPH (**28**) was found to produce an inward (depolarizing) current through hDAT similar to METH (1**5**) (Figure 11).[85] MEPH (**28**) was examined along with (-)MCAT (*S*(-)**16**) and (+)METH (*S*(+)**15**) and the order of potency was found to be (-)MCAT (*S*(-)**16**) (EC_{50} = 0.23 μM) > (+)METH (*S*(+)**15**) (EC_{50} = 0.64 μM) ≥ MEPH (**28**) (0.84 μM).[85]

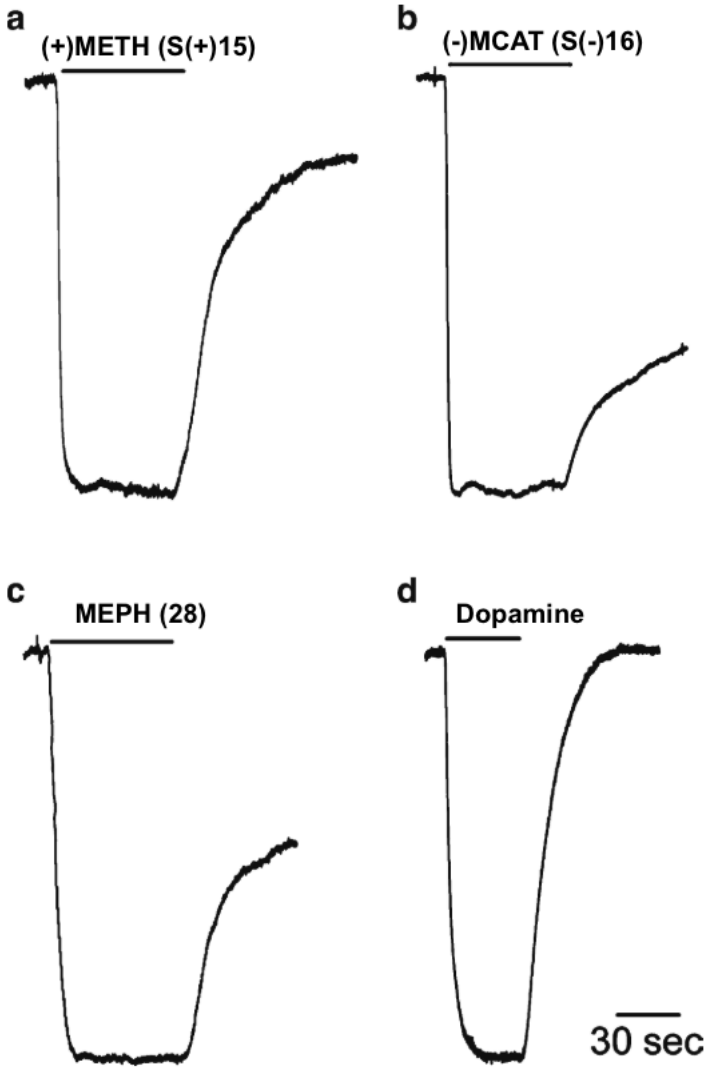

Figure 11. Inward depolarizing currents generated in hDAT by application of 10 μM (+)METH (*S*(+)**15**) (a), (-)MCAT (S(-)**16**) (b), MEPH (28) (c) and dopamine (d) at −60 mV.[85]

On the contrary, it was found that MDPV (**29**) had an opposite effect.[85] MDPV (**29**) produced an outward (hyperpolarizing) current similar to cocaine (Figure 12).[85,86] Moreover, MDPV (**29**) was able to reverse the effect of MEPH (**28**) in a similar manner as cocaine reverses the effect of (+)METH (*S*(+)**15**) and MEPH (Figure 13).[86]

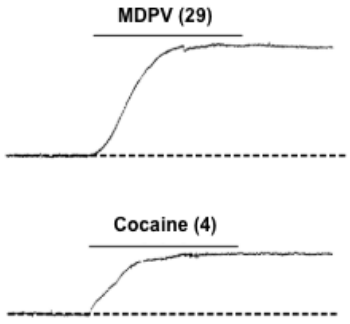

Figure 12. Outward hyperpolarizing current produced in hDAT by application of 10 μM of MDPV (**29**) (above) and cocaine (**4**) (below).[86]

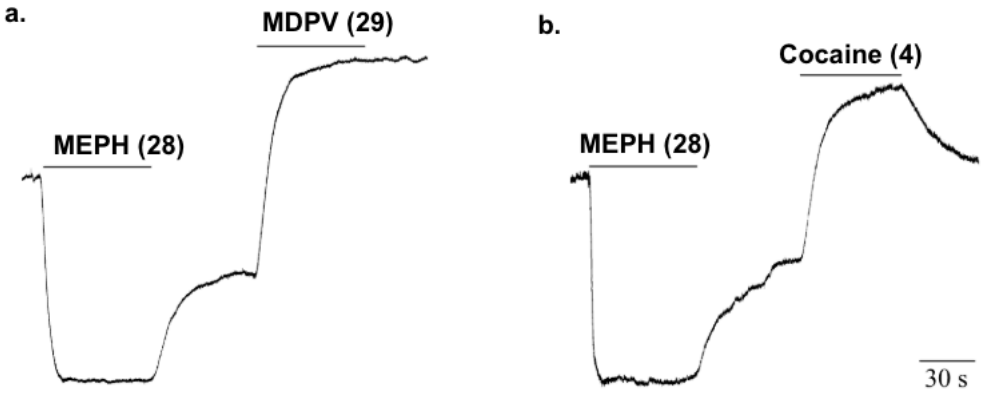

Figure 13. At 10 μM MDVP (**29**) (a) and cocaine (**4**) (b) were able to block the effect of MEPH (**28**), displaying their blocking action at hDAT.[86]

Baumann and co-workers[87] carried out in vitro assays, using rat brain synaptosome, and in vivo studies to examine the bath salts components. It was found that MDPV (**29**) is a potent reuptake inhibitor of DAT and NET but weak at SERT (Table 4). From the in vivo studies, MDPV (**29**) was found to be at least 10-fold more potent than cocaine (**4**) in producing locomotor activation, tachycardia, and hypertension in rats.[87]

Table 4. Effects of bath salt components, AMPH (**2**), and cocaine (**4**) on synaptosomal release and uptake inhibition at DAT, NET, and SERT.[87]

Agents	Release assay EC_{50} (nM)			Reuptake inhibition assay IC_{50} (nM)		
	DAT	**NET**	**SERT**	**DAT**	**NET**	**SERT**
MDMC (**27**)	117	140	234	1232	1031	1017
MEPH (**28**)	51	58	122	762	487	422
MDPV (**29**)*	Inactive	Inactive	Inactive	4.1	26	3329
S(+)**2**	5.8	6.6	698	93	67	3418
Cocaine (**4**)*	Inactive	Inactive	Inactive	211	292	313

*MDPV (**29**) and cocaine (**4**) produced <35% [^{3}H]MPP^+ release.

Homologation of the α-side chain of MDMC (**27**) from methyl to ethyl (butylone, **30**, Figure 14) resulted in reuptake inhibition at DAT, NET, and SERT.[88] In another study conducted by Del Bello et al.[89] it was found that expansion of the methylenedioxy ring of MDMC (**27**) to an ethylenedioxy ring (EDMC, **31**, Figure 14) slightly reduced its potency as a releasing agent at all three transporters. Replacement of the methylenedioxy ring of MDPV (**29**) to a fused phenyl ring (naphyrone, **32**, Figure 14) resulted in reuptake inhibition at the three transporters and was found to be 6- and 15-fold less potent than MDPV (**29**) at NET and DAT, respectively.[88] On the contrary, naphyrone (**32**) was found to be 10-fold more potent than MDPV (**29**) at SERT.[88]

From these studies it was evident that substituents on the terminal amine, α-side chain and the aromatic ring played a significant role in the actions (releasers vs reuptake

inhibitors) and selectivity (DAT, NET, and SERT) of cathinone analogs as reported by Glennon and Dukat.[2]

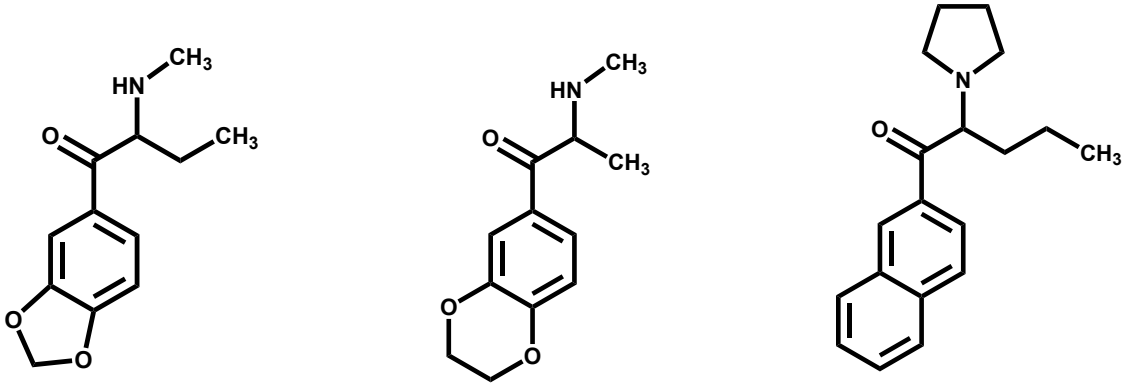

Butylone (**30**) EDMC (**31**) Naphyrone (**32**)

Figure 14. Structures of butylone (**30**), ethylenedioxymethcathinone (EDMC, **31**), and naphyrone (**32**).

3. Synthetic cathinones as releasing agents

As MCAT (**16**)[75] and MEPH (**28**)[87] were already found to be releasing agents at DAT, a number of phenyl ring-substituted MCAT (**16**) analogs were subsequently evaluated.

a. 4-Substituted MCAT

MCAT (**16**) and six other 4-substituted analogs (Table 5) were examined in intracranial self-stimulation (ICSS) and in in vitro studies in order to characterize or identify what physicochemical properties were important for their actions.[90] It was found that all six 4-substituted analogs were able increase DA and 5-HT release via DAT and SERT.[90] MCAT (**16**) was found to be the most potent analog at DAT and 4-trifluoromethylmethcathinone (**38**) was found to be the least potent.[90] There was a strong correlation seen between in

vitro DAT selectivity and ICSS facilitation (Figure 15).[90] The release activity at NET of 4-substituted MCAT analogs were conducted recently by Walther et al.[91]

Table 5. In vitro release potencies (EC_{50}) of 4-substituted MCAT analogs at DAT, NET and SERT.[90,91]

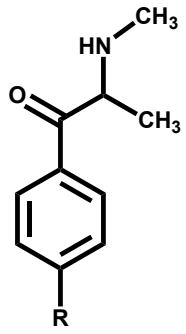

-R	NET (nM)[91]	DAT (nM)[90]	SERT (nM)[90]	DAT vs SERT selectivity*
-H (MCAT, **16**)	22	12.5	3860	309
-F (**33**)	-	83.4	1298	15.4
-Cl (**34**)	33	42.2	144	3.40
-Br (**35**)	100	59.4	60	1.01
-CH_3 (**36**)	63	49.1	118	2.41
-OCH_3 (**37**)	111	506	120	0.24
-CF_3 (**38**)	900	2700	190	0.07

*DAT vs SERT selectivity = SERT EC_{50}/DAT EC_{50}.

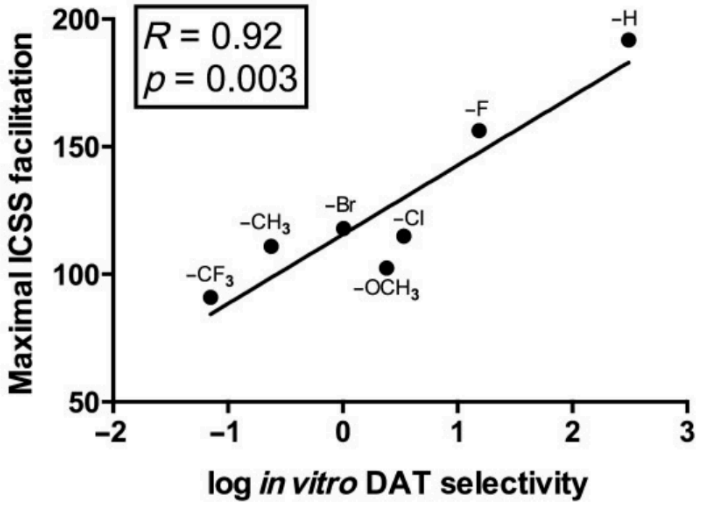

Figure 15. Correlation between in vitro DAT vs SERT selectivity and maximum in vivo ICSS facilitation (shown as percentage of maximum control reinforcement rate).[90]

From these studies it was found that substitution at the 4-position influences the potency and selectivity at DAT and SERT.[90] Increase in the size of the substituent shifts its potency from DAT to SERT.[90] Homology modeling studies on hDAT and human serotonin transporter (hSERT) also showed that the binding pocket associated with the 4-position in hDAT can only accommodate smaller substituents, whereas the larger binding pocket of hSERT can accommodate larger substituents.[92]

b. 3-Substituted MCAT

Five 3-substituted analogs and MCAT (**16**) were tested for their potencies as releasing agents at DAT, NET, and SERT (Table 6).[91] 3-Cl MCAT (**39**) was tested previously[93] and in the most recent study, from our laboratory, its potency was found to be comparable among the three transporters.[91] The 3-Cl MCAT (**39**) and 3-Br MCAT (**40**) analogs have

been previously found and seized from the clandestine market.[94] The potencies of all the 3-substituted MCAT analogs at DAT as releasing agents were 2- to 5-fold higher than the corresponding 4-substituted MCAT (**16**) analogs.[91] The potencies at SERT were about half as compared to the corresponding 4-MCAT analogs and had a narrow range of potency (Table 5).[91]

Table 6. In vitro release potencies (EC_{50}) of 3-substituted MCAT analogs at DAT, NET and SERT.[91]

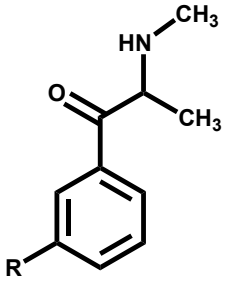

-R	**NET (nM)**[91]	**DAT (nM)**[91]	**SERT (nM)**[91]	**DAT vs SERT selectivity***
-H (MCAT, **16**)	22	21	5853	279
-Cl (**39**)	19	26	211	8
-Br (**40**)	25	21	136	6
$-CH_3$ (**41**)	27	28	268	10
$-OCH_3$ (**42**)	111	109	683	6
$-CF_3$ (**43**)	370	714	281	0.4

*DAT vs SERT selectivity = SERT EC_{50}/DAT EC_{50}.

c. 2-Substituted MCAT

2-Substituted MCAT analogs were found to be the least potent as compared to their 3- and 4-substituted analogs, being 2- to 10-fold less potent than the corresponding 4-substituted analogs.[85] The NET potencies were comparable to their DAT potencies, and the SERT potencies of the 2-substituted analogs were 4 to 47-fold lower than the corresponding 4-substituted analogs (Table 7).[91]

Table 7. In vitro release potencies (EC_{50}) of 2-substituted MCAT analogs at DAT, NET and SERT.[91]

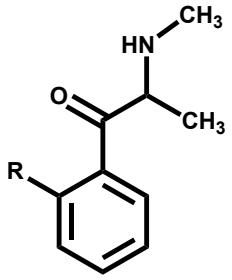

-R	**NET (nM)**[91]	**DAT (nM)**[91]	**SERT (nM)**[91]	**DAT vs SERT selectivity***
-H (MCAT, **16**)	22	25	2592	103
-Cl (**44**)	93	179	2815	16
-Br (**45**)	156	650	2837	4
-CH_3 (**46**)	53	81	490	6
-OCH_3 (**47**)	339	920	7220	8

*DAT vs SERT selectivity = SERT EC_{50}/DAT EC_{50}.

d. Other phenyl-ring substituted MCAT (16)

Blough et al.[95] evaluated a few disubstituted MCAT analogs in rat brain synaptosomes for their ability to release DA and 5-HT (Table 8). On comparing with MCAT, all the three disubstituted MCAT analogs were less potent at DAT and more potent at SERT as releasing agents.[95] Three other aryl-substituted agents were evaluated for their DAT and SERT release potencies.[89] The first two compounds, 1-naphthylmethcathinone (**51**) and 2-naphthylmethcathinone (**52**), were found to be equipotent when compared to MCAT (**16**) at DAT, and 198-fold and 158-fold more potent at SERT as releasing agents, respectively.[95] Lastly, the phenyl ring of MCAT was replaced with an indole ring giving the 3-indole analog (i.e. **53**) which was 2-fold less potent at DAT and 103-fold more potent at SERT when compared to MCAT.[95]

Table 8. DAT and SERT-mediated release activity of disubstituted and other ring substituted analogs of MCAT.[95]

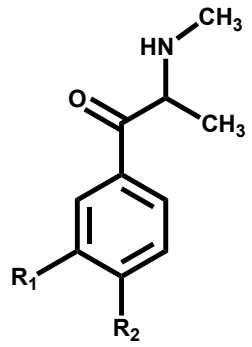

16, 48-50

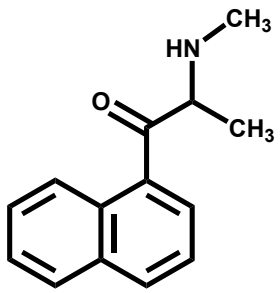

51

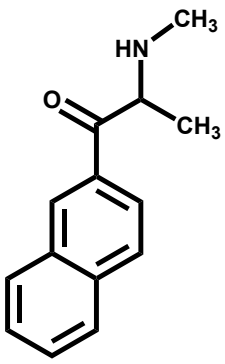

52

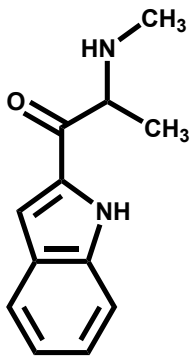

53

Agent	-R1	-R2	DA release (nM)	5-HT release (nM)	DAT vs SERT selevtivity
MCAT (**16**)	-H	-H	50	4270	86
48	-Cl	-Cl	178	74	0.4
49	-F	-F	227	960	4.2
50	-Cl	$-CH_3$	124	41	0.3
51	-	-	55	21	0.4
52	-	-	34	27	0.8
53	-	-	93	41	0.4

*DAT vs SERT selectivity = SERT EC_{50}/DAT EC_{50}.

In summary, substitution at the 2-position was not well tolerated by any of the three transporters.[91,95] However, 3- and 4-substituted analogs were roughly equipotent as releasing agents at DAT and NET with a high correlation but are less potent at SERT.[91] Increasing the steric bulk near the 3- or 4-position of the phenyl ring improved potency towards SERT as a releasing agent which was also seen with the homology modeling studies conducted by Sakloth et al.[92]

4. Synthetic cathinones as reuptake inhibitors

MDPV (**29**) was the first synthetic cathinone, found by our laboratory, to act as a reuptake inhibitor at DAT.[85,86] Therefore, a systematic deconstruction approach was followed to determine which structural feature/s contribute to its unique action.[96] MDPV (**29**) and seven deconstructed analogs (Figure 16) were tested in voltage-clamped (−60 mV) *Xenopus* oocytes transfected with the hDAT and all the analogs were found to act as DAT reuptake inhibitors.[96] Converting MDPV (**29**) (IC_{50} = 135 nM) to its amphetamine analog (i.e., **54**), by removal of the carbonyl group, resulted in more than an 8-fold decrease in its potency (IC_{50} = 1150 nM).[96] Removal of the methylenedioxy group (i.e., α-PVP, **55**) had little effect (IC_{50} = 205 nM), whereas reducing the length of the α-side chain from *n*-propyl to methyl (i.e., **56**) dramatically decreased its potency by 25-fold (IC_{50} = 3540 nM).[96] Replacing the pyrrolidine ring of MDPV (**29**) with the simplest tertiary amine (i.e., **57**) resulted in a 5-fold decrease (IC_{50} = 715 nM) and further conversion to a secondary amine (i.e., **58**, IC_{50} = 7950 nM) and a primary amine (i.e., **59**, IC_{50} = 27000 nM) resulted in 59- and 200-fold decrease in potency when compared to MDPV (**29**), respectively.[96]

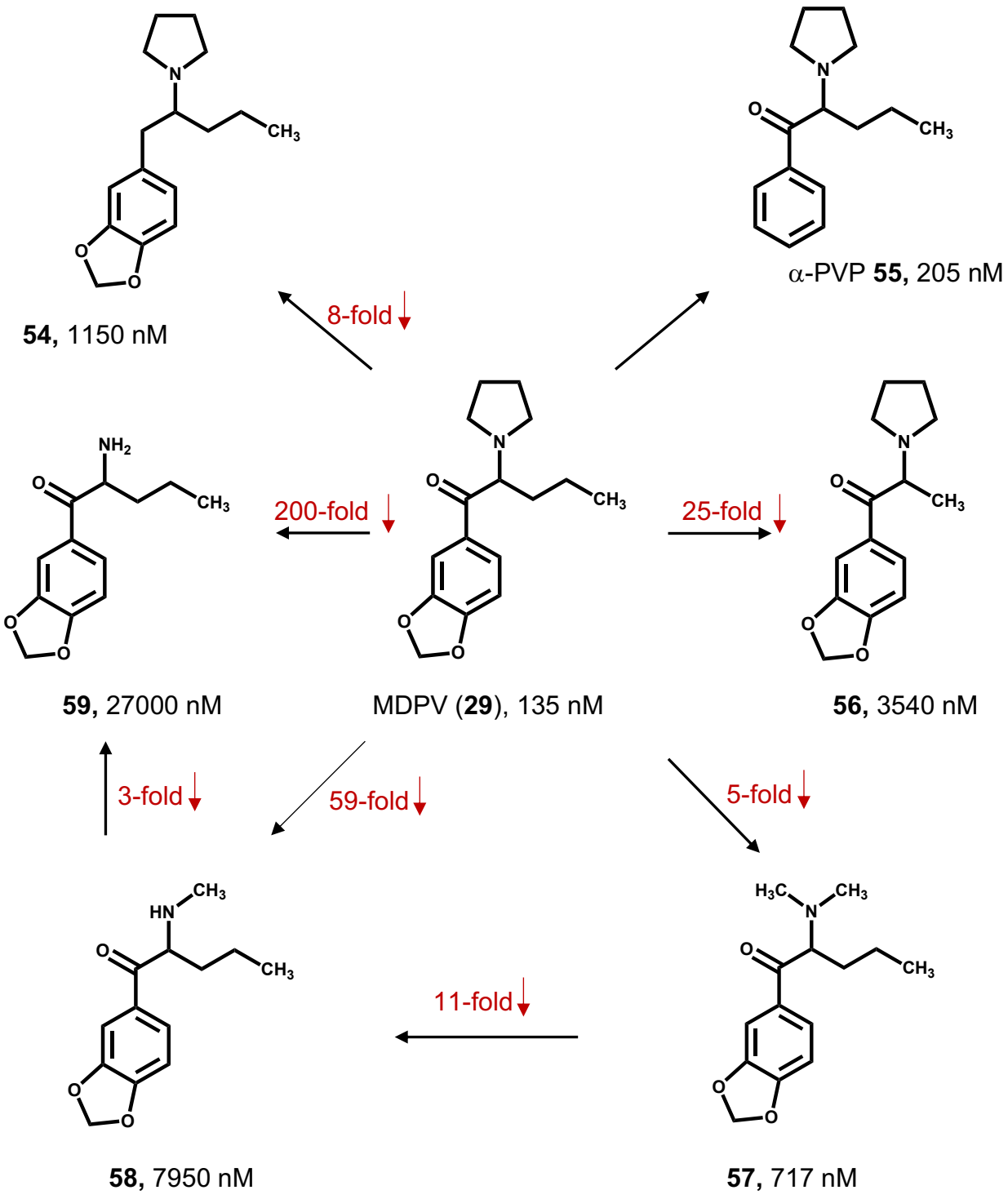

Figure 16. Deconstructed analogs of MDPV (**29**) with their IC_{50} (nM) values tested in voltage-clamped (−60 mV) *Xenopus* oocytes transfected with hDAT.[96]

In a study conducted by Kolanos et al.,[97] racemate MDPV (**29**) and its two isomers were tested for their ability to inhibit the reuptake of [^{3}H]DA. It was found that (+)MDPV (*S*(+)**29**, Figure 17) (IC_{50} = 2.13 nM) was twice as potent as racemic MDPV (**29**) (IC_{50} = 4.85 nM) and 180-fold more potent than (-)MDPV (*R*(-)**29**, Figure 17) (IC_{50} = 382 nM).[97]

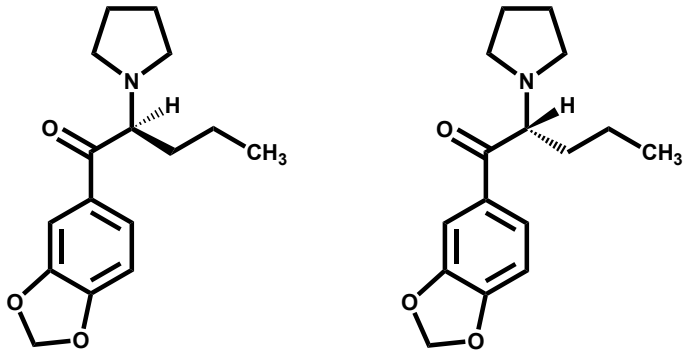

S(+)**29** *R*(-)**29**

Figure 17. Structures of optical isomers of MDPV (**29**).

5. Second generation synthetic cathinones – α-PVP

The first synthesis of α-PVP (**55**) was described by Wander in a British patent in 1963 and it was found to have CNS stimulant action.[98] Its most popular street name "*flakka*" was derived from "la flaca" which is a Spanish slang term for a "beautiful women" as reported by Kolesnikova et al.[99] Other commonly used street names are speed, snow blow, gravel, crystal love, vanilla sky, and sextacy.[99,100] α-PVP (**55**) was not seen on the market prior to 2000 and the EMCDA reported China as its major source.[100] The first seizure of α-PVP (**55**) was reported in 2011 in France and then in Hungary and Poland in 2013-2014.[99] Between 2012 and 2015, a total of 115 deaths associated with α-PVP were reported in Europe.[101] In the United States, it was first encountered in early 2010s

in Florida, Ohio, and Tennessee.[102] α-PVP (**55**) was related to at least 80 deaths between September 2014 and December 2015 in Florida alone as reported by Palamar et al.[103] α-PVP (**55**) was placed in U.S. Schedule I in March 2014.[104]

a. SAR studies on α-PVP

As removal of the methylenedioxy group of MDPV (i.e., α-PVP, **55**) had minimal effect on its potency as a reuptake inhibitor at DAT,[96] a deconstruction and elaboration study was conducted on α-PVP (**55**) (Figure 18).[105,106] Truncating the α-side chain in a stepwise manner from *n*-propyl to ethyl (i.e., α-PBP, **60**), methyl (i.e., α-PPP, **61**) and completely replacing it with -H (i.e., **62**) resulted in an overall 200-fold decrease in potency when tested to inhibit uptake of [^{3}H]DA.[105,106] None of the compounds inhibited the uptake of [^{3}H]5-HT.[106] For the elaboration study, the α-side chain was extended from *n*-propyl to *n*-butyl (i.e., **63**) which resulted in a slight increase in its potency, whereas branching the side chain to *i*-propyl (i.e., **64**) decreased potency by 5-fold.[106] Other substitutions at the α-side chain were also evaluated (Figure 18) and all analogs with changes at the α-position were found to be at least as potent as α-PVP except for the constrained analog **69** which was found to be over 700-fold less potent than α-PVP.[106] All the analogs in this 'deconstruction-elaboration' study were found to be DAT reuptake inhibitors.[106]

Deconstruction

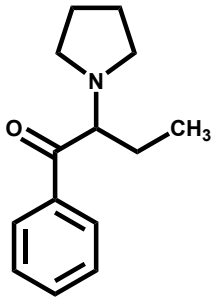

60, (IC_{50} = 63.3 nM)

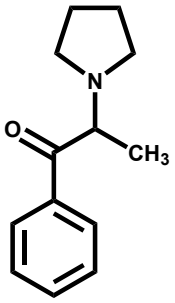

61, (IC_{50} = 196 nM)

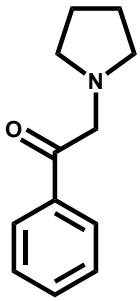

62, (IC_{50} = 3250 nM)

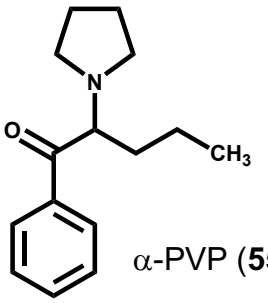

α-PVP (**55**), (IC_{50} = 17.5 nM)

Elaboration

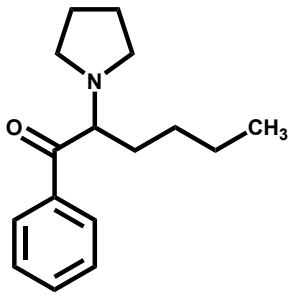

63, (IC_{50} = 11.6 nM)

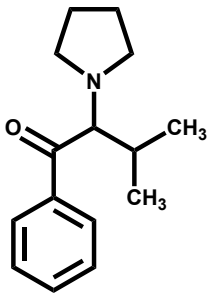

64, (IC_{50} = 92.3 nM)

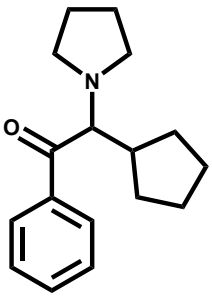

65, (IC_{50} = 17 nM)

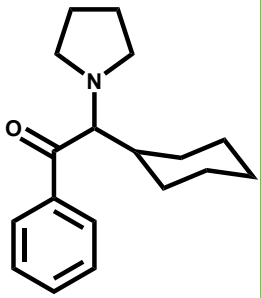

66, (IC_{50} = 8.3 nM)

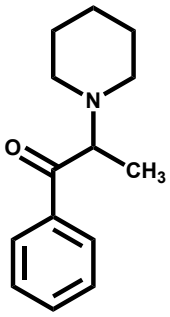

67, (IC_{50} = 2490 nM)

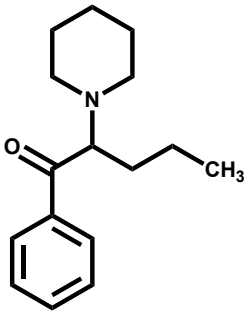

68, (IC_{50} = 128 nM)

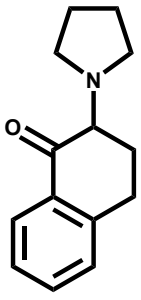

69, (IC_{50} = 12900 nM)

Figure 18. Structures of deconstructed (top in red box) and elaborated (bottom in green box) analogs of α-PVP tested in our laboratory for their ability to inhibit uptake of [^{3}H]DA.[106]

Nelson et al.[107] conducted a conditioned taste avoidance test in rats using racemic and both isomers of α-PVP (Figure 19). It was found that rats injected with the racemate and *S*-isomer displayed avoidance to the saccharin solution.[107] The avoidance shown by 3 mg/kg of racemic α-PVP was found to be similar to 1.5 mg/kg of the *S*-isomer,[107] whereas the *R*-isomer did not induce any taste avoidance even at 6 mg/kg.[107] This study concluded that the S-isomer of α-PVP is the eutomer.[107]

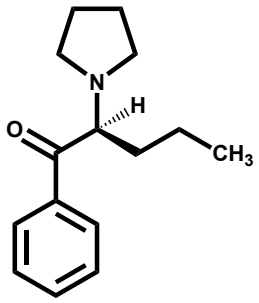

S-α-PVP (**55**)

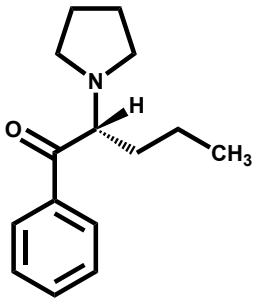

R-α-PVP (**55**)

Figure 19. Structures of the isomers of α-PVP.

E. Methylphenidate

Methylphenidate (MP, **70**, Figure 20) was first synthesized in 1944 (Scheme 2),[108] however its psychostimulant activity was only recognized after a decade as reported by Heal and Pierce.[109] MP (**70**) has two chiral centers and therefore exists as four stereoisomers i.e. the *dextro* and *levo* enantiomers of both *threo* and *erythro*-methylphenidate (Figure 20). MP is a commonly used drug in the United States and although it was initially used as an analeptic agent for reversal of barbiturate-induced coma, now it is mainly used to treat attention deficit/hyperactivity disorder (ADHD) in children and adults.[109,110]

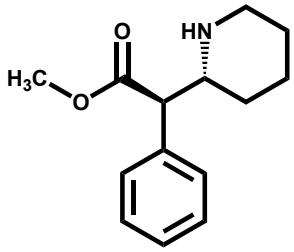

d-threo (2*R*, 2'*R*) *t*MP (**70**)

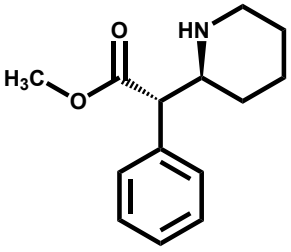

l-threo (2*S*, 2'*S*) *t*MP (**70**)

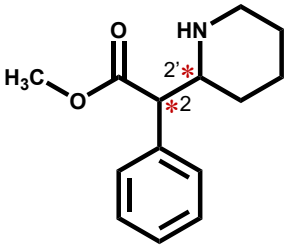

MP (**70**)

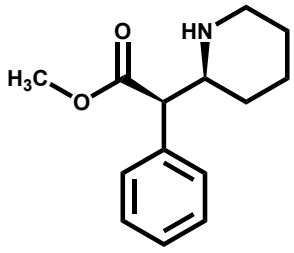

d-erythro (2*R*, 2'*S*) eMP (**70**)

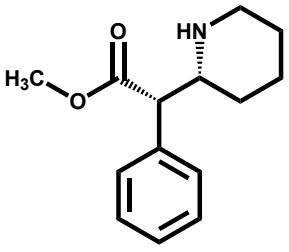

l-erythro (2*S*, 2'*R*) eMP (**70**)

Figure 20. Structures of MP (**70**) and its four isomers.

Scheme 2[a]. Synthesis of MP (**70**) by Panizzon in 1944.[108]

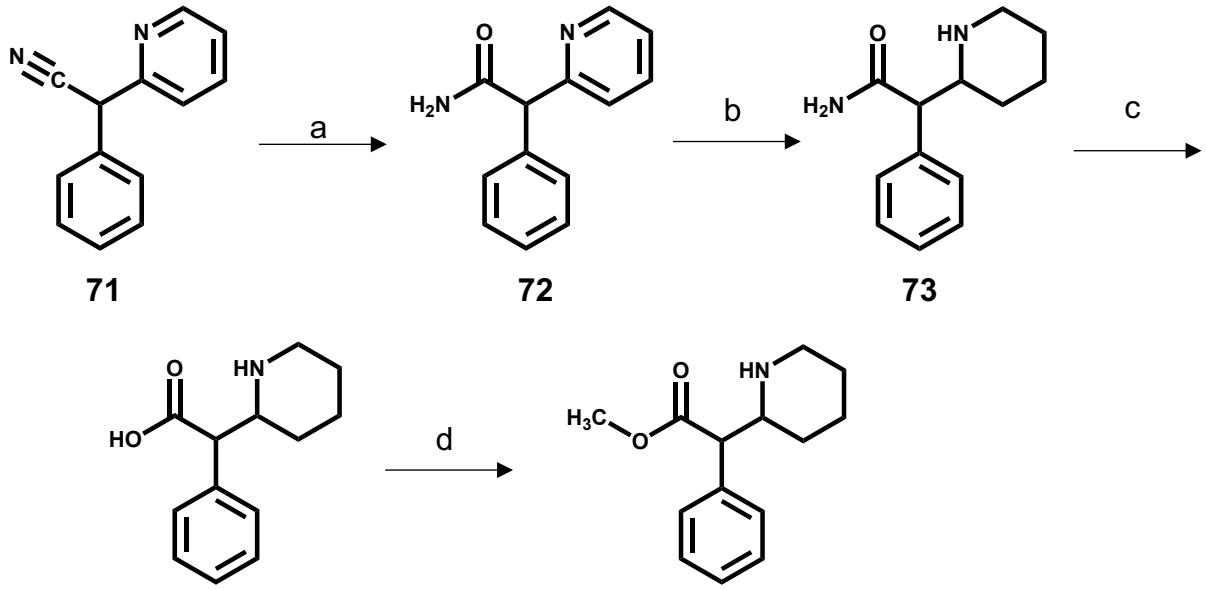

[a]Reagents and conditions: a. H_2SO_4; b. H_2, Pt, CH_3COOH 40 °C; c. HCl, reflux; d. CH_3OH, H_2SO_4.

MP (**70**) was originally patented in 1950 by CIBA Pharmaceuticals (now known as Novartis) for its method of preparation, it was later patented (under the brand name Ritalin) as a treatment of psychiatric disorders in 1954 as reported by Wenthur.[111] Figure 21 shows the timeline of MP (**70**) and its development into different formulations over the years.[111]

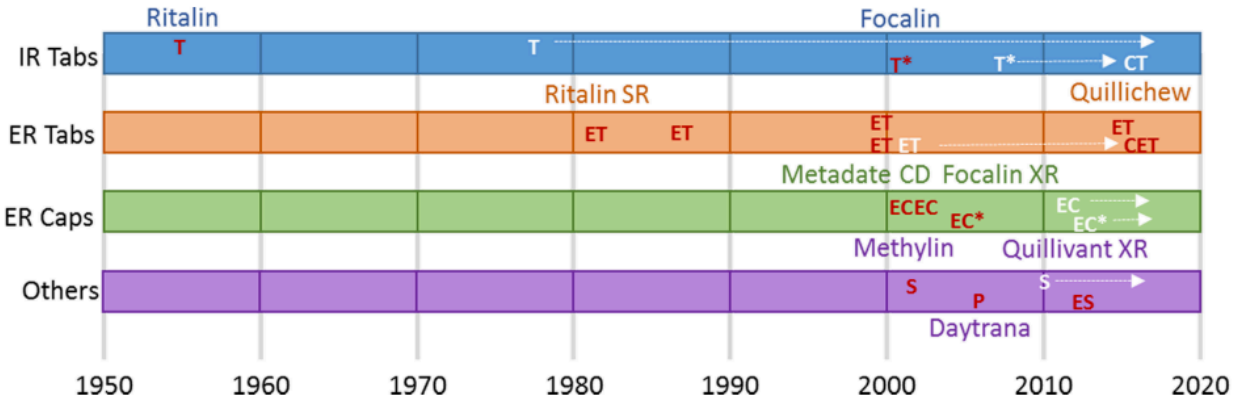

Figure 21. Timeline for FDA approval years for different MP (**70**) formulations and brand names. (T = tablets, IR = immediate release, ER = extended release, ET = extended release tablets, EC = extended release capsules, S = solutions, P = transdermal patch, ES = extended release oral suspension).[111]

1. MP (70) and its isomers

The early formulation of MP (**70**) contained all four isomers; however, a study conducted by Szporny and Görög[5] showed that only the *threo* isomer of MP had a locomotor stimulant effect. Due to this discovery, all the current FDA approved formulations of MP (**70**) contain *dl-threo* MP (*t*MP, **70**) i.e. a 50:50 mixture of *d*- and *l*-isomers of *t*MP as reported by Heal and Pierce.[109] After more than three decades, a study was conducted by Ding et al.,[112] where they evaluated both *d*- and *l-threo* isomers of MP (**70**) using positron emission tomography (PET) studies in human and baboon brains, and microdialysis studies in rats. From the PET studies it was found that after i.v. injection of [^{11}C]*d-threo*-MP and [^{11}C]*l-threo*-MP, only the *d-threo* MP showed specific binding in the basal ganglia, whereas *l-threo* MP was only responsible for nonspecific binding (Figure 22).[112]

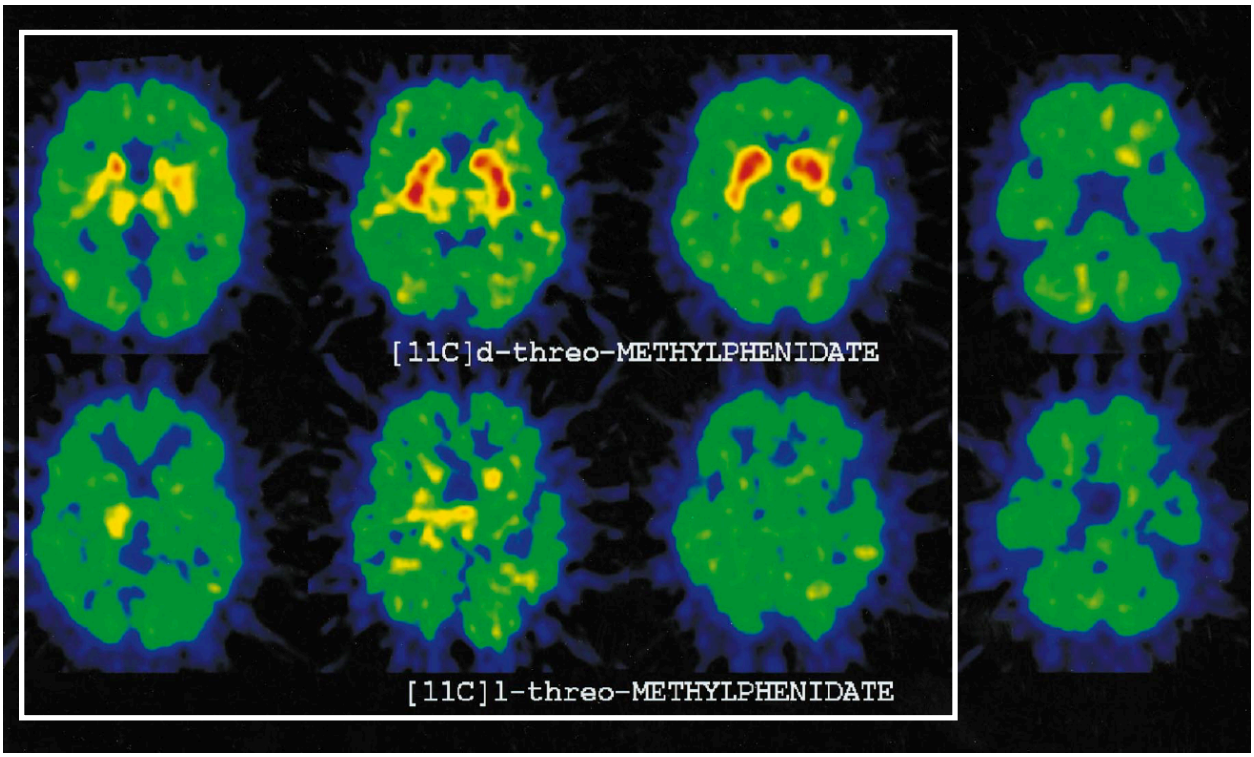

Figure 22. PET images of human brain after injection of [^{11}C]*d-threo*-MP and [^{11}C]*l-threo*-MP. Scans from the top of the brain to the base (left to right). High accumulation of radioactivity is seen in the basal ganglia (white box) only for *d-threo* MP and not for *l-threo* MP.[112]

Microdialysis studies in rats showed that *d-threo* MP (20 mg/kg) increased extracellular striatal DA concentration by 650% at 80 min, as compared to a 450% increase seen with racemic *t*MP (**70**) (20 mg/kg) and negligible increase with *l-threo* MP (20 mg/kg).[112] This study concluded that only the *d-threo* isomer of *t*MP (**70**) is responsible for its stimulant actions. This finding led to clinical development of Focalin® and Focalin XR®; it only consists of *d-threo* MP (also known as dexmethylphenidate), which has been approved by the FDA for the treatment of ADHD in children aged 6-12 years as reported by Heal and Pierce.[109]

2. Pharmacokinetics of *t*MP (70) in humans

In a study conducted by Wargin et al.,[113] in healthy human volunteers and ADHD children, it was found that MP (**70**) was rapidly absorbed and it reached its peak concentration after 2.2 h of oral administration. Other pharmacokinetic data are shown in Table 9.

Table 9. Pharmacokinetics of MP (**70**) in normal adults and ADHD children.[113]

	Dose (mg/kg)	**T_{max} (h)***	**C_{max}* (ng/mL)**	**Cl_e* (L/hr/kg)**	**K (hr^{-1})***	**$t_{1/2}$ (h)***
MP in healthy adults	0.15	2.2	3.5	10.5	0.33	2.05
	0.30	2.1	7.8	10.5	0.30	2.14
MP in ADHD children	0.30	1.5	10.8	10.2	0.28	2.43

*T_{max} = time of peak concentration, C_{max} = peak concentration, Cl_e = oral clearance, K = elimination constant, $t_{1/2}$ = half life.

In another preliminary study conducted by Srinivas et al.,[114] to evaluate the enantiomers of MP, it was found that after a dose of 40 mg of MP (**70**) the T_{max} for both the enantiomers of MP (**70**) was 2 h and the C_{max} was found to be 11.71 ng/mL for *d-threo* MP and 1.97 ng/mL for *l-threo* MP. The area under curve (AUC) calculated for both the enantiomers also indicated that *d-threo* MP (65.24 ng/mL/h) was 8-fold greater than the *l-threo* MP (7.53 ng/mL/h).[114]

3. Metabolism of MP (70) and its isomers

Faraj et al.[115] showed that in healthy human volunteers and a group of patients when 20 mg of *t*MP-^{14}C was administered orally, peak plasma levels of ^{14}C were seen after 2 h and $t_{1/2}$ ranged from 2 to 7 h. From the urinary excretion pattern of ^{14}C it was found that *t*MP (**70**) had complete absorption. The major metabolite of MP (**70**), was found to be ritalinic acid (RA, **71**, Figure 23). About 80% of the urinary ^{14}C consisted of RA (**71**) and other metabolites only accounted for 1.5-2.5%.[115] Figure 23 shows the metabolites of MP.

The metabolism of MP (**70**) was found to be enantiospecific upon intravenous administration. There was a gradual shift seen in the enantiomeric ratio of *d:l* over time and a significant difference between the plasma concentration of *d*- and *l-threo* MP (**70**) is seen as reported by Heal and Price.[109] In a urinary excretion profile for the *t*MP (**70**), *d-threo* MP (**70**) was found to be in 10-fold higher levels than *l-threo* MP (**70**) and the urine had 2- to 3-fold higher levels of *d-threo* RA than *l-threo* RA.[116] These studies suggested that *t*MP (**70**) enantiospecific 'first-pass' metabolism rather than enantiospecific excretion.[116]

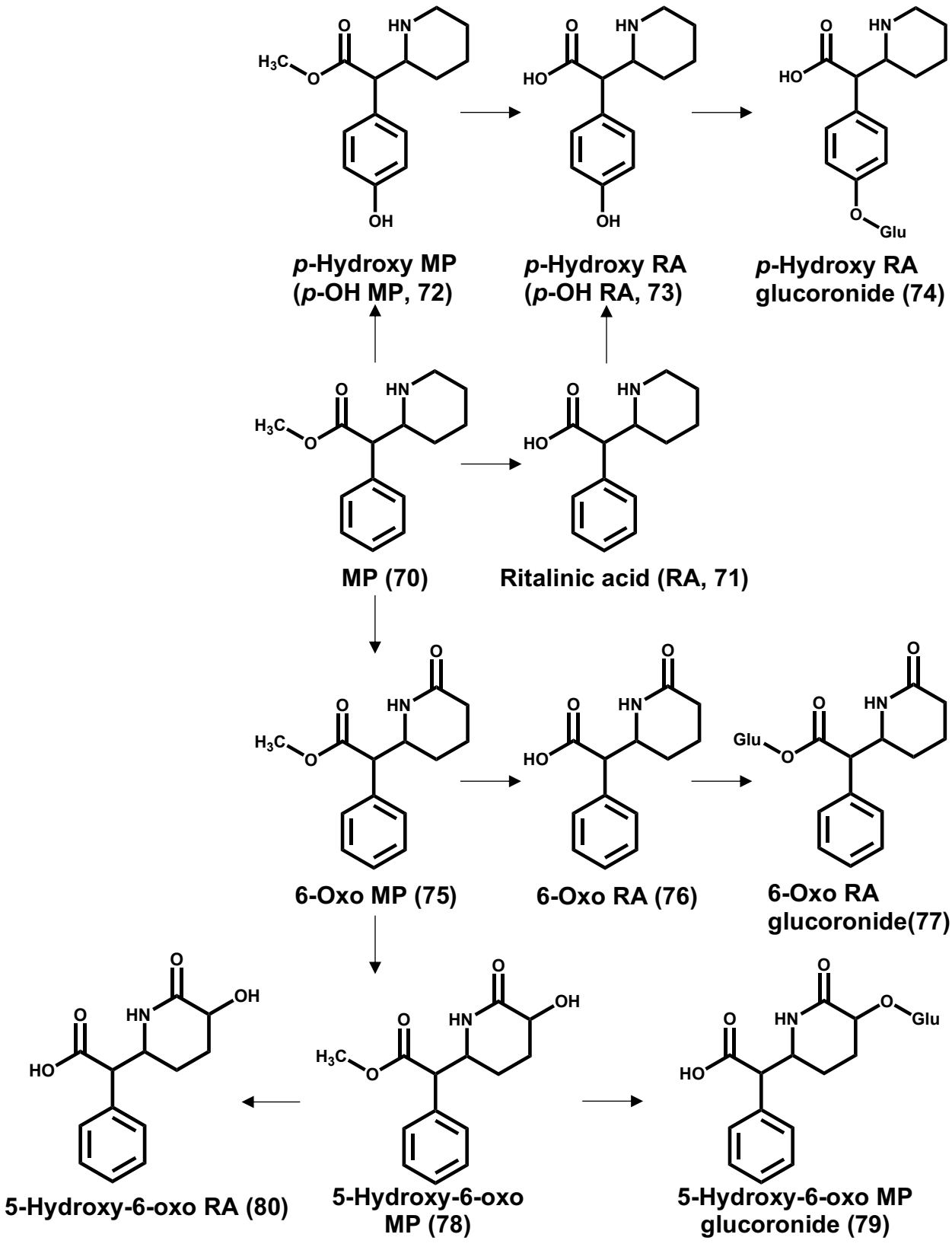

Figure 23. Major metabolic pathway of *dl-t*MP (**70**).[109]

The metabolites were tested for their locomotor activity in mice, and it was found that on i.p. administration *p*-OH MP(**72**, Figure 23) was inactive up to a 100 mg/kg dose.[115] Oxo-MP (**75**, Figure 23) was found to be a locomotor stimulant at a dose of 100 mg/kg and its activity was only 10% that of MP (**70**) at the same dose.[115] In another study conducted by Patrick et al.[117] the metabolites of *threo* and *erythro*-MP (**70**) were synthesized and tested for their locomotor activity by intracerebroventricular administration in rats. It was found that *t*MP (**70**) had a significantly greater maximal effect than the eMP (**70**).[117] Furthermore, *p*-OH *t*MP (**72**) was found to produce significantly greater locomotor activity than the corresponding *p*-OH eMP and also *t*MP (**70**).[117] Both the isomers of RA (**71**) and *p*-OH RA (**73**, Figure 23) produced locomotor activity, however their effect was considerably less than that for *t*MP (**70**).[117]

Metabolism of MP (**70**) primarily occurs through deesterification by carboxyesterase 1A1 (CES1A1) and not by CES2 or CES3. Sun et al.[118] showed that CES1A1 has high catalytic efficiency both for *d*- and *l*-*t*MP (**70**). However, the catalytic efficiency for *l*-*t*MP (k_{cat}/k_m = 7.7 $mM^{-1}min^{-1}$) was found to be greater than that for *d*-*t*MP (k_{cat}/k_m = 1.3-2.1 $mM^{-1}min^{-1}$).[118] This decrease in the catalytic efficiency of CES1A1 for *d*-*t*MP (**70**) may also contribute to higher potency of *d*-*t*MP (**70**) as compared to *l*-*t*MP (**70**) in vivo.[118]

4. Pharmacology of MP (70) and its isomers

a. In vitro neurochemistry

In a rat brain homogenate study conducted by Anderson,[119] *t*MP (**70**) was found to be a potent inhibitor of DAT (IC_{50} = 281 nM) and NET (IC_{50} 103 nM). *t*MP (**70**) showed less than 10% inhibition of 5-HT at 30 μM.[119] In another study, *d-threo* MP (**70**) and *l-threo* MP (**70**) were tested for inhibiting 0.1 μM [^{3}H]DA and [^{3}H]NE uptake in synaptosomal preparations of rat hypothalamus and striatum.[120] *d-threo* MP (**70**) was found to be 10-fold more potent as an inhibitor both of [^{3}H]DA and [^{3}H]NE than *l-threo* MP (**70**).[120] In the same study, *t*MP (**70**) and both of its isomers were also evaluated for the release of catecholamines from synaptosomal preparations of rat hypothalamus and striatum, and neither racemic MP (**70**) nor its isomers produced any release of NE and produced only modest release of DA which was not statistically significant when compared with AMPH which was used as positive control.[120] These studies suggested that MP (**70**) and its isomers act as DAT and NET reuptake inhibitors and not as releasers.

b. In vivo neurochemistry

In vivo microdialysis experiments were conducted to access extracellular levels of DA and 5-HT in rat caudate putamen and NE in hippocampus due to *t*MP (**70**) (10, 20, and 30 mg/kg), and compared it to the effect produced by AMPH (2.5 mg/kg).[121] Similar to AMPH, *t*MP (**70**) increased DA in the caudate putamen in a dose-dependent manner, although, 20 mg/kg of *t*MP (**70**) was required to produce similar responses to 2.5 mg/kg AMPH.[121] *t*MP (**70**) also increased NE levels in the hippocampus; however, none of the concentrations of *t*MP altered extracellular 5-HT.[121] This study also showed that *t*MP (**70**)

enhanced NE efflux for a longer period of time as compared to DA and, at higher doses, a ceiling effect was observed with NE but not with DA. This concluded that *t*MP (**70**) shifts to a dopaminergic profile at higher doses.[121]

5. Structure-activity relationship studies on MP (70)

Many investigators have focused on the SAR of MP (**70**) as reported by Wenthur.[111] Various analogs have been synthesized with phenyl-ring substituents, changes in the terminal amine, changes in the piperidine ring, and with modifications of the ester group.

a. Phenyl ring substituents

An investigation conducted by Pan et al.[122] in 1994 focused on the role of bromine substitution at the 2-, 3-, and 4-position of the phenyl ring of *t*MP (**70**). In an in vitro binding assay using rat brain membranes, all the three bromo-substituted analogs were found to inhibit the binding of [^{3}H]WIN 35,428 (a selective DAT ligand) and [^{3}H]nisoxetine (a selective NET ligand) with the rank order of potency: 3-bromo *t*MP (**86**) > 4-bromo *t*MP (**93**) > 2-bromo *t*MP (**81**) > *t*MP (6-, 20-, 9-fold more potent than *t*MP, respectively).[122] However, all three analogs and *t*MP (**70**) were found to be weak inhibitors of [^{3}H]paroxetine (a selective SERT ligand).[122] Extracellular dopamine levels in the striatum of conscious rats increased by a factor of 4 after 20 mg/kg of 4-bromo *t*MP (**93**) was administered i.p. The mean increase in DA levels for 3-bromo *t*MP (**86**) was about half that compared to 4-bromo *t*MP (**70**) and an intermediate increase was seen for 2-bromo *t*MP(**81**).[122] In follow-up studies conducted by Pan et al. where the 2-, 3-, and 4-bromo-substituted *t*MP analogs were resynthesized and retested, 2-bromo *t*MP (**81**) was found

to be 20-fold less potent than *t*MP (**70**) in inhibiting [^{3}H]WIN 35,428 as reported by Deutsch et al.[9]

A series of 2-, 3-, and 4-substituted *t*MP (**70**) analogs and five eMP (**70**) analogs (Table 10) were evaluated in [^{3}H]WIN 35,428 binding and [^{3}H]DA uptake assays.[9] All the eMP analogs were found to be less potent than their corresponding *t*MP analogs. In terms of *t*MP analogs, all the 2-substituted analogs were found to be less potent than their corresponding 3- or 4-substituted analogs, with methoxy having the largest loss in activity (ratio of IC_{50} for positions 2/4 = 1200), followed by bromo (270), chloro (95) and fluoro (41).[9] Based on the X-ray crystal structures of 4-Cl *t*MP (**95**) and 2-OCH_3 *t*MP (**85**) (Figure 24) it was concluded that, substituents at the 2-position do not induce a large conformational change in the molecule and that the loss in the potency of the 2-substituted analogs was due to a direct steric interaction with the receptor and not because of a conformational change of the ligand itself.[9]

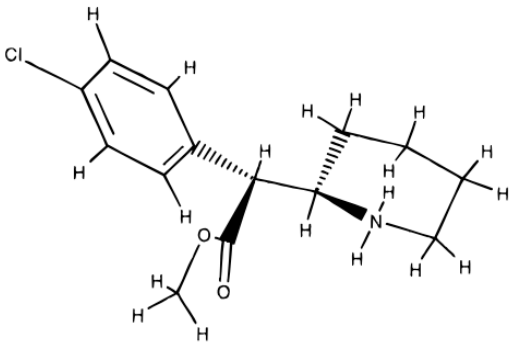

4-Cl *t*MP (95)

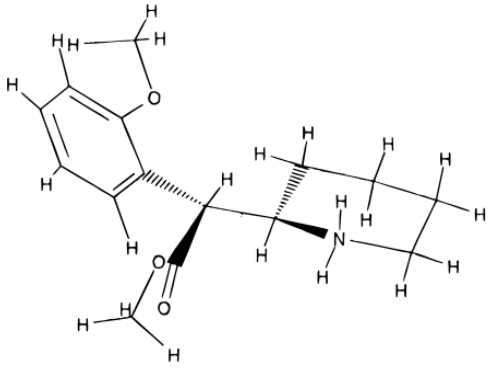

2-OCH_3 *t*MP (85)

Figure 24. X-ray structures of 4-Cl *t*MP (**95**) and 2-OCH_3 *t*MP (**85**) hydrochloride.[9]

Having an electron-withdrawing group (EWG) at the 3- or 4-position of the phenyl ring increased binding potency; on the other hand, electron-donating groups (EDG) were found to be less potent than *t*MP (**70**).[9] A significant difference was seen in the potencies of 3- and 4-substituted analogs. For groups such as -F, -Cl, -Br and -CH_3, both 3- and 4-substituted analogs were more potent than *t*MP (**70**).[9] Larger groups, such as 4-NO_2 (**100**) and 4-tBu *t*MP (**94**), were found to be significantly less potent than *t*MP (**70**).[9] Two 3,4-disubstituted analogs (3,4-diCl and 3,4-diOCH_3) were evaluated and 3,4-diCl *t*MP (**102**) was found to be equipotent to 3-Cl *t*MP (**87**), whereas 3,4-diOCH_3 *t*MP (**103**) was 3-fold less potent than 3-OCH_3 *t*MP (**92**).[9] Table 10 below shows the IC_{50} values of all the analogs in inhibition of [^{3}H]WIN 35,428 binding and [^{3}H]DA uptake assay.[9]

Table 10. Inhibition of [^{3}H]WIN 35,428 binding and [^{3}H]DA uptake of *t*MP, eMP and phenyl ring-substituted analogs.[9,119]

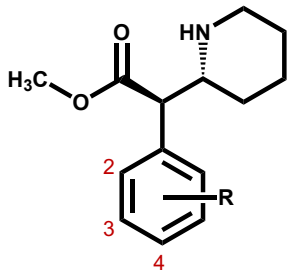

***t*MP (70)**

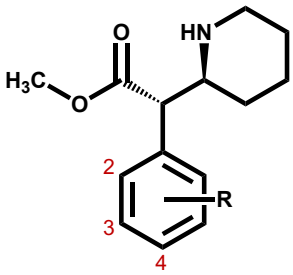

eMP (70)

-R	**[^{3}H]WIN 35,428 binding (IC_{50}, nM)**	**[^{3}H]DA uptake (IC_{50}, nM)**
	***t*MP analogs (70)**	
*t*MP (**70**)	83	224
2-Br (**81**)	1870	3410
2-Cl (**82**)	1950	2660
2-F (**83**)	1420	2900
2-OH (**84**)	23100	35800
2-OCH_3 (**85**)	101000	81000
3-Br (**86**)	4	13
3-Cl (**87**)	5	23
3-F (**88**)	41	160
3-CH_3 (**89**)	21	100
3-NH_2.HCl (**90**)	265	578
3-OH (**91**)	321	790
3-OCH_3 (**92**)	288	635
4-Br (**93**)	7	26

-R	[^{3}H]WIN 35,428 binding (IC_{50}, nM)	[^{3}H]DA uptake (IC_{50}, nM)
4-*t*-Bu (**94**)	13500	9350
4-Cl (**95**)	21	74
4-F (**96**)	35	142
4-I (**97**)	14	65
4-CH_3 (**98**)	33	126
4-NH_2.HCl (**99**)	35	115
4-NO_2 (**100**)	494	1610
4-OH (**72**)	98	340
4-OCH_3 (**101**)	83	293
3,4-diCl (**102**)	5	7
3,4-diOCH_3 (**103**)	810	1760
3,5-diCH_3 (**104**)	4690	-
3,5-diCl (**105**)	67	-
3,4-benzo (**106**)	11	-
	eMP analogs (70)	
2-Br (**107**)	38100	59000
2-Cl (**108**)	52500	61000
3-Cl (**109**)	378	1540
2-OCH_3 (**110**)	139000	290000
4-*t*Bu (**111**)	41300	52500

In a more recent study conducted by Misra et al.[8] three additional disubstituted analog were evaluated for their DAT binding affinities. 3,5-diCH_3 *t*MP (**104**) was found to be approximately 60-fold less potent than its parent, *t*MP (**70**), whereas 3,5-diCl (**105**) and 3,4-benzo *t*MP (beta naphthyl analog, **106**) were found to be 1.3 and 8-fold more potent than *t*MP (**70**).[8]

b. Modifications at the ester group

In an early study conducted by Portoghese and Malspeis,[123] the methyl group of the ester was replaced by other alkyl groups and cyclic substituents (Table 11) and examined for their central stimulant action relative to *t*MP (**70**). Out of the twelve substituents tested, only the ethyl ester (i.e., **112**) retained substantial activity (i.e., 80% of the stimulant activity relative to *t*MP); all other analogs showed reduced effects.[123]

Table 11. Central stimulant actions of methylphenidate analogs with varying ester groups relative to *t*MP (**70**).[123]

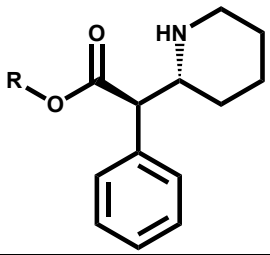

-R	Central stimulant activity relative to 70
Methyl (*t*MP, **70**)	1.00
Ethyl (**112**)	0.80
n-Pr (**113**)	0.20
i-Pr (**114**)	0.33
n-Bu (**115**)	0.13
i-Bu (**116**)	0.10
sec-Bu (**117**)	0.20
n-Pentyl (**118**)	<0.10
Cyclopentyl (**119**)	<0.10
Cyclohexyl (**120**)	<0.10
Benzyl (**121**)	<0.10
2-Methoxyethyl (**122**)	0.20
2-Chloroethyl (**123**)	0.13

An analog where the methyl ester group of MP (**70**) was replaced with a phenyl ring (i.e., deoxypipradrol, **124**) was evaluated for the uptake of DA and NE in rat synaptosomes by

Ferris et al.[124] *R*(-)Deoxypipradrol (**124**, Figure 25) (IC_{50} = 0.35 μM) was found to be 10-fold more potent than *S*(+)deoxypipradrol (**124**) (IC_{50} = 4 μM) in releasing NE from rat brain tissue.[124] *R*(-)Deoxypipradrol (**124**) was 27- and 15-fold more potent than *S*(+)deoxypipradrol (**124**) and *d-threo* (2*R*,2'*R*) *t*MP (**70**), respectively, in inhibiting DA reuptake and 15-fold more potent than both *S*(+)deoxypipradrol (**124**) and *d-threo* (2*R*, 2'*R*) *t*MP (**70**) in inhibiting NE reuptake in rat brain slices.[124]

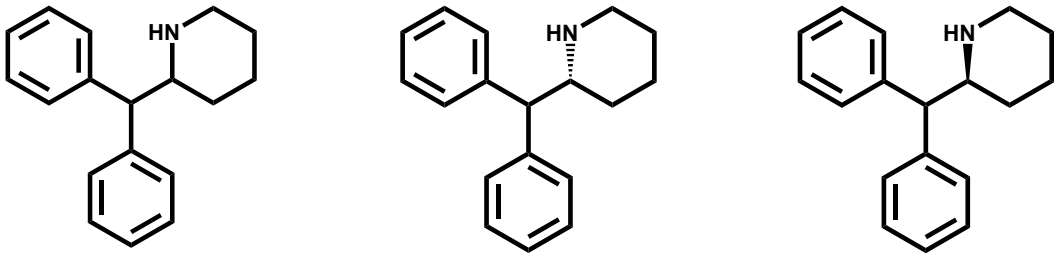

Racemic deoxypipradrol (**124**) | *R*(-)deoxypipradrol (*R*-**124**) | *S*(+)deoxypipradrol (*S*-**124**)

Figure 25. Structures of racemic deoxypipradrol (**124**) and its optical isomers.

Misra at el.[8] evaluated a few other analogs where they replaced the methyl ester of *t*MP (**70**) with different functional groups and examined their binding affinity at DAT (Table 12). All the compounds displayed reduced affinity for DAT except for an ether analog (i.e., **126**), which was found to be nearly equipotent to *t*MP (**70**).[8] Complete removal of the ester of *t*MP (i.e., 2-benzylpiperidine, **130**) reduced the binding affinity at DAT by 85-fold (IC_{50} = 6360 nM) and reduced [^{3}H]DA reuptake potency by 38-fold (IC_{50} = 8800 nM) as compared to *t*MP (**70**) (IC_{50} =75 and 230 nM, binding affinity and [^{3}H]DA uptake, respectively).[125] Although Kim et al.[125] showed the correct structure of **130**, their methods section showed the synthesis of 2-phenylpiperidine. Furthermore, their melting point was not consistent with that mentioned in the literature.[126,127] See later discussion of **169**.

Table 12. DAT binding affinity of *t*MP analogs with ester group modifications of *t*MP (**70**).[8,125]

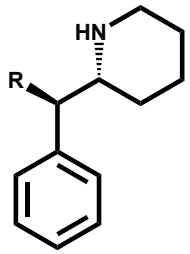

125-130

-R	**[^{3}H]WIN 35,428 binding (IC_{50}, nM)**
-CO_2CH_3 (*t*MP, **70**)	83
-CH_2OH (**125**)	448
-CH_2OCH_3 (**126**)	97
-CO_2CH_2Ph (**127**)	1020
-$CH_2O(CO)CH_3$ (**128**)	690
-CO_2NH_2 (**129**)	1730
-H (**130**)[125]	6360

c. Substitution at the piperidinyl amine

Misra et al.[8] evaluated different aliphatic and aromatic substituents at the piperidinyl nitrogen in DAT binding assay. Converting the secondary amine of the piperidine ring to the simplest tertiary amine by replacing -H with -CH_3 (i.e., **131**) reduced the DAT binding affinity by 6-fold. All the nitrogen-substituted analogs and their DAT binding affinities are shown in Table 13.

Table 13. DAT binding affinity of *t*MP analogs with different piperidine nitrogen substituents.[8]

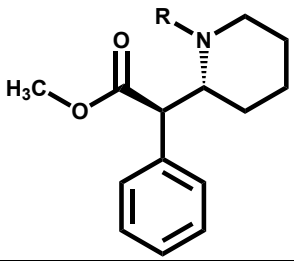

-R	[^{3}H]WIN 35,428 binding (IC_{50}, nM)
-H (*t*MP, **70**)	83
-CH_3 (**131**)	499
-CH_2CHCH_2 (**132**)	597
-CH_2CCH (**133**)	821
-CH_2Ph (**134**)	53
-$(CH_2)_2Ph$ (**135**)	678
-$(CH_2)_3Ph$ (**136**)	267
-$(CH_2)_4Ph$ (**137**)	205
-$(CH_2)_5Ph$ (**138**)	1570
-$(CH_2)_6Ph$ (**139**)	656
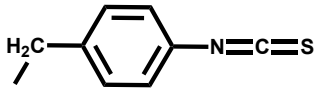 (**140**)	422
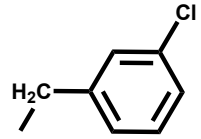 (**141**)	106
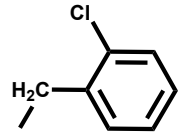 (**142**)	243

-R		[^{3}H]WIN 35,428 binding (IC_{50}, nM)
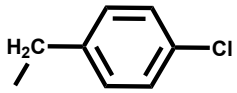	(**143**)	31
	(**144**)	113
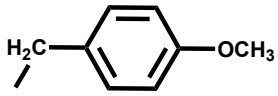	(**145**)	79
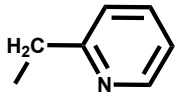	(**146**)	369
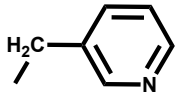	(**147**)	173
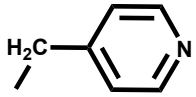	(**148**)	128
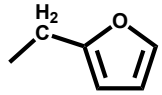	(**149**)	536
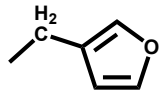	(**150**)	459
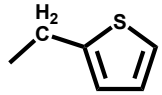	(**151**)	224
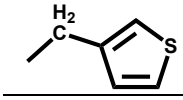	(**152**)	143

From the above data it was concluded that substituents at the piperidinyl nitrogen atom decrease DAT binding affinity.[8] The loss in the potency ranged from 1.3- to 19-fold compared to *t*MP (**70**), except for analogs containing a benzyl ring i.e. **134**, **143**, and **145**.[8] Having more than one methylene group between the piperidinyl nitrogen atom (i.e., **135**-**139**) decreased binding affinity. Moreover, only 4-Cl substitution on the phenyl ring (i.e., **143**) led to a 3-fold increase in binding affinity compared to *t*MP (**70**).[8]

d. Piperidine ring modifications

Analogs with changes in the piperidine ring were synthesized and evaluated in DAT binding and DAT reuptake assays by Deutsch et al.[128] Analogs with smaller (five-membered) and larger (seven- and eight-membered) ring systems were synthesized (Table 14). Five- (i.e., **156**), seven- (i.e., **157**), and eight-membered ring (i.e., **158**) analogs were found to be less potent than *t*MP (six-membered ring, **70**) by a factor of 4, 2, and 8, respectively in DAT binding assays.[128] When the piperidine ring was replaced by a morpholine ring (i.e., **159**), the binding potency was reduced by 15-fold as compared to *t*MP (**70**).[128] Supporting the binding data, all the analogs synthesized in this study were found to be less potent than *t*MP (**70**) in a DA reuptake assay.[128]

Table 14. DAT binding and [^{3}DA] uptake data of *t*MP analogs with modifications of the piperidine ring.[128]

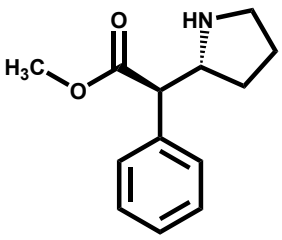

156

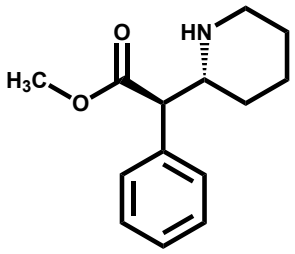

***t*MP (70)**

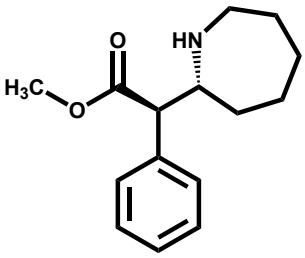

157

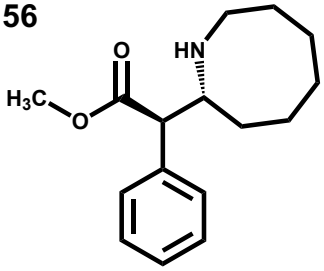

158

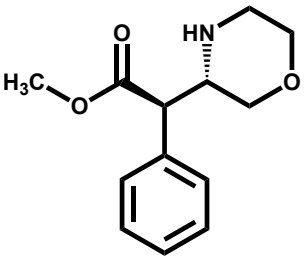

159

Ring modification	[^{3}H]WIN 35,428 binding (IC_{50}, nM)	[^{3}H]DA uptake (IC_{50}, nM)
*t*MP (**70**)	83	224
5-membered (**156**)	355	885
7-membered (**157**)	197	701
8-membered (**158**)	623	1590
Morpholine (**159**)	1250	9930

6. Crystal structure of *t*MP (70)

Due to the presence of single bonds in the MP (**70**) structure, it is conformationally flexible and it was important to determine which conformation was responsible for its biological activity.[129] The X-ray crystallographic structure of the HCl salt of *l-threo* (2*S,2*'*S*) *t*MP (**70**) was successfully obtained by Froimowitz et al.[129] and with the help of conformational analysis obtained for both enantiomers of *t*MP and *r*MP it was concluded that the (2*R,2*'*R*) configuration of *t*MP (**70**) is the active enantiomer. The conformational analysis of the *t*MP (**70**) isomer indicated that the carbonyl oxygen of the ester is in close proximity to the piperidinyl nitrogen atom and forms an intramolecular hydrogen bond, which helps stabilize the *t*MP conformation.[129] The only difference between both enantiomers of *t*MP (**70**) was a slightly different orientation of the ester group.[129] Figure 26 shows the global minimum of *t*MP (**70**), eMP (**70**) and the crystal structure of the inactive enantiomer *l-threo* (2*S*, 2'*S*) *t*MP HCl.[129] In another study, Froimowitz et al.[130] obtained crystal structures of five analogs of *t*MP (**70**), and all the five structures had similar 3D conformations when compared to the global minimum obtained for *d-threo* (2*R*, 2*R*') *t*MP.

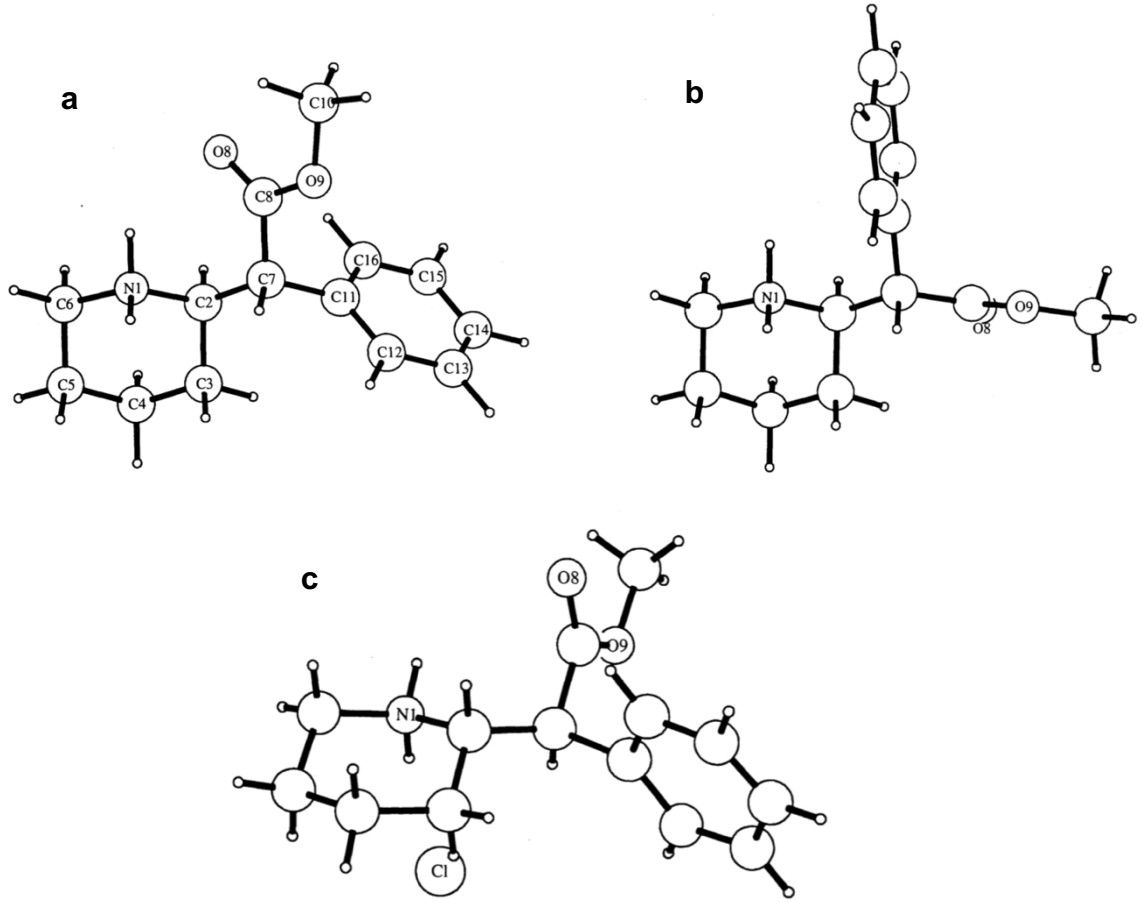

Figure 26. Global minimum of *t*MP (**a**) and eMP (**b**) and the crystal structure of *l-threo* (2*S*, 2'*S*) *t*MP (**c**).[129]

III. Specific aims

Synthetic cathinones are a novel class of drugs of abuse that have drawn considerable attention worldwide over the last decade. They are chemically related to cathinone (**1**), which is a naturally occurring stimulant obtained from the plant *Catha edulis*.[3] Although the plant might have been characterized in the 19th century, the earliest recorded use of it dates back to the 1300s.[28] Since then >150 analogs of synthetic cathinones have appeared on the clandestine market and their number is growing every year.[2] Early cathinones were known to act as substrates at the monoamine transporters (DAT, NET, and SERT); however, newer synthetic cathinones have diverse mechanism(s) of action.[2] In 2010 Iverson[80] reported a popular drug combination called 'bath salts' which mainly consisted of MDMC (**27**), MEPH (**28**) and MDPV (**29**). MDPV was the first synthetic cathinone found to act as a DAT reuptake inhibitor similar to cocaine (**4**).[86] Due to this varying pharmacology and mechanisms of action of synthetic cathinones, it is important to study them on a case-by-case basis but this will be time consuming and expensive.

*t*MP (**70**) is another recognized CNS stimulant and has a mechanism of action similar to cocaine.[109] The SAR of *t*MP (**70**) as a DAT blocker has been extensively studied by a number of groups over the years.[111] There is structural similarity between *t*MP (**70**) and

certain synthetic cathinones (i.e., **160** where R' is an extended alkyl group such as *n*-propyl).

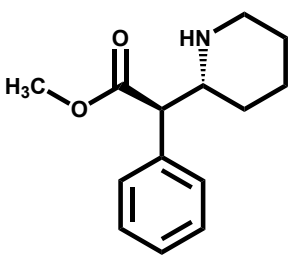

***t*MP (70)**

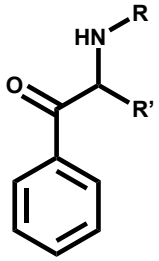

160

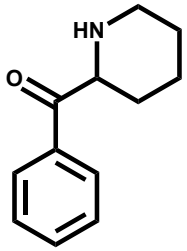

161

Compound **161** is a conformationally-constrained analog of **160**, and might be considered a hybrid of MP (**70**) and α-PVP. Compound **161** was previously prepared in our laboratory and found (at a single concentration of 10 μM) that it behaved as a DAT reuptake inhibitor. This prompted the present investigation.

Aim 1. To conduct molecular modeling/docking studies with *t*MP (70) and hybrid analog 161 to determine how they might bind at DAT

Approach:

- Generate homology models of hDAT from a dDAT crystal structure
- Dock *t*MP (**70**) and hybrid analog **161** and study their interactions to determine their binding modes
- Conduct Hydrophobic INTeraction (HINT) studies on *t*MP (**70**) and analog **161**

Aim 2. To prepare and examine a series of hybrid analogs (2-benzoylpiperidines) and examine their actions at DAT

Approach:

- Synthesize a series of hybrid analogs (benzoylpiperidines); specifically, the following compounds will be prepared:

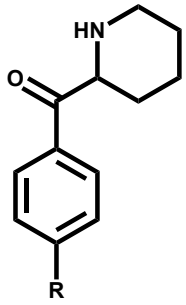

R = -H, **161**
R = -CH_3, **162**
R = -C_2H_5, **163**
R = -Cl, **164**
R = -Br, **165**
R = -OCH_3, **166**
R = -CF_3, **167**

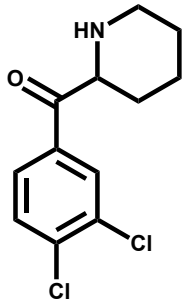

168

These particular substituents were selected because of the difference in their physicochemical properties (that could be useful if QSAR studies were to be subsequently conducted), and they were studied for their DAT reuptake potency in the *t*MP series[8,9] and displayed a range of potency.

- Determine functional activity of these hybrid analogs at hDAT by live-cell imaging

Aim 3. To determine the necessity of the carbonyl oxygen atom of 161 for DAT reuptake inhibition

Approach:

- Synthesize the descarbonyl analog, **169**, of the hybrid parent **161**

  (Analog **169** should not be confused with **130**; analog **130** had the correct structure in Ref. 125 however the experimental section showed the synthesis of 2-phenylpiperidine; therefore, to avoid confusion, we are using a different identification number. That is, **169** ≠ **130**).

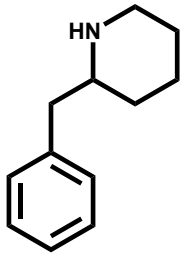

169

- Conduct docking studies on descarbonyl analog **169** at hDAT homology models to determine if it has a binding pose similar to **161**
- Determine the functional activity of the descarbonyl analog **169** at hDAT by live-cell imaging

IV. Results and discussion

Aim 1. To conduct molecular modeling/docking studies with *t*MP (70) and hybrid analog 161 to determine how they bind at DAT

A. hDAT homology modeling studies

Knowing that *t*MP (**70**) is a reuptake inhibitor of DAT[119] we investigated the interactions of *t*MP (**70**) with DAT on a molecular level. Analog **161** was previously tested in our laboratory at a single concentration of 10 μM and was found to be a DAT reuptake inhibitor.[131] It was of interest to investigate if *t*MP (**70**) and hybrid analog **161** have any common interactions at DAT by conducting molecular modeling studies. DAT belongs to the SLC6 family of transporters and the crystal structure of hDAT is not available; therefore, we utilized the crystal structure of the *Drosophila melanogaster* dopamine transporter (dDAT) co-crystallized with cocaine (**4**) (PDB ID: 4XP4) as our template.[132] We generated one hundred homology models using MODELLER 9.10 and compared it with the crystal structure of dDAT using SybylX 2.1.1 and determined that they had a root mean square deviation (RMSD) of 0.183 Å. Figure 27 shows overlapping structures of (**a**) the dDAT crystal structure (light pink) and the homology model (blue-white) and (**b**) a close-up view of the binding pocket. The amino acid residues for our homology model are labeled in parenthesis. Almost all the residues in the binding pocket seem to overlap.

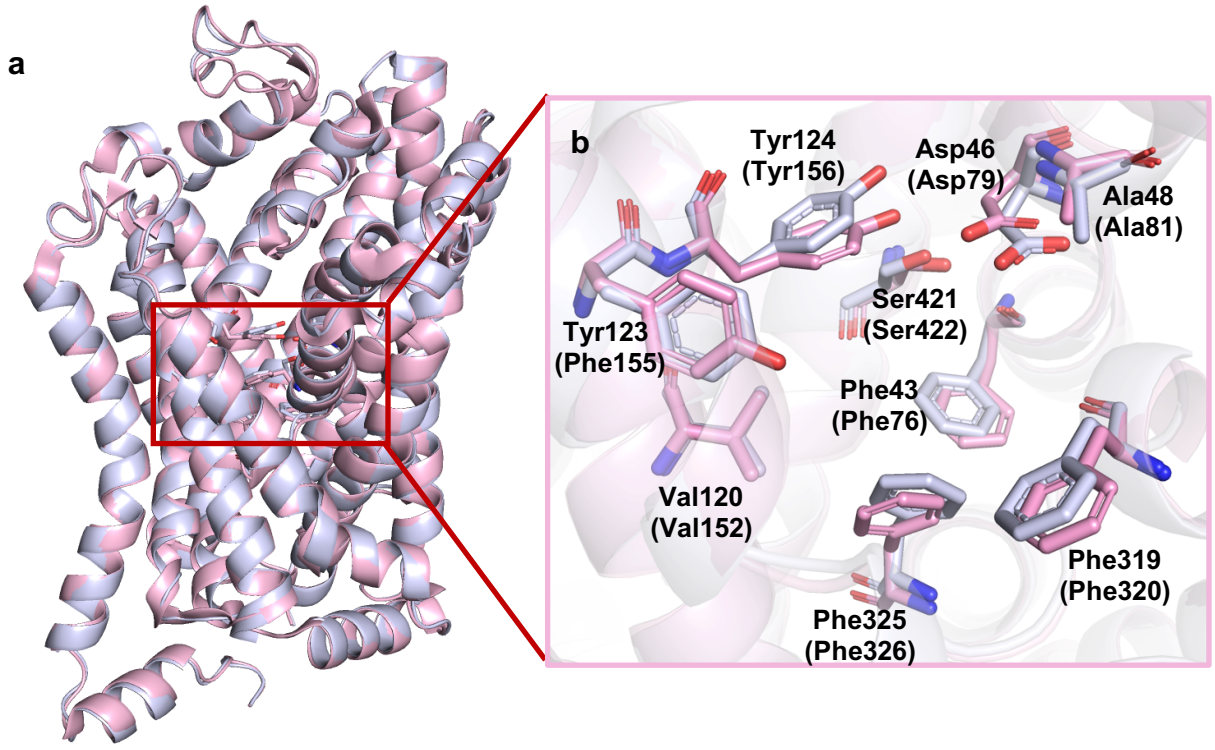

Figure 27. (**a**) Overlapping structures of the dDAT crystal structure (light pink) (PDB ID: 4XP4, 2.8-Å resolution) and a homology model of hDAT (blue-white) (**b**) a close-up of the binding pocket with the residues of the crystal structure (light pink colored capped sticks) and the homology model (blue-white colored capped sticks). The residues of our model are in parenthesis.

B. Construction and alignment of hDAT models

The sequence of the dDAT structure was obtained as a FASTA file from the Protein Databank (PDB ID: 4XP4) and the sequence for the hDAT was obtained from the Universal Protein Resource (UniProt) database using the accession code Q01959. Both, the dDAT and hDAT sequences were aligned using Clustal W 2.0[133] (Figure 28). Due to a lack of corresponding residues, the first 57 residues of the N-terminus, the last 20 residues of the C-terminus, and 12 residues of extracellular loop 2 were not modelled. The two sodium ions and a chloride ion were modelled in the binding site since they might

affect the overall structure of the transporter.

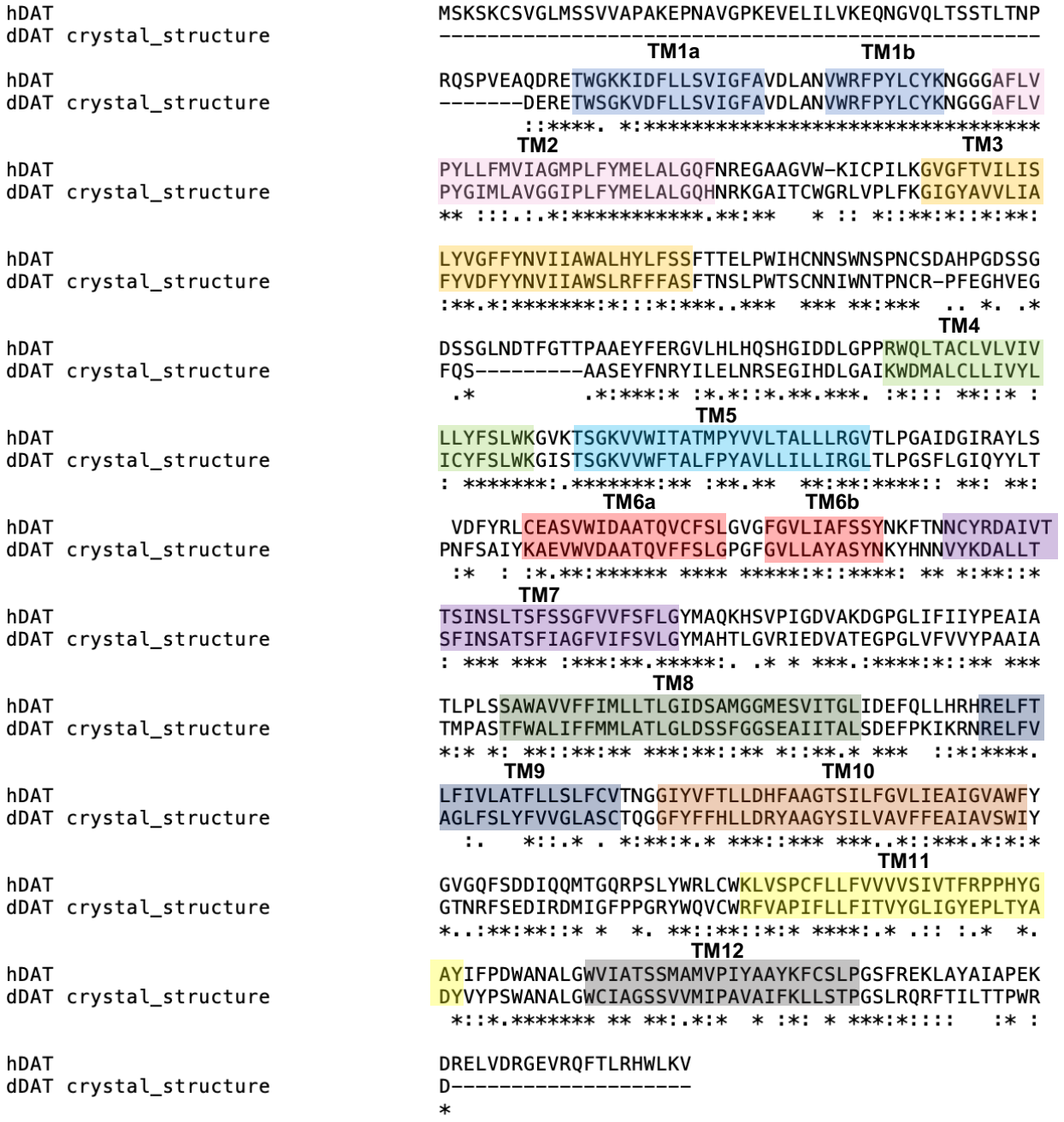

Figure 28. Clustal W 2.0-based sequence alignment of the dDAT crystal structure (PDB ID: 4XP4) and hDAT (UniProt accession code Q01959). The highlighted boxes represent transmembrane (TM) helices. Symbols below each sequence indicate the degree of amino acid conservation: '*' for fully conserved residue, ':' for strong conservation, '.' for weak conservation, and no symbol indicates non-conserved residues.

C. Validation

In order to support our studies, we docked cocaine (**4**) to one hundred homology models generated for hDAT and validated the interactions we obtained with the interactions observed in the dDAT crystal structure co-crystallized with cocaine. The aspartate residue (Asp79) was used to define a 10-Å binding pocket using the docking software GOLD suite 5.6.1.[134] In our model, cocaine was found to have a hydrogen bond between the tropane nitrogen atom and Asp79 residue (Figure 29a) similar to that of the crystal structure.[132] There was also an edge-to-face interaction with the benzyl ring of cocaine and Phe326 (Figure 29b).

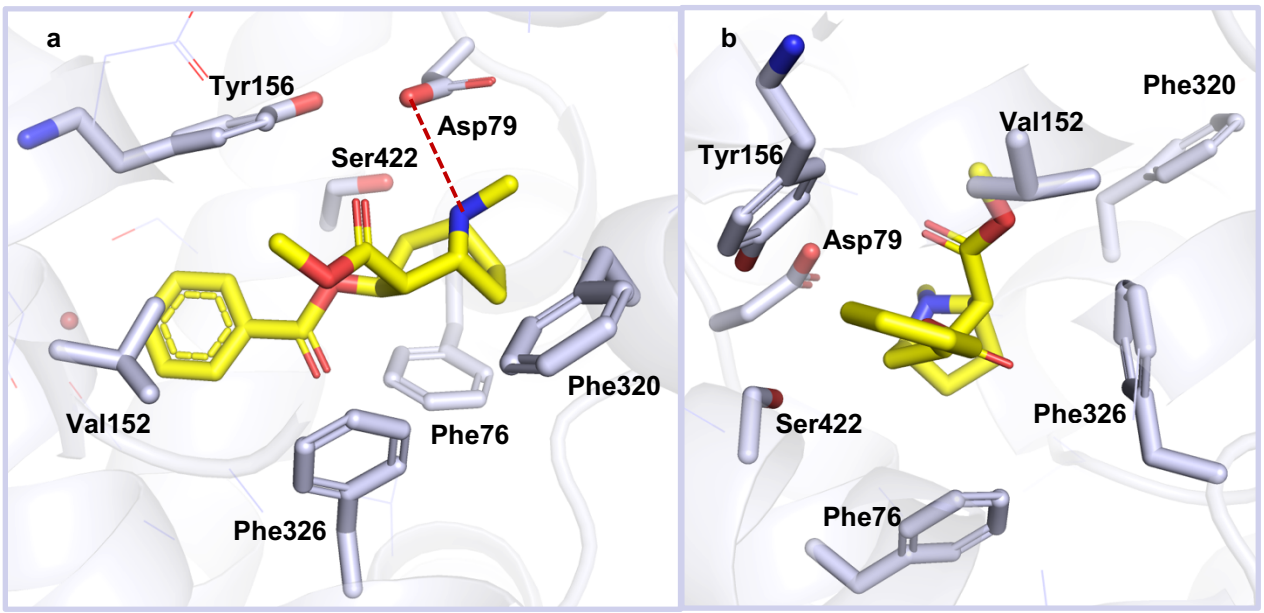

Figure 29. a. Structure of cocaine (yellow) docked in the binding site of our hDAT model. The red broken line shows the hydrogen bond between the nitrogen atom of cocaine and Asp79. **b.** A side-view of the binding site showing an edge-to-face interaction between the phenyl ring of cocaine and Phe326.

A Ramachandran plot of a hDAT model, having the highest GOLD score, was obtained using PROCHECK analysis (Figure 30). The Ramachandran plot uses torsion angles to describe protein conformation, and the amino acids are divided into two large regions representing α-helices and β-sheets, and a smaller region representing the backbone conformation.[135,136] The colors in the plot show if the region is favored or not, e.g. most favored (red), additionally allowed region (yellow), generously allowed region (light yellow), and disallowed region (white). For our hDAT model 96.7% of the amino acids were in the most favored region, and 3.3% in the additionally allowed region. Three glycine residues (Gly258, Gly500, and Gly585) were found in the disallowed region; however, they were not near the binding pocked of our hDAT model. Gly258 and Gly500 were found in the extracellular loop, whereas Gly585 was found in the C-terminus; therefore, they would have no effect on our docking studies. We carried out our docking studies using these validated hDAT models.

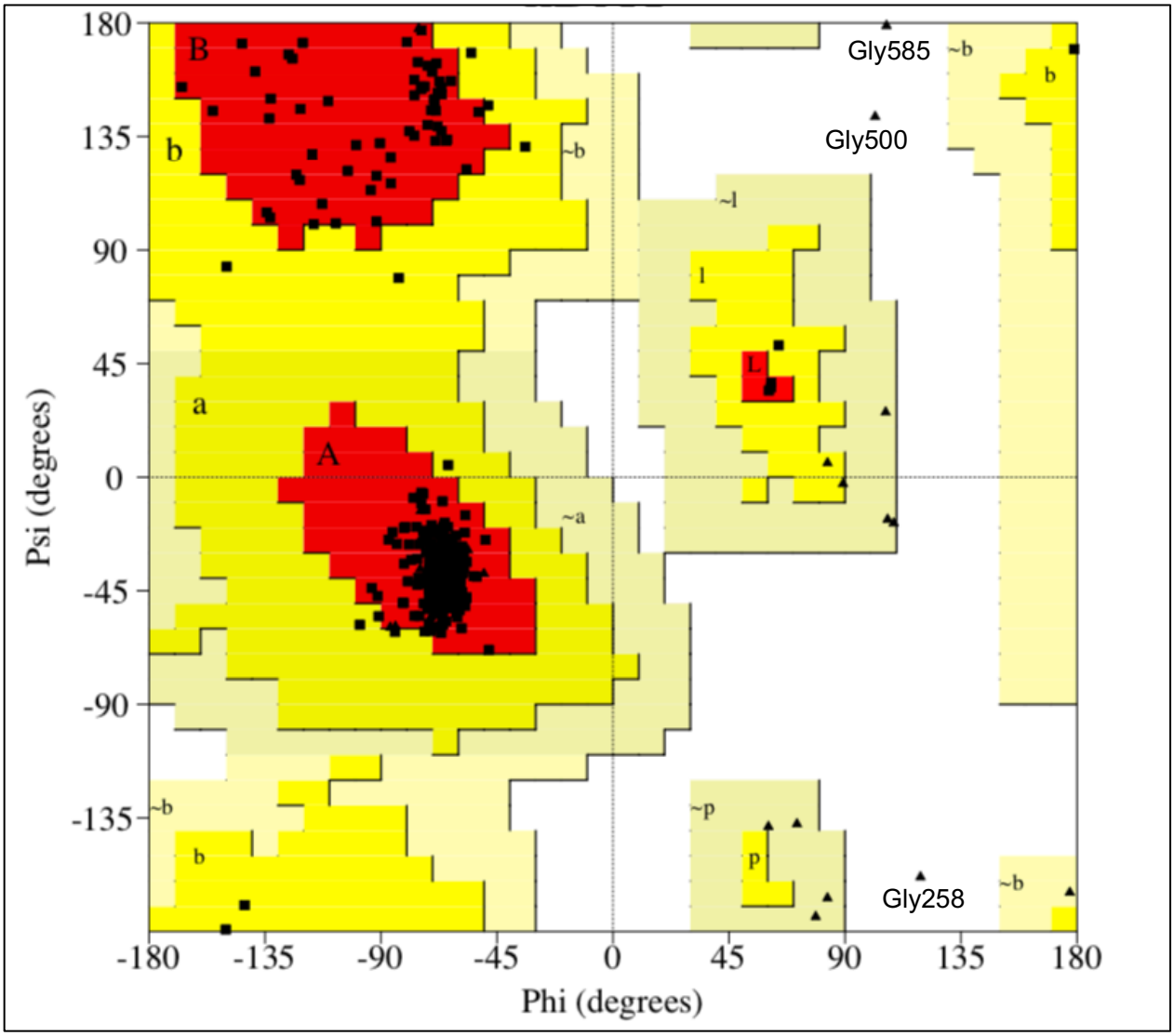

Figure 30. Ramachandran plot of our optimal hDAT model. Phi (X-axis) and Psi (Y-axis) represent backbone conformation angles of amino acid residues. Three glycine residues were found in the disallowed region (white) of the plot; however, they were not in the proximity of the binding pocket.

D. Docking studies with *t*MP (70) and hybrid analog 161

*t*MP (**70**) and the hybrid analog **161** were sketched using SybylX 2.1.1, energy-minimized using the Tripos Force Field, and then docked ten times in each of the one hundred models of hDAT using the Asp79 residue to define the binding pocket. For *t*MP (**70**), two poses were obtained, and in pose 1 the nitrogen atom of the piperidine ring was found to be involved in a bifurcated interaction with Asp79 and Ser422, whereas the carbonyl oxygen atom formed a hydrogen bond with the Ser422 (Figure 31). Figure 31a shows all the interactions between *t*MP (**70**) (pose 1) and the hDAT model and Figure 31b shows *t*MP (**70**) in a surface format to give an idea of how it occupies the binding pocket.

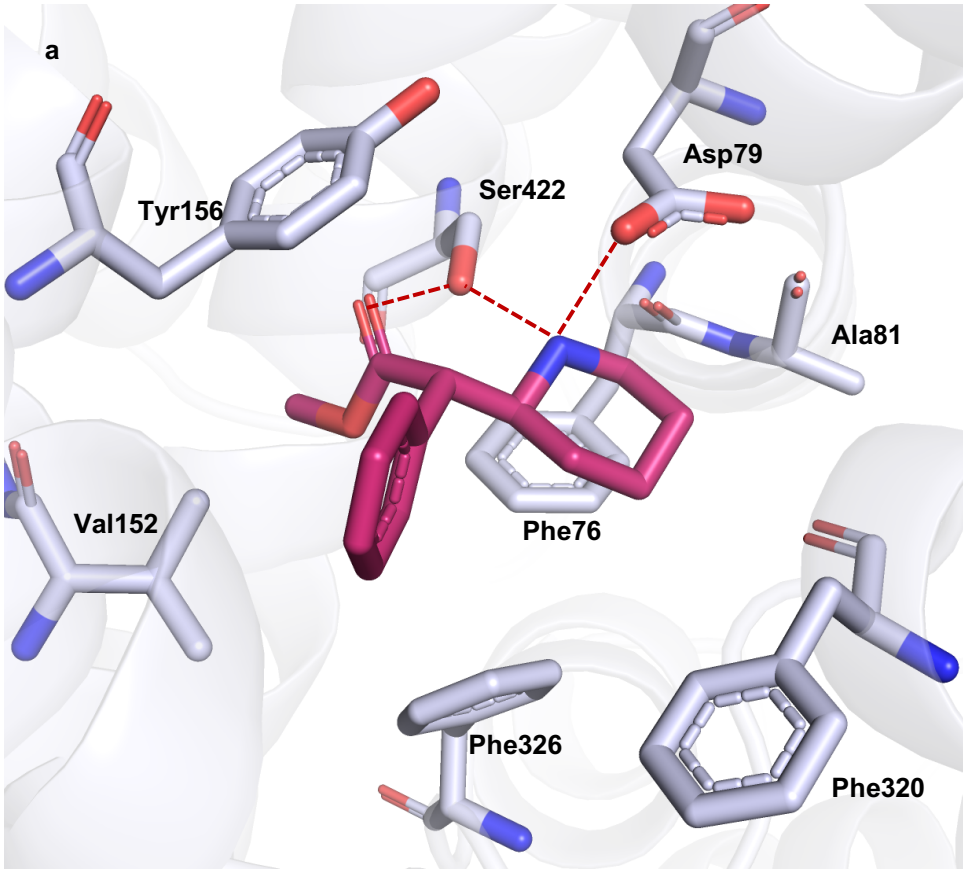

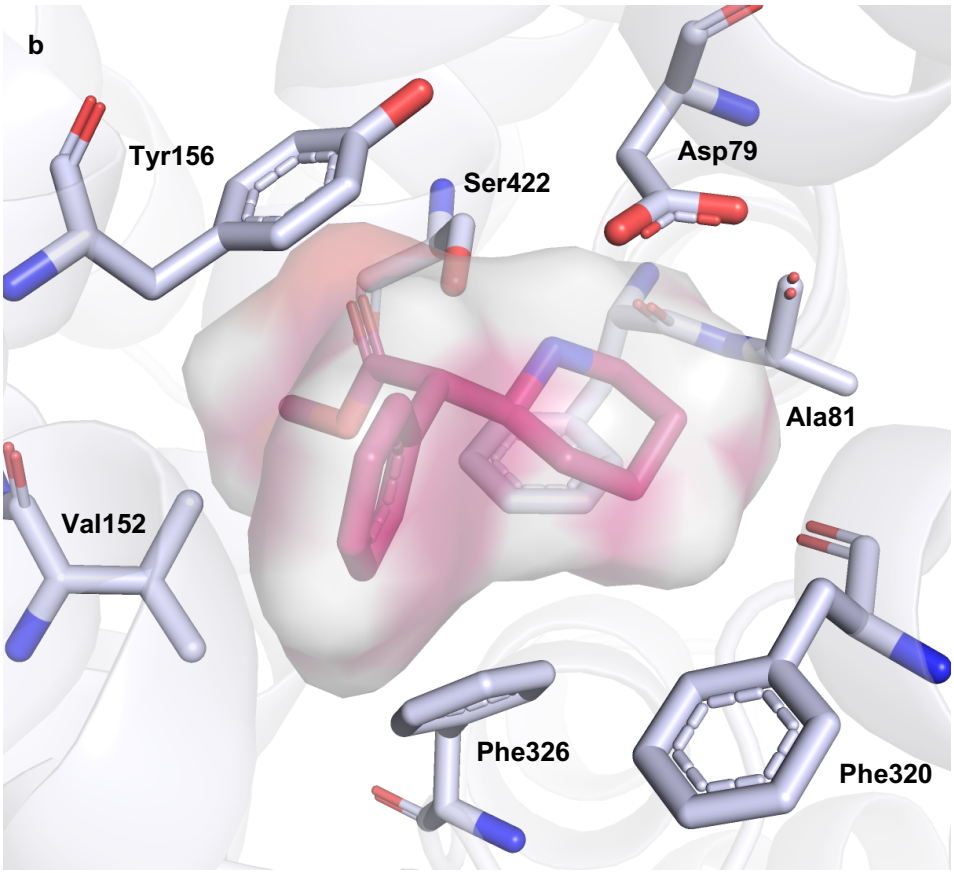

Figure 31. a. Pose 1 of *t*MP (magenta) (**70**) docked at the binding site of our hDAT model (blue-white). The nitrogen atom of *t*MP (**70**) forms a bifurcated interaction with Asp79 and Ser422, and the carbonyl oxygen atom of *t*MP (**70**) forms a hydrogen-bond interaction with Ser422 (shown in red broken lines). Other hydrophobic residues such as Phe 76, Ala81, Val152, Phe320 and Phe326 are shown in blue-white capped sticks. **b**. *t*MP (**70**) as a surface representation, showing how it occupies the binding pocket.

Pose 2 of *t*MP (**70**) was obtained in our docking studies, and only one hydrogen bond was found between the nitrogen atom of the piperidine ring and Asp79 instead of the bifurcated interaction seen in pose 1. Due to the flexible nature of the ester group of *t*MP (**70**), it was seen that there was no hydrogen bond between the carbonyl oxygen atom and Ser422. Figure 32 shows the pose 2 of *t*MP (**70**) docked in our homology model.

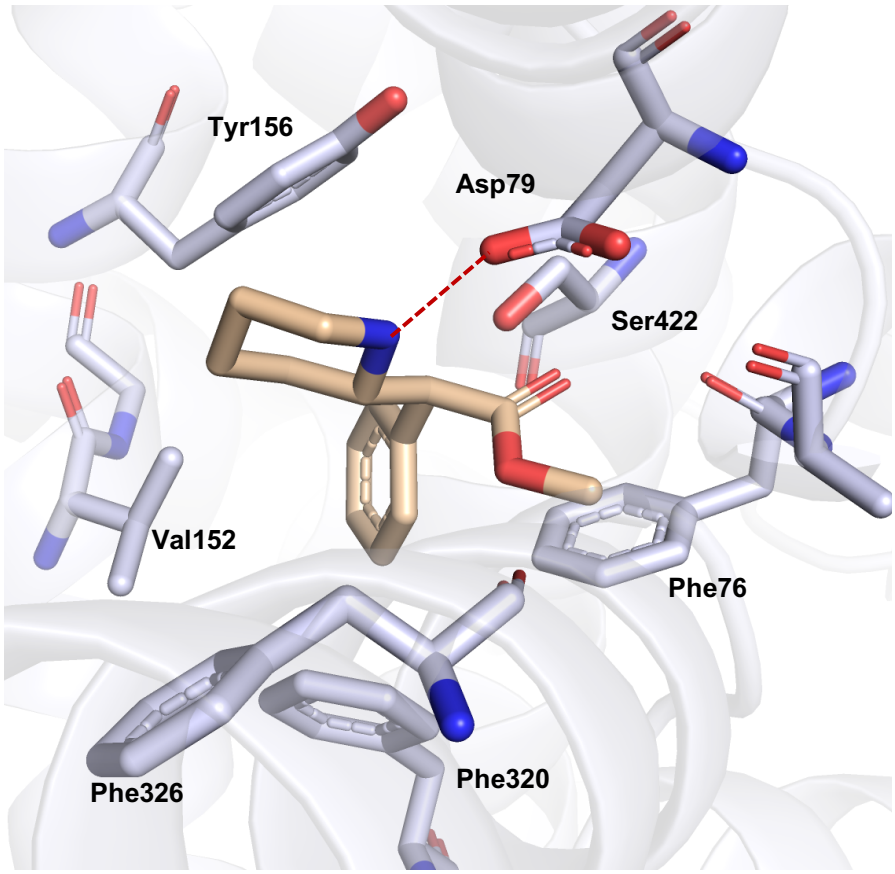

Figure 32. Pose 2 of *t*MP (**70**) (wheat color) docked at the binding site of our hDAT homology model. The nitrogen atom forms a single hydrogen bond with the Asp79 and there is a loss of a hydrogen bond between the carbonyl oxygen atom and Ser422.

The crystal structure of *t*MP (**70**) suggested that there is formation of an intramolecular hydrogen bond between the piperidine nitrogen atom and the carbonyl oxygen atom of the ester.[130] Pose 1 and pose 2 were overlaid to see the differences between the two comformations and the distance between the nitrogen atom and the carbonyl oxygen atom was measured in PyMOL 2.0.7. The distances were found to be 3.0 Å for pose 1 and 3.8 Å for pose 2 (Figure 33). Pose 1 of *t*MP (**70**) seems more likely to form an intramolecular hydrogen bond interaction (since it is <3.5 Å) and has the necessary

interaction as previously studied by Schmitt and Reith;[137] therefore, it might be considered more consistent with the crystal structure. All further studies mentioned below were conducted using pose 1 of *t*MP (**70**).

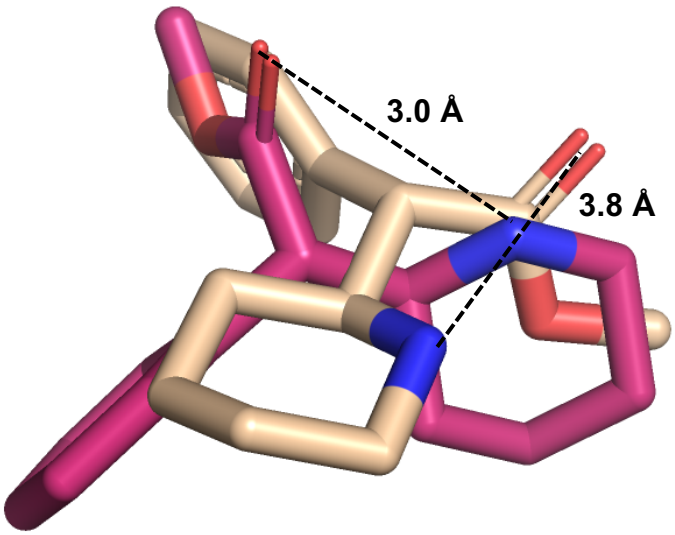

Figure 33. Pose 1 (magenta) and pose 2 (wheat) of *t*MP (**70**) overlaid; the distance between the piperidine nitrogen atom and carbonyl oxygen atom of the ester is shown is black broken lines.

The parent hybrid analog **161** was also docked in a similar fashion at the various hDAT models and it was found that, like *t*MP (**70**), the nitrogen atom of analog **161** did not form a bifurcated interaction. However, there was a hydrogen bond interaction between the nitrogen atom of **161** and Asp79 and carbonyl oxygen atom of **161** and Ser422. Figure 34a. shows analog **161** docked in the hDAT model with hydrogen bond interactions, and Figure 34b. shows analog **161** in space-filling spheres.

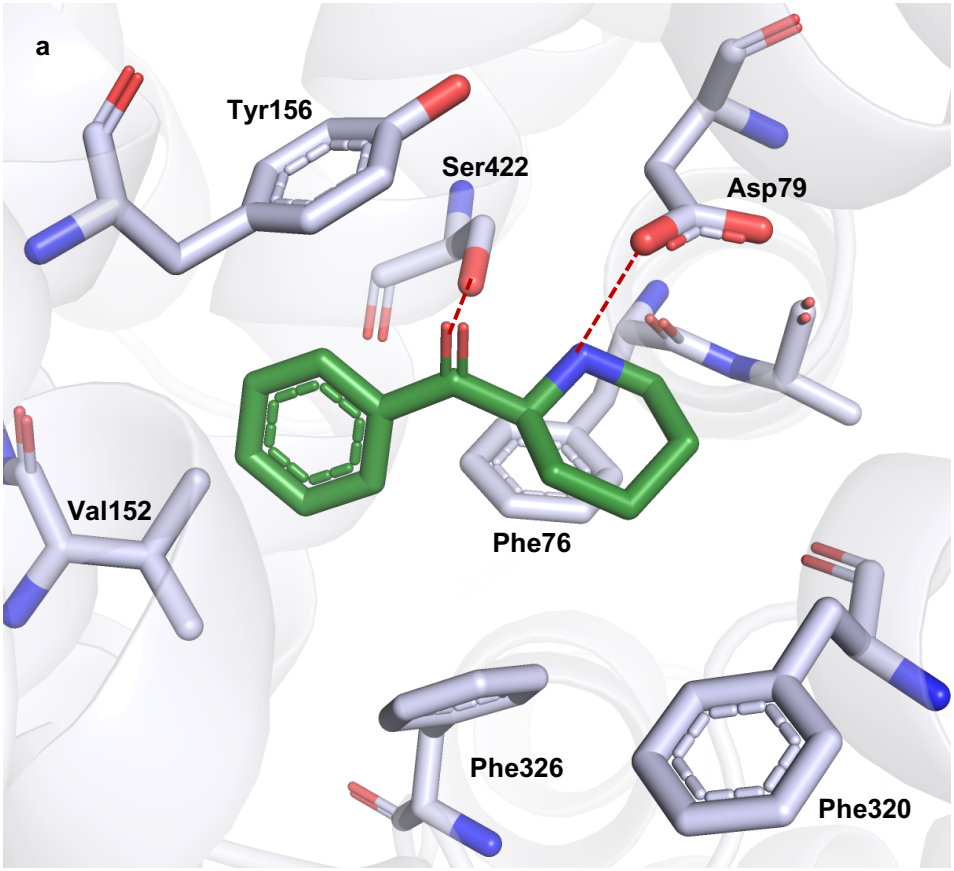

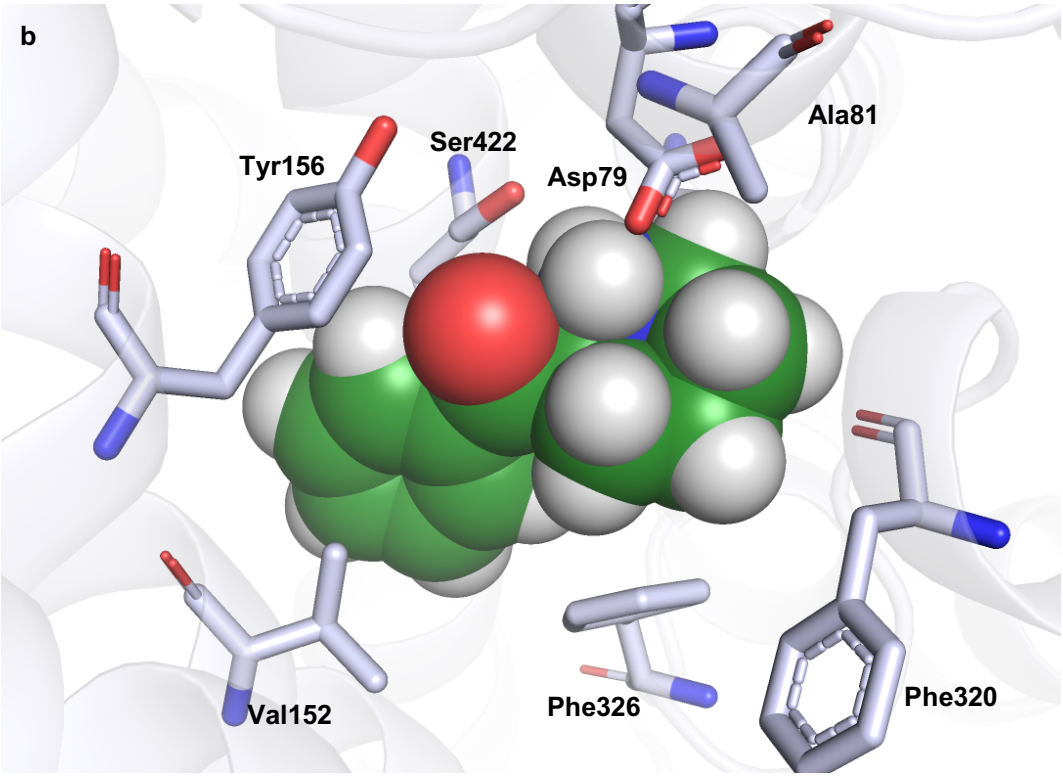

Figure 34. a. Analog **161** (forest green) docked in our hDAT model (blue-white). The nitrogen atom and the carbonyl oxygen atom of **161** forms a hydrogen bond interaction with Asp79 and Ser422, respectively. Other hydrophobic residues such as Phe76, Ala81, Val152, Phe320 and Phe326 are shown in blue-white capped sticks. **b.** Analog **161** represented as space filling spheres in the binding pocket.

E. Hydropathic INTeraction analysis

Hydropathic INTeraction (HINT) analysis[138,139] was performed in order to quantify the interactions seen in our docking studies. HINT is a program that primarily calculates the hydrophobic environment of a ligand and a protein.[139] HINT analysis takes both favorable and unfavorable interactions into account and provides a score for all the observed interactions; a high positive score suggests favorable interactions between ligand and protein.[139]

HINT analysis was performed using Sybyl 8.1. Both *t*MP (**70**) and **161** were found to have positive HINT scores (575 and 995, respectively). Table 15 shows the breakdown of the HINT scores for *t*MP (**70**) and **161** based on hydrophobic and polar interactions and Table 16 shows the breakdown of the polar interactions with respect to Asp79 and Ser422.

Table 15. Table showing distribution of favorable (green) and unfavorable (red) HINT score for *t*MP (**70**) and analog **161**.

Ligand	Total HINT score	Favorable score			Unfavorable score		
		Hydrogen bond	Acid/ Base	Hydrophobic	Acid/ Acid	Base/ Base	Hydrophobic /Polar
*t*MP (**70**) (Pose 2)	575	1245	933	441	-79	-912	-1053
161	995	1007	761	482	-108	-329	-817

Table 16. Polar HINT score breakdown of *t*MP (**70**) and analog **161** based on Asp79 and Ser422 residues.

Ligand	Total polar score	Interacting atom of the ligand	Polar interactions with Asp79	Polar interactions with Ser422
*t*MP (**70**)	2178	Nitrogen atom	1188	27
(Pose 2)		Carbonyl oxygen	-	192
161	1768	Nitrogen atom	982	-
		Carbonyl oxygen	-	38

F. Discussion

*t*MP (**70**) is an FDA approved drug for the treatment of ADHD and it primarily acts at the dopamine transporter as a reuptake inhibitor.[111] Earlier synthetic cathinones were known to act as substrates at the monoamine transporter; however, newer cathinones act as DAT reuptake inhibitors.[2] It is known that having a bulky α-side chain (e.g. *n*-propyl of α-PVP) converts synthetic cathinones from releasing agents to reuptake inhibitors.[2] Therefore, we designed a series of hybrid analogs where we ligated the α-side chain of α-PVP to the terminal amine to resemble the piperidine ring of *t*MP (**70**), and the ester group of *t*MP (**70**) was replaced with a carbonyl oxygen atom giving us our parent hybrid analog **161.** Analog **161**, which was previously synthesized in our laboratory, was found to be a DAT reuptake inhibitor in a preliminary assay, at a single (10 μM) concentration.[131]

Using the dDAT crystal structure co-crystallized with cocaine as a template, we created a population of one hundred homology models of hDAT. We validated our models by docking cocaine, and our final model had interactions similar to those seen in the dDAT crystal structure. We conducted a PROCHECK analysis and obtained a Ramachandran plot, and 96.7% of the amino acids were found in the favored region and only three glycine residues were found in the disallowed region. The binding pocket of DAT is hydrophobic in nature and is surrounded by hydrophobic amino acids such as Phe76, Ala81, Val152, Phe320 and Phe326.

After validating our model, we docked *t*MP (**70**) and hybrid analog **161**, previously sketched in using SybylX 2.1.1, ten times in one hundred models. Two poses were

obtained for *t*MP (**70**) in our docking studies and both had different poses due to the flexible nature of the *t*MP structure. In pose 1, the piperidine nitrogen atom of *t*MP was found to form a bifurcated interaction with Asp79 and Ser422 and the carbonyl oxygen atom of the ester group of **70** formed an additional hydrogen bond with Ser422. On the contrary, for pose 2, there was only one hydrogen bond between the piperidine nitrogen atom and Asp79, and the interaction between the carbonyl oxygen atom and Ser422 was lost. When pose 1 and pose 2 of *t*MP was overlaid, it was seen that the phenyl ring and the ester chain was flipped and this might have led to the loss in the interaction with Ser422. Froimowitz et al.[130] have shown that the intramolecular hydrogen bond between the piperidine nitrogen atom and the carbonyl oxygen atom stabilizes the crystal structure of *t*MP (**70**). The distances between the piperidine nitrogen atom and the carbonyl oxygen atom were measured and it was found that pose 1 (3.0 Å) had an acceptable distance to form a hydrogen bond. Pose 1 had all the favorable interactions with the hDAT model and therefore, pose 1 was selected for our HINT studies.

For analog **161**, the piperidine nitrogen atom did not form a bifurcated interaction with Asp 79 and Ser422; instead, one hydrogen bond interaction was seen between the nitrogen atom and Asp79. The carbonyl oxygen atom of **161** was also found to have a hydrogen bond interaction with Ser422. HINT analysis was performed on *t*MP (**70**) and analog **161** and both were found to have a positive score (575 and 995, respectively). Even though *t*MP had a higher total polar score, its total HINT score was found to be lower than that of **161** and this might be attributed to greater hydrophobic/polar clashes seen for *t*MP (**70**).

Due to the loss of one interaction in our hybrid analog **161**, as compared to *t*MP (**70**), in our homology modelling studies, the prediction was that analog **161** would be less potent as a DAT reuptake inhibitor than *t*MP (**70**). Hybrid analogs were synthesized and tested for their functional activity and this is discussed in Aim 2.

Aim 2. To prepare and examine a series of *t*MP/cathinone hybrid analogs (i.e., 2-benzoylpiperidines) and examine their actions at DAT

We designed our hybrid molecules based on MP structures due to four important reasons:

i. *t*MP and cathinone have some structural resemblance (vide supra)

ii. Certain cathinone analogs behave as DAT reuptake inhibitors similar to cocaine

iii. *t*MP, another DAT reuptake inhibitor, is widely abused

iv. Extensive SAR and SAFIR studies have been conducted on MP, but little is known about cathinone SAR

We aim to conduct parallel SAR studies between *t*MP (**70**) and synthetic cathinones, which means, '*if parallel changes in the structure of hybrid analogs result in parallel shifts in activity, both the t*MP *series and the hybrid analog series might be binding at DAT in a similar manner.'* The concept is an extension of the Portoghese hypothesis as cited by Foye and Lemke.[140]

In a study conducted by Misra et al.[8] 80 different analogs of *t*MP (**70**) were synthesized, of which twenty-nine analogs had changes only in the phenyl ring, and their DAT binding affinity was measured. We synthesized a series of eight analogs, of which seven analogs were monosubstituted at the 4-position of the phenyl ring and one was a 3,4-disubstituted analog (i.e. 3,4-dichloro). We chose the particular set of substituents due to differences in their physicochemical properties and their wide range in DAT binding affinity as shown by Misra et al.[8] for their corresponding *t*MP analogs.

All synthesized compounds were examined as DAT reuptake inhibitors to determine their IC_{50} values and later examined as releasing agents (at one concentration) to confirm that these hybrid analogs (**161**-**168**) act only as reuptake inhibitors, and not as releasing agents, at DAT. The synthesis of these compounds is outlined below.

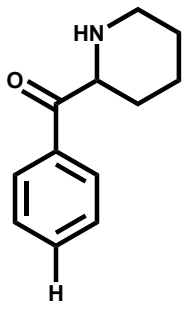

161

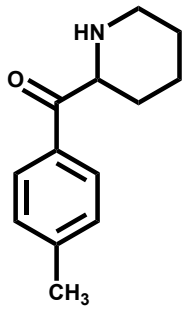

162

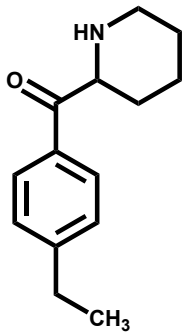

163

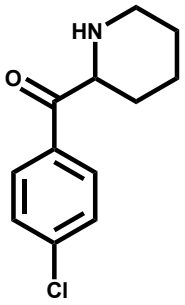

164

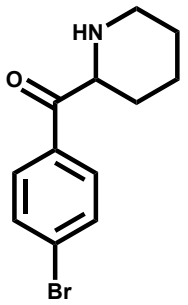

165

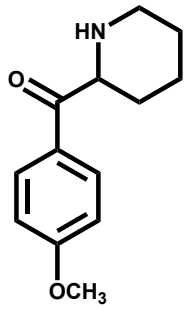

166

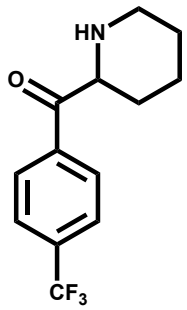

167

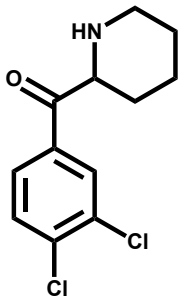

168

A. Synthesis

Since our parent hybrid analog **161** was previously synthesized in our laboratory by Sakloth et al.,[131] its exact synthetic procedure was followed. However, during this attempt the desired compound was not obtained. Scheme 3 shows the synthetic procedure that was attempted first, but failed, and the scheme that was eventually successful in obtaining analog **161**. For our first attempt, we used pipecolic acid (**170**) as our starting material and converted it to pipecolic acid chloride **171** using PCl_5 and methylene chloride at 0 °C.

The obtained acid chloride (i.e., **171**) was analyzed using melting point (mp) and IR spectroscopy, and was subsequently used in a Friedel-Crafts acylation reaction in the presence of anhydrous benzene and $AlCl_3$. The reaction mixture was stirred at room temperature for 18 h and then at 60 °C for 24 hours. During this heating, the reaction mixture started to turn black in color and eventually it solidified. More solvent was added to achieve dissolution, but it remained solid. IR spectroscopy was performed on the black solid and it did not display any carbonyl peaks. The product was not identified. After this failed attempt, another procedure was followed where 2-benzoylpyridine (**172**) (Scheme 3) was first reduced to phenyl (2-piperidinyl)methanol (**173**) using AcOH and Pt/C on a Parr hydrogenator. The intermediate alcohol (i.e., **173**) obtained was then oxidized using Jones reagent to obtain the desired final product **161** and was converted to its hydrochloride salt. The oxidation reaction and the preparation of Jones reagent was accomplished using the procedure described for the synthesis of MDPV by Kolanos et al.[97] We are unable to determine why the earlier preparation failed in our hands. Nevertheless, the current product had a similar mp as the product earlier described by Sakloth.[131]

Scheme 3[a]. Synthesis for parent hybrid analog **161**.

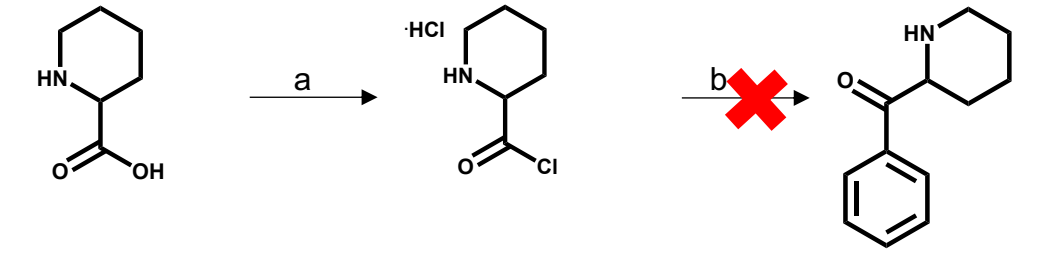

170 **171** **161**

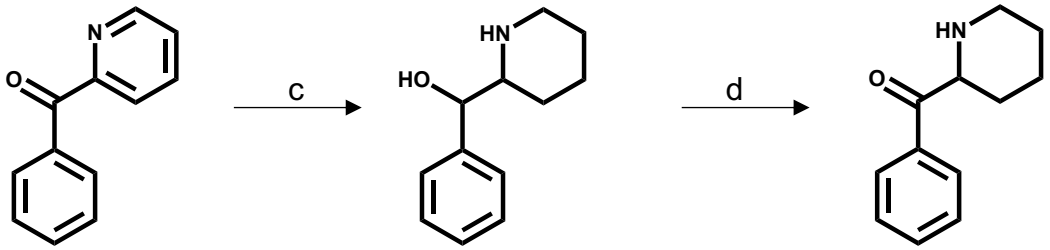

172 **173** **161**

[a]Reagents and conditions: a. PCl_5, CH_2Cl_2; b. benzene, $AlCl_3$, 40 °C; c. AcOH, 5% Pt/C, 30-40 psi, rt, 6h; d. Jones reagent, 0 ºC, 1h, rt, 18h.

Analogs **162** and **163** (Scheme 4) were prepared by a one-pot Friedel-Crafts acylation reaction using N-Boc-pipecolic acid (**174**) as starting material. Anhydrous toluene and ethylbenzene were used as the solvent, respectively. Thionyl chloride ($SOCl_2$) and DMF were used to obtain the acid chloride *in situ* at 0 °C and as soon as the ice-bath was removed, the color of the reaction mixture changed from bright orange to black and, over the next 30 min, the reaction mixture turned into a black solid which had the appearance of a charred solid. IR spectroscopy was performed and no carbonyl peaks were detected; moreover, the carbonyl peaks that were seen in the starting material also disappeared. For our next approach we eliminated DMF and carried out a neat reaction using $SOCl_2$

and the starting material (i.e. **174**); however, we obtained the same result. With two failed procedures, we changed our chlorinating agent and used PCl_3 instead of $SOCl_2$. The reaction was carried out in an N_2 atmosphere and IR spectra were obtained on the reaction mixture where we noticed the presence of an acid chloride peak. Having confirmed the presence of the desired acid chloride, we added freshly sublimed $AlCl_3$ at 0 °C and allowed the reaction mixture to stir overnight. Thin-layer chromatography (TLC), to check the progress of the reaction, displayed a new product. Scheme 4 shows the synthetic schemes that failed and the one that was eventually successful.

Scheme 4[a]. Synthesis of analogs **162** and **163**.

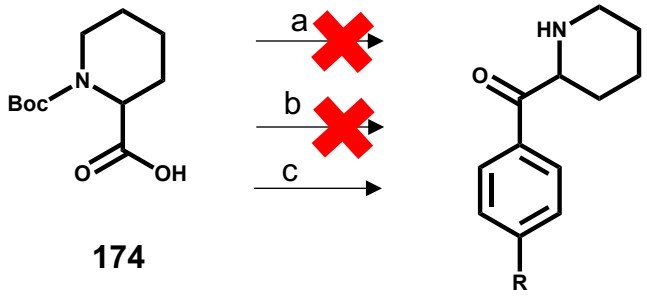

174

162 R = -CH_3
163 R = -C_2H_5

[a]Reagents and conditions: a. $SOCl_2$, DMF, solvent for **162** was toluene and for **163** was ethylbenzene; b. $SOCl_2$, solvent for **162** was toluene and for **163** was ethylbenzene; c. PCl_3, 0 °C, solvent for **162** was toluene and for **163** was ethylbenzene, rt, 16-24 h.

The same procedure shown in Scheme 4c was carried out to obtain analogs **164** and **165**. For analog **164** (Scheme 5), we used *N*-Boc-pipecolic acid (**174**) and anhydrous bromobenzene as starting materials and obtained our acid chloride using PCl_3; however

when $AlCl_3$ was added, and the reaction was carried out at room temperature, no progress in the reaction was seen after 2 h. The reaction mixture was allowed to stir for 48 h and TCL analysis showed no progress. Halogens are *ortho* and *para* directing but they are also deactivating groups and, therefore, for our next attempt, we decided to reflux the reaction instead of letting it stir at room temperature. While monitoring the reaction, we saw some change on TLC analysis; however, on comparing TLC spots it was found that the Boc group of the *N*-Boc-pipecolic acid (**174**) was deprotected, giving us pipecolic acid (**170**). To tackle this deprotection issue, we protected the nitrogen atom with a formyl group which is stable against $AlCl_3$.[141] Pipecolic acid (**170**) was protected using formic acid and acetic anhydride, which generates acetic formic anhydride *in situ*. The *N*-formyl-pipecolic acid was used for the one-pot Friedel-crafts reaction and analog **176** was successfully obtained. The formyl group was removed by refluxing **176** in a mixture of HCl/EtOH. Analog **165** has a bromine atom at the 4-position, and therefore the same procedure was followed using bromobenzene giving us the final product **165** (Scheme 5).

Scheme 5[a]. Synthesis of analogs **164** and **165**.

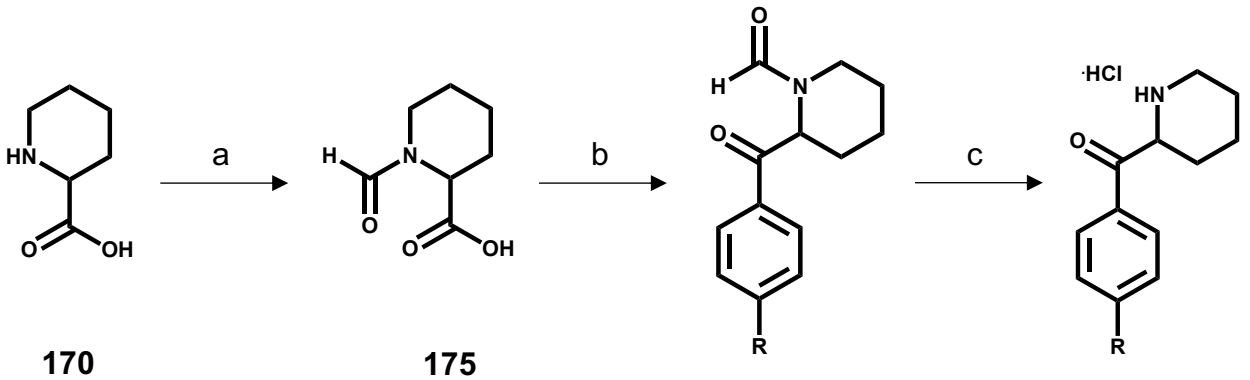

170 **175** **176 R = Cl** **177 R = Br** **164 R = Cl** **165 R = Br**

[a]Reagents and conditions: a. $(CH_3CO_2)_2O$, HCOOH, rt, 1h; b. (i) *p*-substituted benzene, PCl_3, 60 ºC, 2h, (ii) $AlCl_3$, rt, 16-18h; c. HCl/EtOH, reflux, 3h.

The trifluoromethyl group is an EWG and a meta directing substituent and, therefore, the Friedel-Crafts acylation approach should mostly give us a 3-substituted analog. Hence, we used an organo-lithium approach to synthesize analog **167**, previously reported by Thai et al.[142] for similar compounds. Scheme 6 shows an outline of the reaction. The reaction involved the synthesis of two intermediates (i.e., a Weinreb amide and an organolithium compound) and, eventually, reacting them at -23 ºC (in a mixture of dry ice and CCl_4). For our first intermediate, we used N-Boc-pipecolic acid as starting material, which was reacted with *N,O*-dimethylhydroxylamine hydrochloride, TEA, and a coupling agent (benzotriazol-1-yloxy)tris(dimethylamino)phosphonium hexafluorophosphate (BOP) to give us a Weinreb amide (i.e. **178**). To obtain the organolithium intermediate, 4-bromo trifluoromethylbenzene (**180**) was reacted with 2.5 M *n*-BuLi at -40 ºC (in a mixture of dry ice and acetonitrile). For the final step, the organolithium reagent generated *in situ*

was added in a dropwise manner to a stirred solution of **178** in anhydrous ether to give compound **167**.

Scheme 6[a]. Synthesis of analogs **166**, **167**, and **168**.

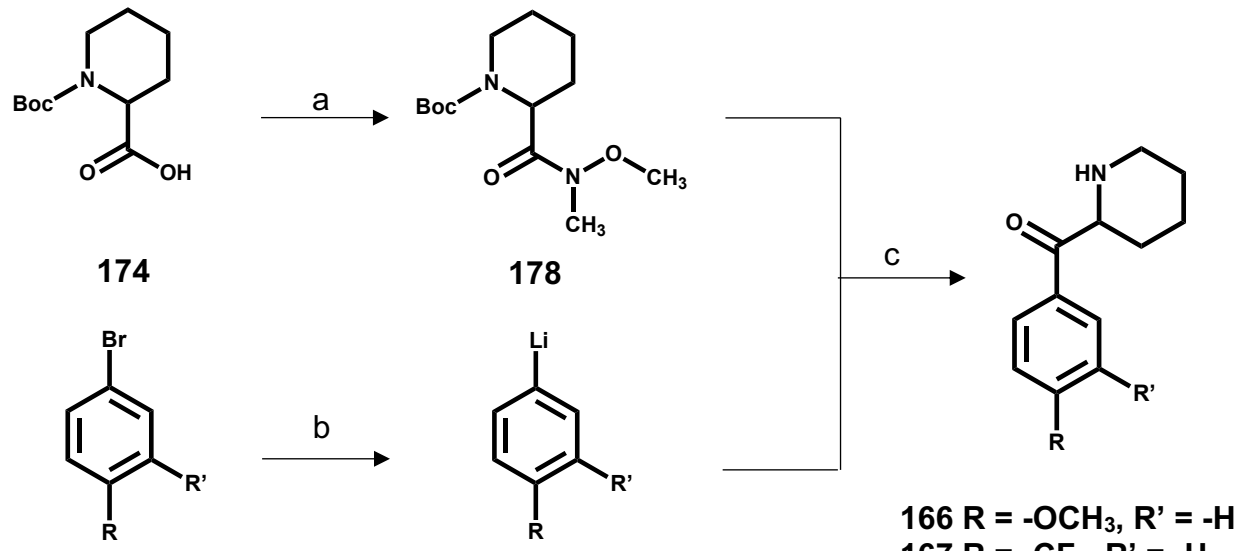

179 R = -OCH_3, R' = -H
180 R = -CF_3, R' = -H
181 R = -Cl, R' = -Cl

182 R = -OCH_3, R' = -H
183 R = -CF_3, R' = -H
184 R = -Cl, R' = -Cl

166 R = -OCH_3, R' = -H
167 R = -CF_3, R' = -H
168 R = -Cl, R' = -Cl

[a]Reagents and conditions: a. *N,O*-dimethylhydroxylamine hydrochloride, TEA, BOP, rt, 3h; b. 2.5 M *n*-BuLi in hexane, -40 ºC, 3h; c. Et_2O, -23 ºC.

Scheme 4c and 5 were used in an attempt to synthesize analog **166**, however both synthetic schemes failed to provide the desired product. Therefore, Scheme 6 outlined above, was used to synthesize analogs **166** and **168** using 4-bromoanisole and 1-bromo-3,4-dichlorobenzene, respectively, as starting material to give an organolithium intermediate. The advantages of Scheme 6 over Schemes 4 and 5 were the ease of

synthesis, fewer impurities, and fewer by-products, and the final products were easier to purify and recrystallize.

B. APP^+ uptake assay

After the synthesis of our desired targets, DAT reuptake data were obtained. As preliminary data had shown that the parent analog **161** acted as a DAT reuptake inhibitor, and it was also known that having a bulky α-side chain shifts the activity of compounds from DAT releasers to DAT reuptake inhibitors,[2] we predicted that all the compounds in our current series would also be reuptake inhibitors. Functional activity studies were conducted in Dr. Jose Eltit's laboratory in the Department of Physiology and Biophysics, School of Medicine, Virginia Commonwealth University.

APP^+ uptake assays were performed in human embryonic kidney (HEK293) cells which stably expressed hDAT. Live-cell imaging was conducted for this assay using epifluorescence microscopy. The assay was performed for compounds that acted as reuptake inhibitors at the monoamine transporters. APP^+ is a known DAT substrate,[143] and was used as a positive control. The test compounds, if reuptake inhibitors, compete with the APP^+ signal and the potency of the test compound is directly proportional to the inhibition of the APP^+ signal. A preliminary APP^+ uptake assay was first conducted at two concentrations (1 and 10 μM) in order to determine the potency of the hybrid analogs, and then complete dose-response curves were obtained for each of the hybrid analogs using six different concentrations. Analogs were tested in triplicate at each concentration

and the experiments were repeated on a separate day to give reliable data. Figure 35 shows the raw data of control APP^+ at 3 μM (**a**) and our parent analog **161** at 1 μM (**b**).

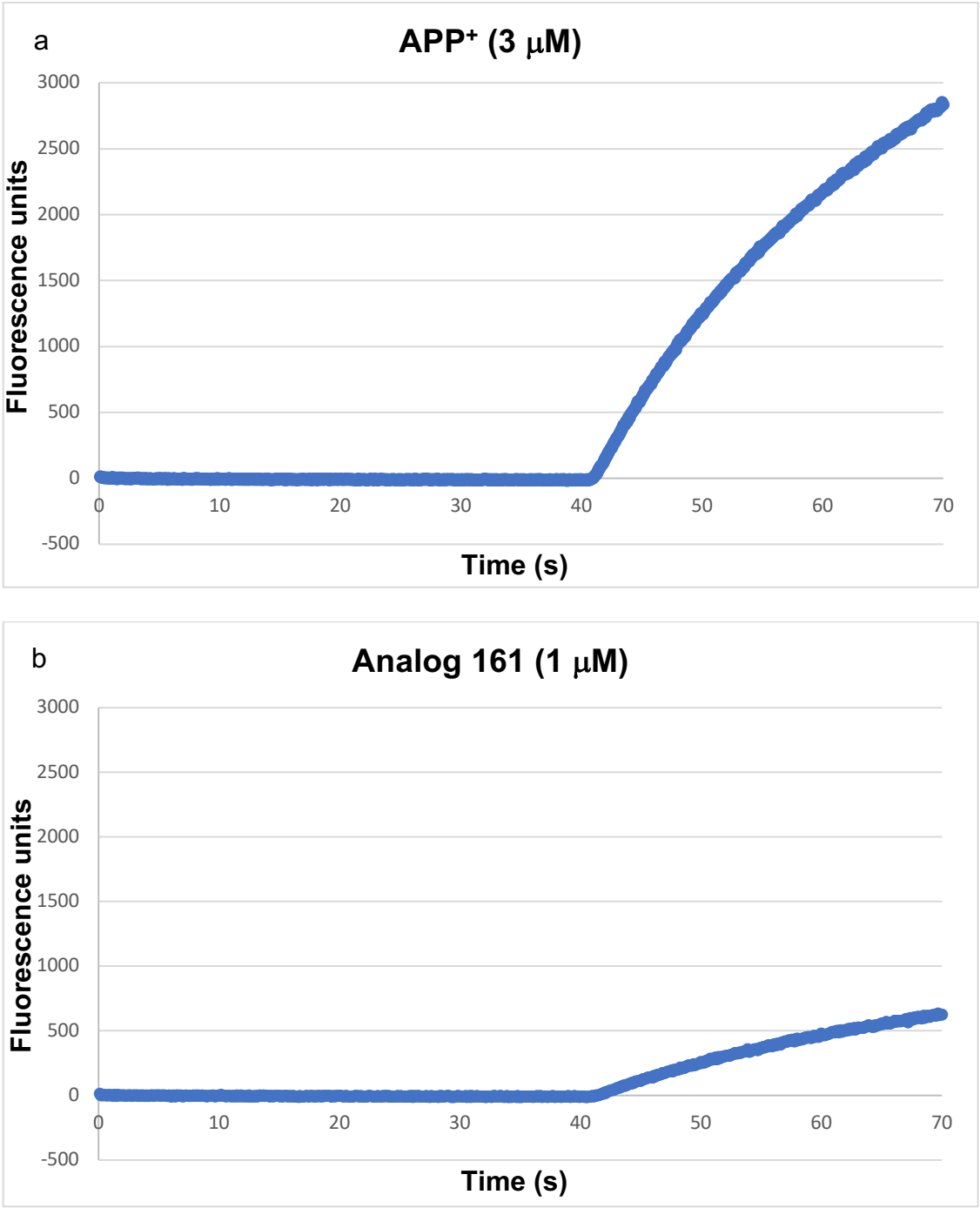

Figure 35. Raw traces of APP^+ (**a**, 3 μM) and analog **161** (**b**, 1 μM) in the APP^+ uptake assay using live-cell imaging.

Using the DsRed signal, the focal plane of monolayered transfected cells was identified, and then the APP^+ signal was measured using a wavelength of 460 nm for excitation and 540 nm for emission.[143,144] The data were analyzed using Fiji (Image J) 2.0 and the dose-response curves were plotted using GraphPad Prism 8.0. Figure 36 shows all the dose response curves of our hybrid analogs along with *t*MP (**70**), and cocaine (**4**), which were tested for comparison; and Table 17 shows the IC_{50} values of the above-mentioned compounds.

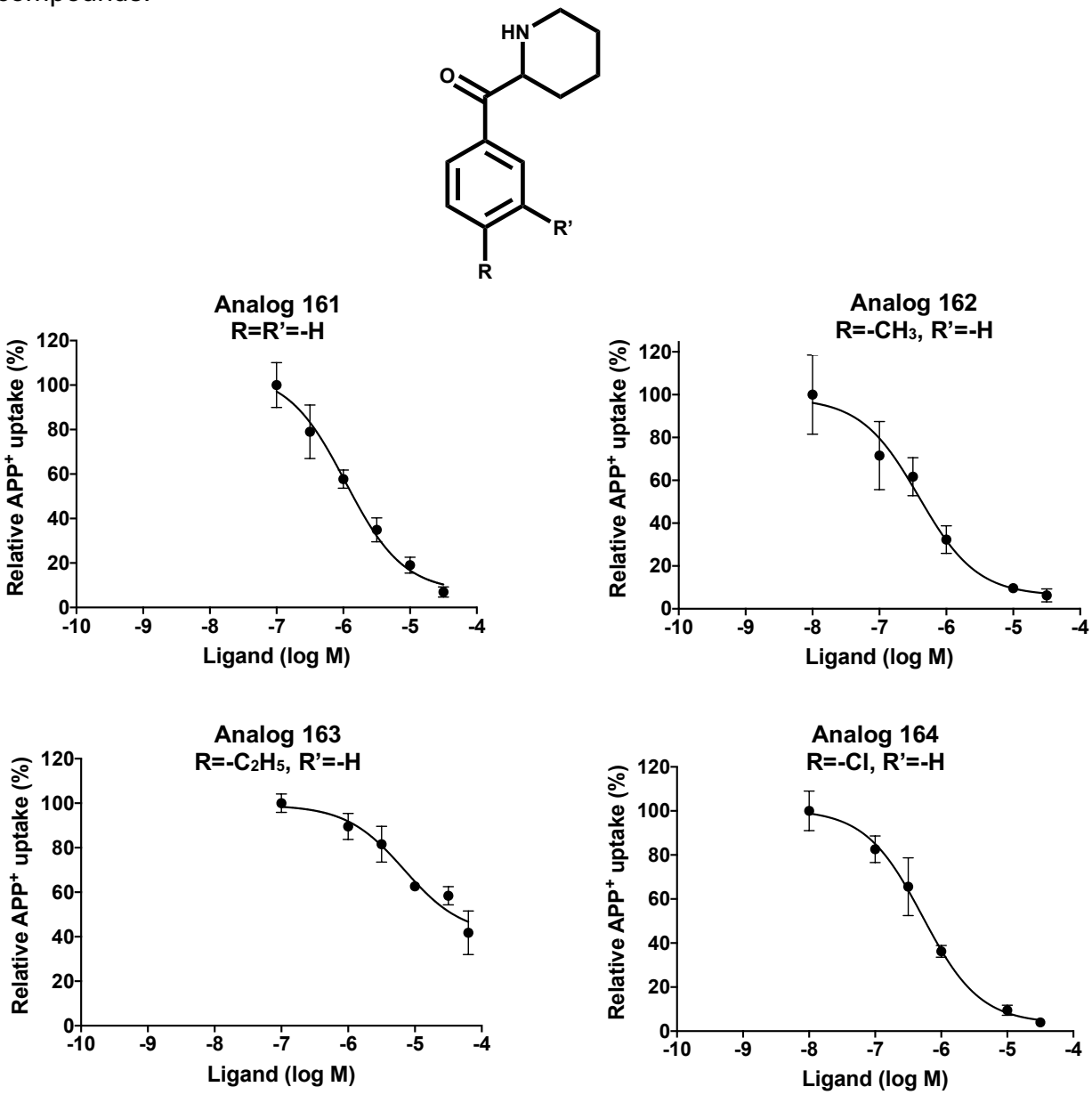

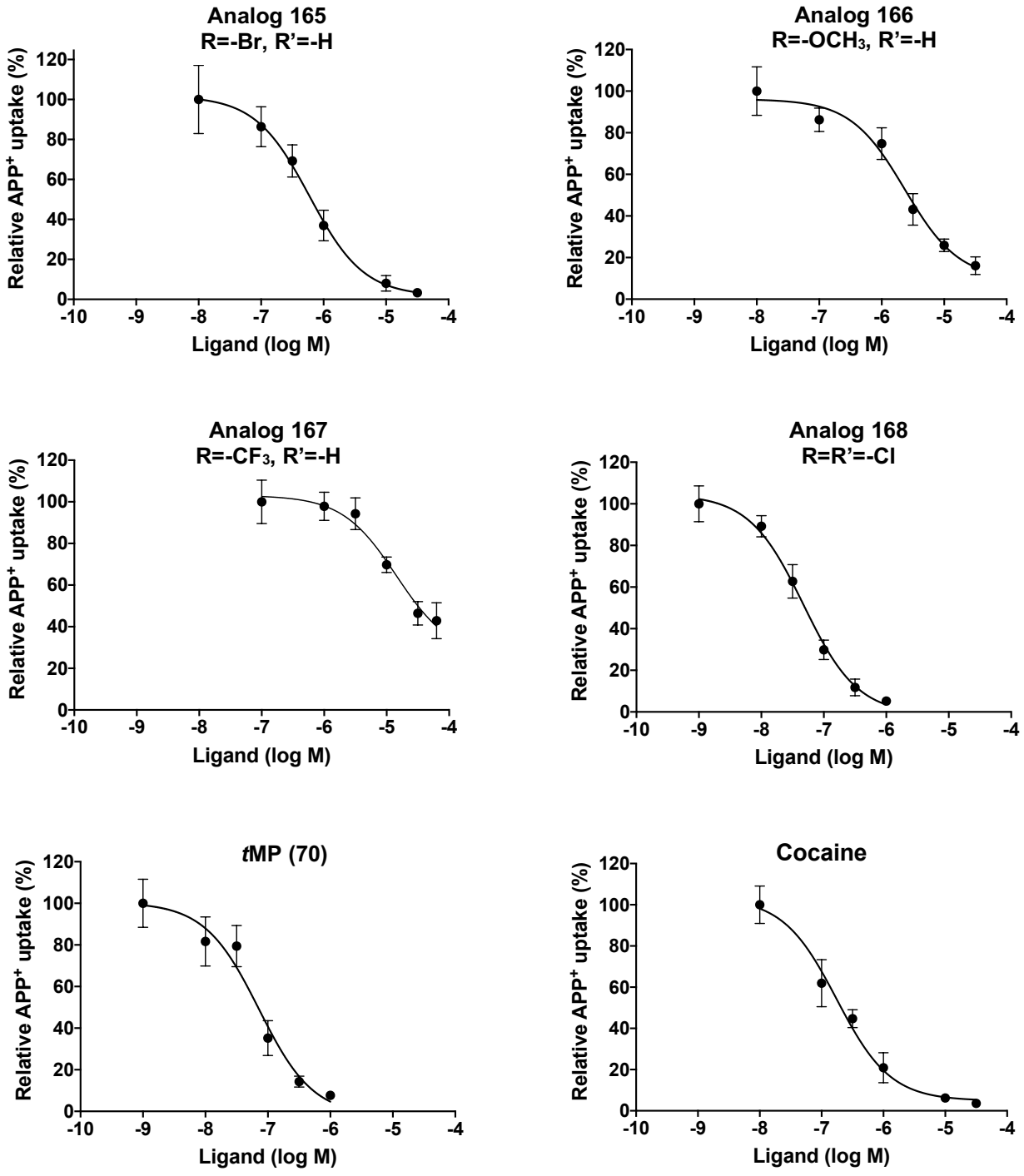

Figure 36. Dose-response curves of our benzoylpiperidine analogs (**161**-**168**), *t*MP (**70**), and cocaine (**4**) in an APP^+ uptake assay at hDAT.

Table 17. IC_{50} values of hybrid analogs **161**-**168**, *t*MP (**70**), and cocaine (**4**) in an APP^+ uptake assay at hDAT.

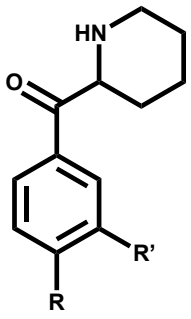

161-168

Ligand	-R	-R'	IC_{50} (nM) ± S.E.M.	pIC_{50}
161	-H	-H	1080 ± 190	5.96
162	$-CH_3$	-H	380 ± 80	6.42
163	$-C_2H_5$	-H	6900 ± 1900	5.16
164	-Cl	-H	520 ± 60	6.28
165	-Br	-H	590 ± 100	6.22
166	$-OCH_3$	-H	2340 ± 400	5.63
167	$-CF_3$	-H	14300 ± 4000	4.84
168	-Cl	-Cl	47 ± 6	7.32
*t*MP (**70**)			72 ± 10	7.14
Cocaine (**4**)			170 ± 20	6.76

C. Intracellular Ca^{2+} determination

Voltage-gated Ca^{2+} channels are important because they translate an electric signal in the plasma membrane into changes in cytosolic Ca^{2+} signals.[145] At rest, the intracellular concentration of Ca^{2+} is low (~100 nM) and the leak current is balanced by the efflux of Ca^{2+} through high-affinity, low-capacity plasma membrane Ca^{2+} ATPase (PMCA); however, upon depolarization the Ca^{2+} channel opens and Ca^{2+} concentration might increase by 10-100-fold as reported by Steele and Eltit.[145] Normally, the extracellular concentration of Ca^{2+} is approximately 10000-fold greater than the intracellular Ca^{2+} concentration (i.e., ~2 mM) and the negative cell membrane potential results in a large electrochemical gradient. This leads to a strong influx of Ca^{2+} when the channel is open. During depolarization, the intracellular Ca^{2+} concentration is directly proportional to the number of Ca^{2+} channels that are open, as reported by Steele and Eltit.[145] As the intracellular Ca^{2+} concentration increases, low-affinity, the high-capacity Na^{+}/ Ca^{2+} exchanger (NCX) is activated, in order to balance the high Ca^{2+} concentration.[145] During repolarization the majority of the open-state Ca^{2+} channel shifts to the closed-state, which decreases the net influx of Ca^{2+} and efflux through NCX decreases intracellular Ca^{2+} to the initial resting stage.[145] Figure 37 describes the scheme of Ca^{2+} fluxes in cells expressing DAT and voltage gated Ca^{2+} channels. The image is adapted from Steele and Eltit.[145]

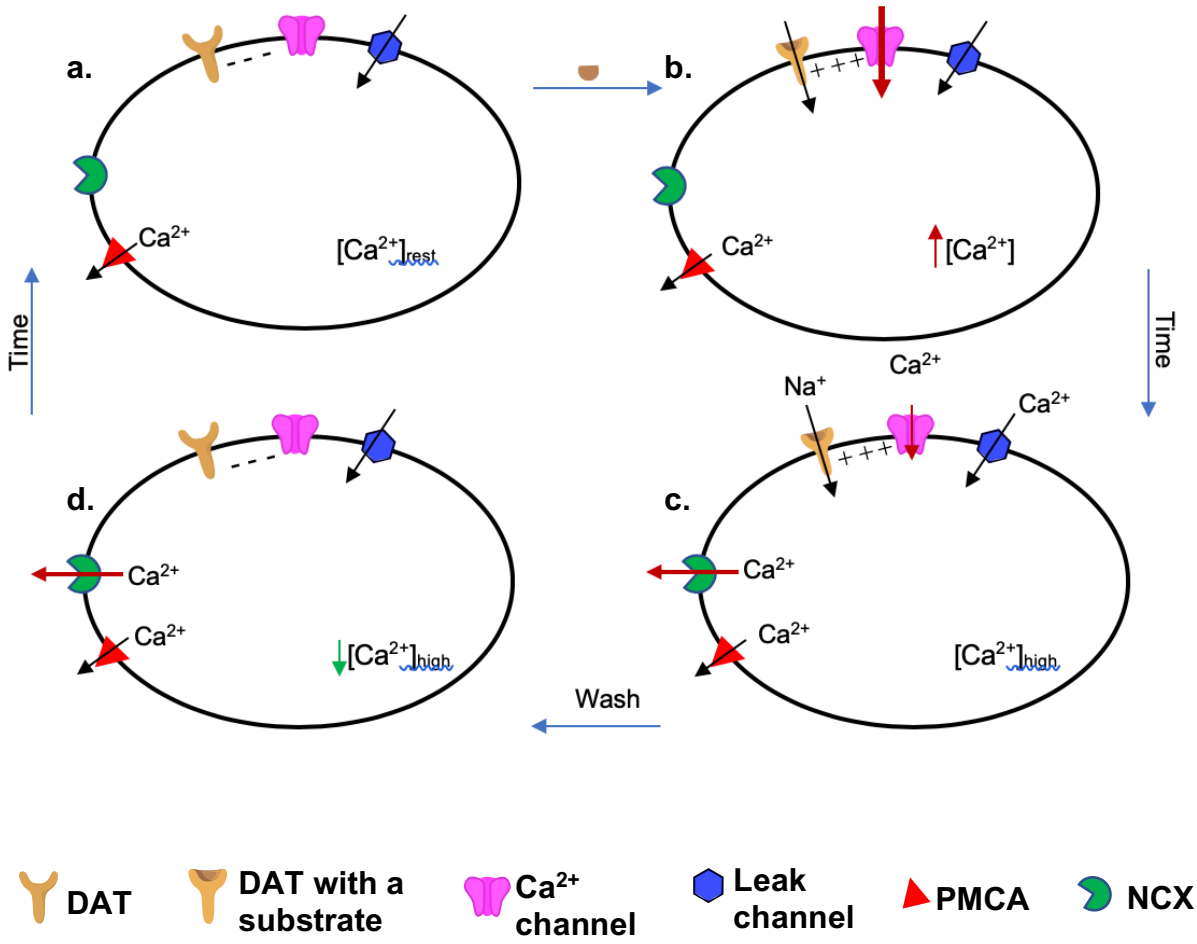

Figure 37. Ca^{2+} fluxes scheme in HEK293 cell expressing hDAT and voltage-gated Ca^{2+} channel. **a**. At rest, the Ca^{2+} concentration is low and the influx due to the leak current is balanced by PMCA. **b**. DAT substrate causes depolarization resulting in opening of Ca^{2+} channels resulting in influx of Ca^{2+}. **c**. Ca^{2+} channel starts getting deactivated and the influx of Ca^{2+} reduces, the excess of intracellular Ca^{2+} is effluxed by NCX. **d**. Removal of the substrate results in repolarization, closing of Ca^{2+} channels and eventually reaching the resting stage **a**. Adapted from Steele and Eltit.[145]

We co-expressed hDAT with a voltage-gated Ca^{2+} channel in order to evaluate our hybrid analogs for their release potential. HEK239 cells stably expressing hDAT were co-expressed with $Ca_v1.2$ in combination with its auxiliary subunits β_3, $\alpha_2\delta$ and a fluorescent protein EGFP. The cells were loaded with Ca^{2+}-sensitive Fura-2 for 40 min and then washed twice with the imaging solution (IS). The measurements were done using an excitation wavelength of 340 nm and the EGFP fluorescence were measured at 490 nm. DA was used as control for this assay and as we knew that our hybrid analogs were DAT reuptake inhibitors, we evaluated our compounds only at one concentration (10-times their IC_{50}). This was done to confirm that the hybrid analogs only acted as reuptake inhibitors and not as releasers or have any mixed actions at DAT. Analogs **163** and **167** were not evaluated in the Ca^{2+} assay due to their low potency in the APP^+ assay. Figure 38 shows the trace of all the hybrid analogs in the Ca^{2+} assay with DA used as the standard.

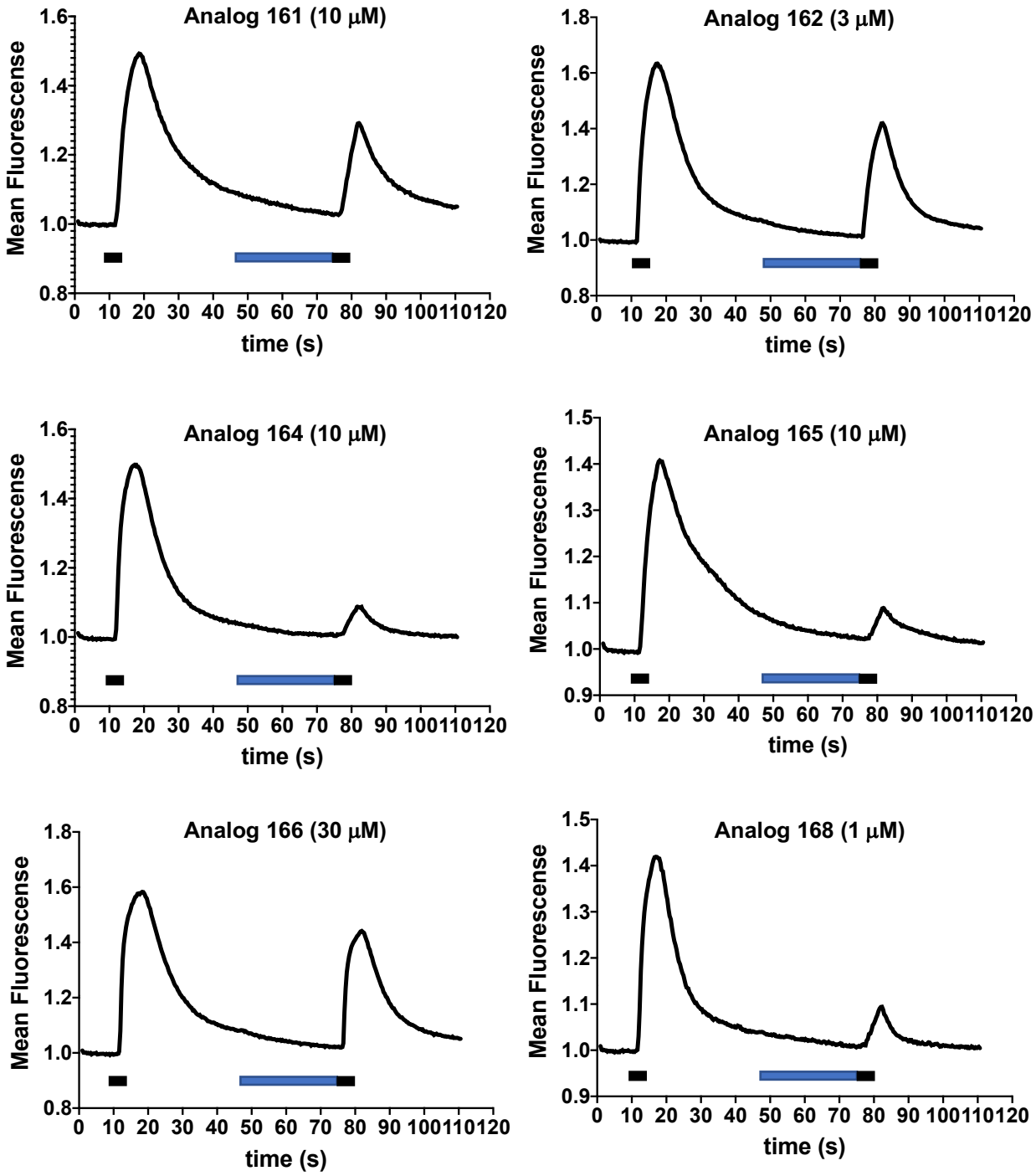

Figure 38. Graphs obtained from the Ca^{2+} assay. The analogs were tested at approximately 10-times their IC_{50}. The first peak represents a DA (10 μM) signal followed by a wash (30 s), then the corresponding analog was perfused for 30 s (shown in blue), followed by a mixture of the analog and 10 μM DA for 5 s. The second peak shows that the hybrid analogs successfully blocked hDAT resulting in weaker signals of DA as compared to the first signal.

All hybrid analogs (**161**-**168**) were found to be reuptake inhibitors and none behaved as substrates at DAT. Of the hybrid analogs tested, the 3,4-dichloro analog (i.e., **168**) was the most potent, and 1.5-fold more potent than *t*MP (**70**). The order of potency for our series was: 3,4-dichloro (**168**) > 4-CH_3 (**162**) > 4-Cl (**164**) ~ 4-Br (**165**) > 4-H (**161**) > 4-OCH_3 (**166**) > 4-C_2H_5 (**163**) > 4-CF_3 (**167**). A comparison between DAT reuptake potencies[9] and radioligand binding affinity[8] for 25 *t*MP analogs (2-, 3-, and 4-substituted) was made, and a significant correlation was obtained (r = 0.98) between the two data sets (Figure 39). This indicated that DAT functional potency of the *t*MP analogs parallels their binding affinity, and this allowed us to use the binding data of *t*MP series as a surrogate for their functional data. Therefore, we compared our APP^+ uptake assay data with the literature binding data for the corresponding analogs. We used the binding data, since the functional data for 4-C_2H_5 *t*MP and 4-CF_3 *t*MP were not available. For the eight 2-benzoylpiperidines examined, there was a significant relationship between their potencies and the DAT binding affinity of their corresponding *t*MP analogs (r = 0.91, n = 8) (Figure 40). The obtained results suggested that the SAR of *t*MP (**70**) might be applicable to the synthetic cathinones.

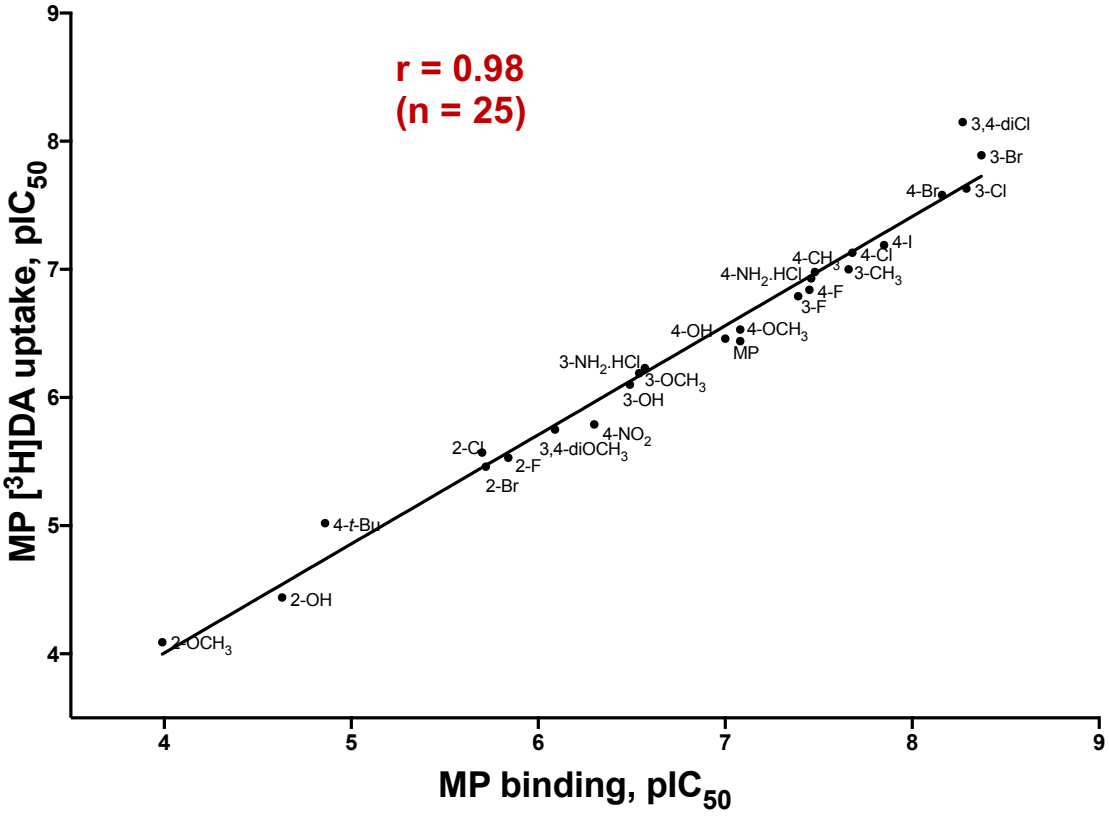

Figure 39. Relationship between the reported DAT transporter binding data of *t*MP analogs (X-axis)[8] and their [^{3}H]DA reuptake data (Y-axis).[9]

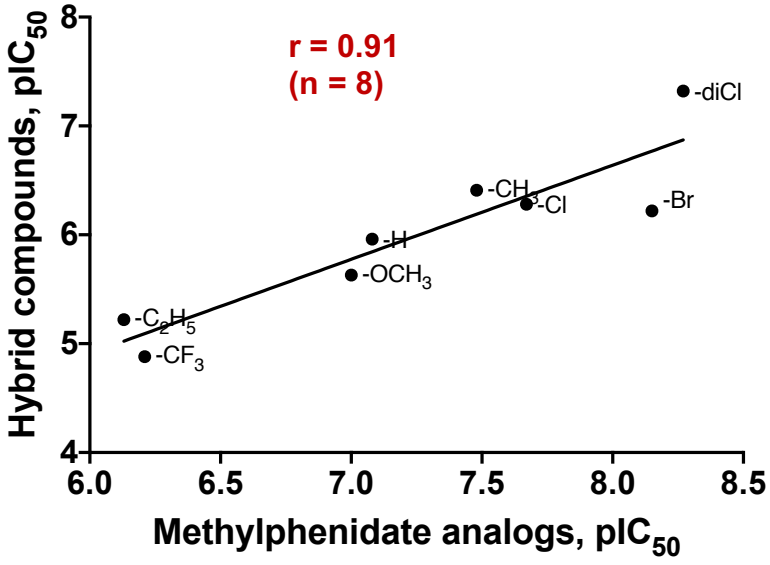

Figure 40. Correlation between the binding data of *t*MP analogs[8] (X-axis) and APP^+ uptake assay data (Y-axis) for the corresponding 2-benzoylpiperidines.

D. Discussion

We designed a series of eight hybrid analogs based on the structure of *t*MP (**70**) and α-PVP. *t*MP (**70**) was chosen for the current study as it acts as a DAT reuptake inhibitor, it shares structural similarity with synthetic cathinones, it is widely abused, and its SAR has been extensively studied. From previous studies conducted in our lab, it was found that having an extended α-side chain converts a cathinone analog from a substrate to a reuptake inhibitor at DAT.[2] Following this lead, we ligated the α-side chain of α-PVP to the terminal amine making a piperidine ring similar to the *t*MP structure. We replaced the methyl ester of the *t*MP with a carbonyl group, which gave us our first hybrid analog (2-benzoylpiperidine).

Our hypothesis, for the current study, was to conduct parallel SAR studies between the *t*MP and the hybrid series, and if parallel changes in the structure of the hybrid analogs resulted in a parallel shift in activity, both the *t*MP series and the hybrid analog series might be binding at DAT in a similar manner. We focused on 4-substituted analogs for the present study and synthesized a series of eight compounds. We chose these particular substituents because they had different physicochemical properties; their *t*MP analogs had been already studied, and they displayed a range in potencies.[8,9]

For synthesis we used a Friedel-Crafts acylation reaction, with Boc protected pipecolic acid for analogs **162** and **163**, and *N*-formyl protected pipecolic acid for analogs **164** and **165**, as our starting material. Surprisingly, using $SOCl_2$ as our chlorinating agent did not give us our desired acid chloride and therefore we used PCl_3 instead. Analogs **166**, **167**,

and **168** were synthesized using an organolithium reaction and that reaction was found to give few by-products and the crude product was easier to purify and recrystallize as compared to the Friedel-Crafts acylation reaction products. Analog **161** was synthesized by reduction of 2-benzoylpyridine (**172**) followed by oxidation of the alcohol intermediate (i.e., **173**) using Jones reagent.

Analog **161** was previously synthesized and evaluated in our lab and at a single concentration it was found to act as a DAT reuptake inhibitor. APP^+ uptake studies were conducted on our analogs using HEK293 cells stably expressing hDAT in live-cell imaging. Preliminary studies, at two concentrations (1 and 10 μM), were conducted on the hybrid analogs and, based on the results, complete dose-response curves were obtained. The 3,4-dichloro analog (**168**, IC_{50} = 47 nM) was found to be the most potent and the 4-trifluoromethyl analog (**167**, IC_{50} = 14300 nM) was found to be the least potent. Analog **168** was the only compound that was found to be more potent than *t*MP (**70**) in the APP^+ uptake assay.

The hybrid analogs were also evaluated in intracellular Ca^{2+} imagining to confirm their mechanism of action. Intracellular Ca^{2+} imagining was conducted for the monoamine transporter substrate and this would tell us if our analogs have any substrate activity or any mixed action. The analogs were evaluated only at a single concentration (10 x IC_{50}) and none of the analogs were found to have substrate activity.

The hybrid analogs in the present study were found to be DAT reuptake inhibitors. We carried out a comparison between the DAT reuptake functional potency and radioligand binding affinity for 25 *t*MP analogs with substituents at the 2-, 3-, and 4-position of the aryl ring. We obtained a correlation coefficient (r) of 0.98 between the two data sets, which suggested that the functional potency of *t*MP analogs parallels their binding affinity at DAT. Therefore, we were able to correlate our APP^+ data with the literature binding data for *t*MP (**70**), and obtained a high correlation (r = 0.91). These studies suggested that the SAR of *t*MP (**70**) analogs could be applicable to the present cathinone-related compounds as DAT reuptake inhibitors.

Aim 3. To determine the necessity of the carbonyl oxygen atom of synthetic cathinones for DAT reuptake inhibition

Many investigators have conducted SAR studies on the ester group of *t*MP (**70**) with various alkyl and aryl substituents.[8,123,124] DAT binding studies conducted by Misra et al.[8] showed that the ester group of *t*MP (**70**) can be replaced by other groups such as a methoxymethyl (i.e., **126**), hydroxymethyl (i.e., **125**), and an amide (i.e., **129**). To determine the influence of the carbonyl oxygen atom on the action of hybrid analog **161**, we synthesized the descarbonyl analog **169**, to give an amphetamine-type analog. We conducted docking and HINT studies on analog **169** using our hDAT homology model and later evaluated the DAT functional activity of **169** in an APP^+ uptake and intracellular Ca^{2+} assay.

A. Docking studies on analog 169

As described in the results of Aim 1, we sketched analog **169** in SybylX 2.1.1 and docked it ten times in one hundred hDAT homology models. We found the presence of a hydrogen bond between the piperidine nitrogen atom and Asp79 similar to what we found with parent analog **161** and *t*MP (**70**). Since analog **169** does not have the carbonyl oxygen atom, the hydrogen bond interaction between the oxygen atom and Ser422 was lost. Figure 41a. shows the docking of analog **169** (orange) in our hDAT model and the hydrogen bond interaction is represented by red broken line and figure 41b. show analog **169** is a space-filling spheres.

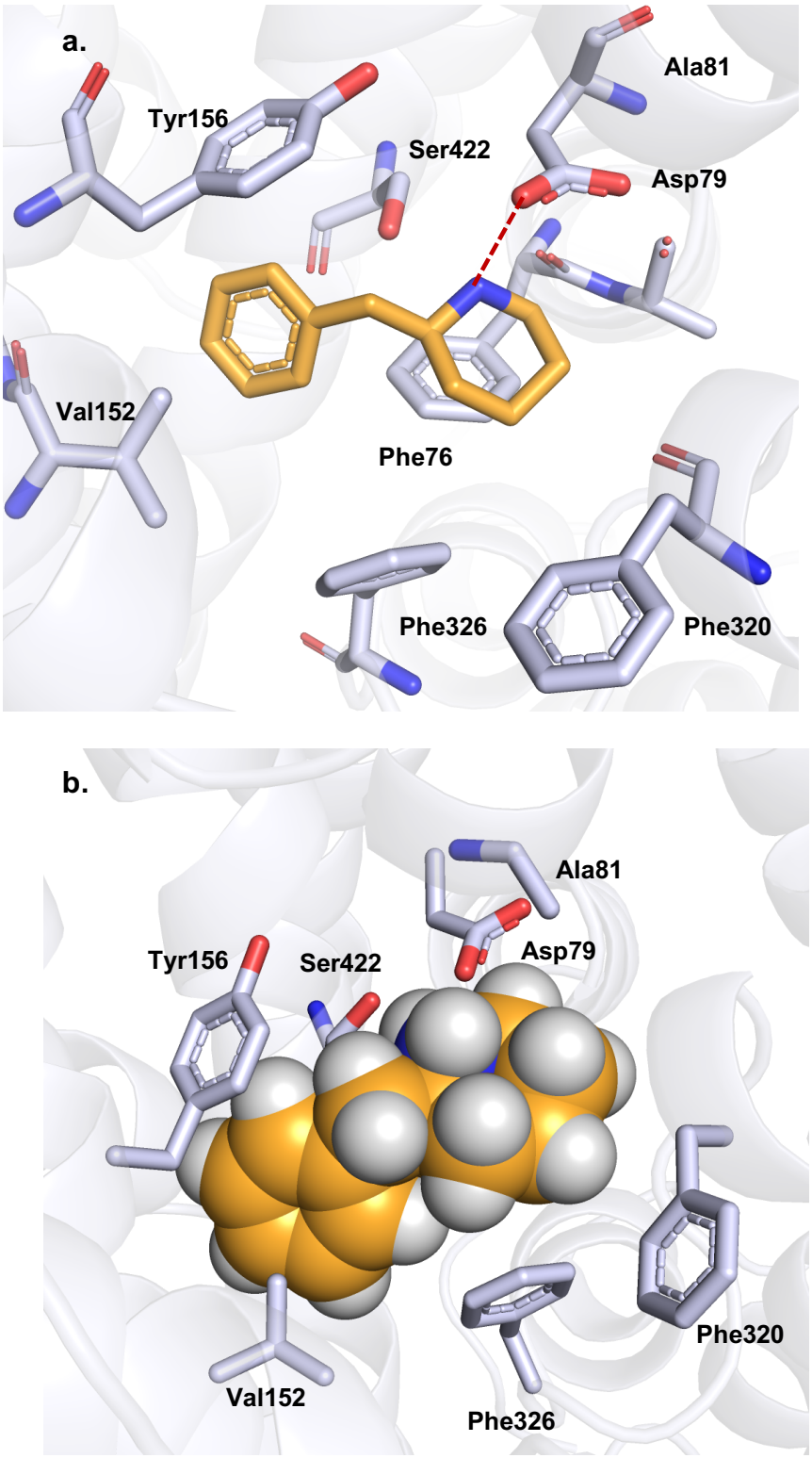

Figure 41. a. Analog **169** (orange) docked in our hDAT model and red broken line shows interaction between piperidine nitrogen atom and Asp79. **b.** Analog **169** (orange) shown is space-filling spheres.

Based on our docking studies, we predicted that analog **169** might be less potent than our parent analog **161**, since it loses one hydrogen bond interaction with Ser422 due to the absence of the carbonyl oxygen atom. Figure 42a shows overlapping structures of analog **161** and **169**, Figure 42b shows a side view of the overlapping structures. Both analogs **161** (forest green) and **169** (orange) were found to have similar poses.

a.

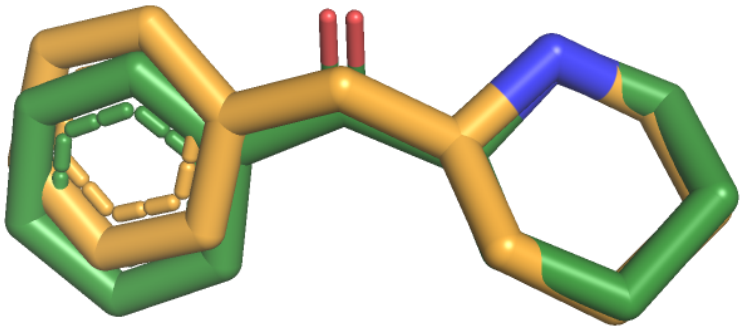

b.

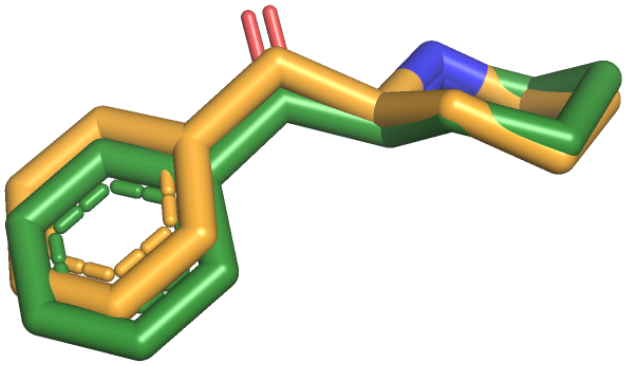

Figure 42. a. Overlapping structures of analogs **161** (forest green) and **169** (orange). **b**. showing the side view of the structures.

B. HINT analysis

HINT studies were conducted on the descarbonyl analog **169** using Sybyl 8.1. A high positive total HINT score (1508) was obtained indicating that analog **169** had favorable interactions with the protein. Table 18 shows the breakdown of favorable and unfavorable interactions between analog **169** and our hDAT model.

Table 18. Table showing distribution of favorable (green) and unfavorable (red) HINT score for analog **169**.

Ligand	Total HINT score	Favorable score			Unfavorable score		
		Hydrogen bond	Acid/ Base	Hydrophobic	Acid/ Acid	Base/ Base	Hydrophobic/ Polar
169	1508	924	784	508	-103	3.2	-610
161	995	1007	761	482	-108	-329	-817
***t*MP (70)**	575	1245	933	441	-79	-912	-1053

C. Synthesis

The synthesis of the descarbonyl analog **169** was straightforward. 2-Benzoylpyridine (**172**) was reduced on a Parr hydrogenator in the presence of 5% Pt/C and AcOH to give the alcohol intermediate (i.e., **173**). The reaction progress was monitored using TLC analysis and no further reduction occurred. A stronger acid was added in order to reduce the hydroxy group. Perchloric acid was added in a catalytic amount and the reaction mixture was allowed to undergo reduction on the Parr hydrogenator for 72 h, eventually giving us our desired product **169** (Scheme 7).

Scheme 7[a]. Synthesis of analog **169**.

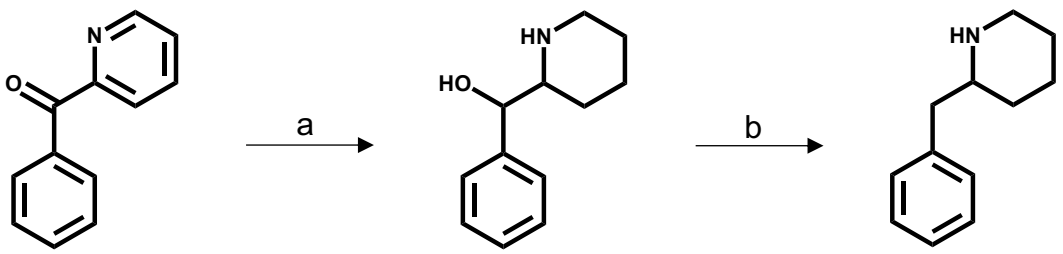

172 **173** **169**

[a]Reagents and conditions: a. AcOH, 5% Pt/C, 30-40 psi, rt, 6h; b. AcOH, $HClO_4$, 5% Pt/C, 50-55 psi, rt, 72h.

D. APP^+ uptake assay

During the synthesis of analog **169**, phenyl(2-piperidinyl)methanol (**173**) was obtained as an intermediate. Therefore, we included analog **173** in our functional studies. As described in results and discussion of Aim 2, preliminary studies were conducted on analogs **169** and **173** at two concentrations (1 and 10 μM). Figure 43 shows the trace obtained from the preliminary studies of APP^+ uptake studies. From the results obtained in the preliminary studies, complete dose-response studies were conducted to obtain IC_{50} values. Figure 44 shows the dose-response curves of analogs **169** and **173** and Table 19 shows their IC_{50} values.

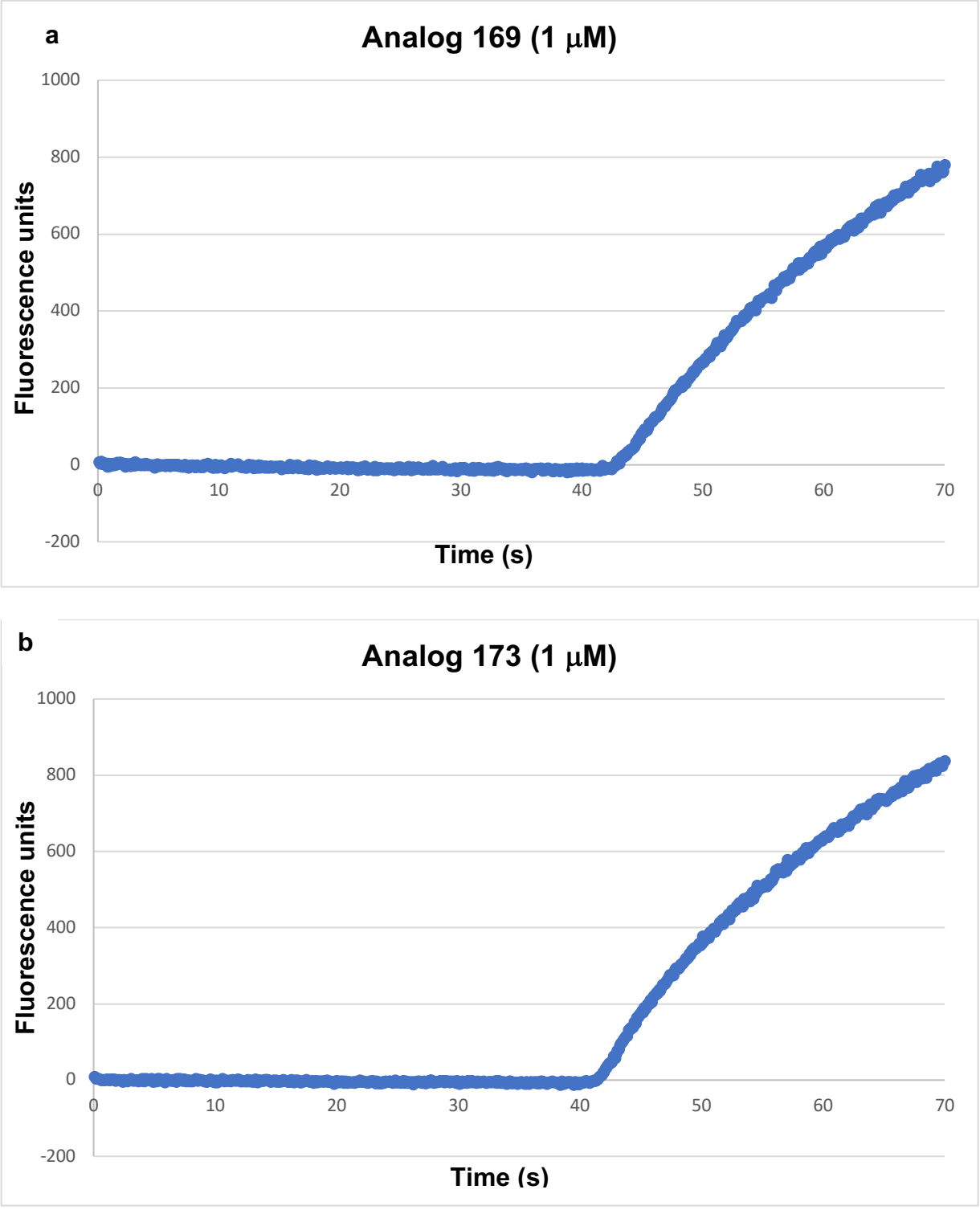

Figure 43. Raw traces of analogs **169** (**a**, 1 μM) and **173** (**b**, 1 μM) in the APP^+ uptake assay using live-cell imaging.

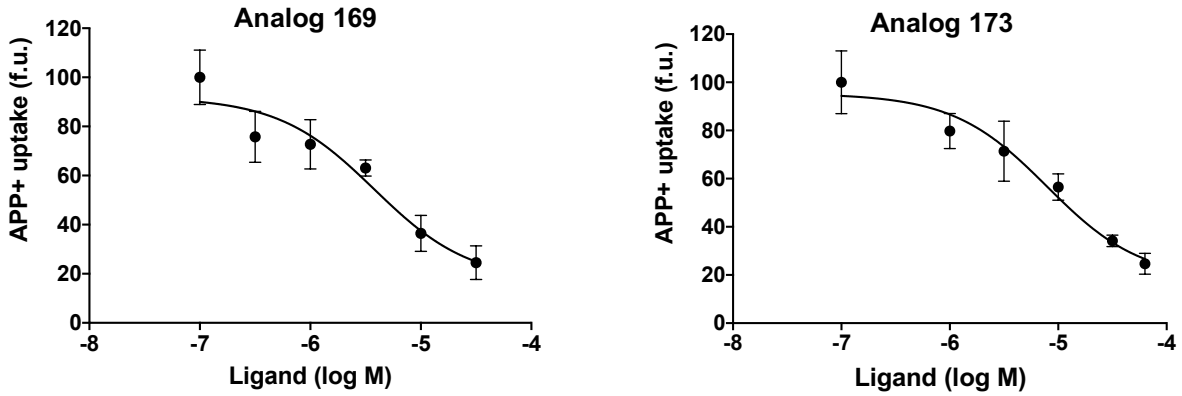

Figure 44. Dose-response curves of analogs **169** and **173** in the APP^+ uptake assay.

Table 19. IC_{50} values of analogs **169**, **173** and **161** in APP^+ uptake assay.

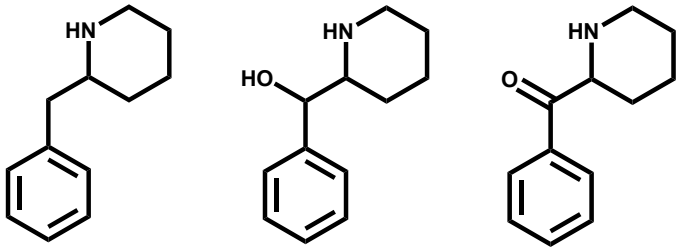

169 **173** **161**

Ligand	IC_{50} (nM) ± S.E.M.	pIC_{50}
169	3780 ± 1200	5.42
173	7900 ± 2200	5.10
161	1080 ± 190	5.96

As predicted by our docking studies, analog **169** was found to be 3.5-fold less potent than the parent analog **161**, and this suggests that the carbonyl oxygen atom of the parent analog is not critical for the compound to act as a DAT reuptake inhibitor. Nevertheless,

the carbonyl group appears to help in improving the potency of these types of analogs. On the contrary, analog **173**, was found to be a weak DAT reuptake inhibitor in our assay. Analog **173**, contains two chiral centers and therefore consists of four isomers (diastereomers); however, for the present study, we only synthesized the racemic mixture. Hence, at this point we cannot predict which isomer is responsible for its activity. It might be possible that only one isomer is the active isomer, and due to the presence of other inactive isomers, activity appears to be low. In order to know which isomer is responsible for activity, we would have to synthesize all the four isomers and evaluate their functional activity at DAT.

E. Intracellular Ca^{2+} determination

Like other analogs mentioned in Aim 2, we evaluated analog **169** at approximately 10-times its IC_{50} value to check for its releasing effects at DAT. Figure 45 shows the trace obtained from the Ca^{2+} assay, DA (10 μM) was used as the substrate. In the assay, HEK293 cells were first perfused with the imaging solution (IS) for 10 s, followed by DA for 5 s which gives the first peak (Figure 45), the DA is then washed for 30 s and then analog **169** was applied for 30 s and no peak was seen. Finally, **169** and DA mixture was applied which gave the second peak. Analog **169** acted as a DAT blocker due to the reduced intensity of the second peak as compared to the first peak. The peak intensity is directly proportional to the number of Ca^{2+} channels that are open. It can be concluded that analog **169** does not have any DAT releasing activity.

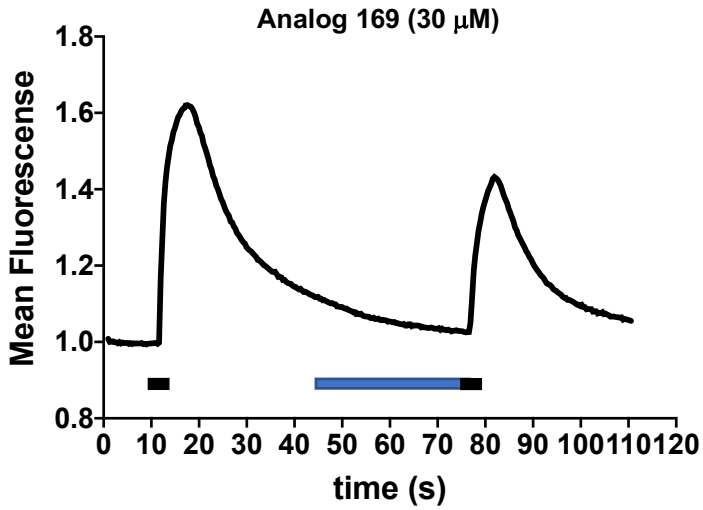

Figure 45. Graph obtained from the Ca^{2+} assay for DA (left), analog **169**, and analog **169** in combination with DA (right).

F. Discussion

Previous studies have showed that the ester group of *t*MP is not required for its binding at DAT and it can be replaced by other functional groups such as hydroxylamine, amide and methoxymethyl.[8] Therefore, in order to understand the importance of the carbonyl oxygen atom for the activity of synthetic cathinones, we synthesized descarbonyl analog **169** and conducted docking and HINT studies using our hDAT models, and evaluated it in the APP^+ uptake and intracellular Ca^{2+} assay. It might be noted that **169** was not identical to **130** (Table 12) reported earlier.

Our docking study showed us that there was one hydrogen bond interaction between the piperidine nitrogen atom and Asp79. Unlike our parent analog **161** and *t*MP (**70**), analog **169** does not have a substituent on the βC and therefore it lost the hydrogen bond

interaction with Ser422 which was seen in the previous two analogs. Due to this loss of a hydrogen bond interaction we predicted that analog **169** might be less potent than analog **161** for its DAT functional activity.

Supporting our docking studies, analog **169** was found to be 3.5-fold less potent than analog **161** in APP^+ uptake studies. Analog **173** was an intermediate obtained during the synthesis of analog **169** and therefore we included it in our APP^+ uptake studies. Analog **173** was found to be 7.3- and 2-fold less potent than analogs **161** and **169**, respectively. However, analog **173** has two chiral centers and therefore contains four isomers. During the synthesis of analog **169**, we only obtained a racemic mixture and hence we cannot predict that which isomer of analog **173** is responsible for its activity. In order to identify the eutomer we will have to synthesize all the four isomers and evaluate them in the APP^+ uptake assay.

Along with the APP^+ uptake assay, analog **169** was also evaluated in an intracellular Ca^{2+} determination assay. Analog **169** did not have a releasing effect at DAT even at 30 μM concentration. From our current study we found that the carbonyl oxygen atom is not critical for the compound to act as a DAT reuptake inhibitor, however it helps in improving the activity of these types of synthetic cathinones.

V. Conclusion and future work

A parallel SAR approach using *t*MP has provided us with important information and helped expand our knowledge about the structural features of synthetic cathinones as DAT reuptake inhibitors. *t*MP, apart from being used for the treatment of ADHD in children, is a Schedule II drug and it shares some structural similarity with synthetic cathinones. Similar to newer synthetic cathinones, *t*MP primarily acts at DAT as a reuptake inhibitor and is widely abused. In our current study we synthesized a series of methylphenidate/cathinone hybrid compounds and evaluated their functional activity at DAT.

It was found that analogs bearing structural features of MP do not alter the activity of related cathinones from being DAT reuptake inhibitors. Previously, our laboratory had shown that a bulky amine and/or extended α-side chain changes the activity of synthetic cathinones from releasers to reuptake inhibitors at DAT.[2] The current research supported

our previous findings showing that when the α-side chain of α-PVP was ligated to the terminal amine to form a piperidine ring and the methyl ester group of MP is replaced by carbonyl group it retained DAT reuptake inhibition activity.

Our docking studies using hDAT homology models suggested that *t*MP and 2-benzoylpiperidines might bind at DAT in a similar manner. 2-Benzoylpiperidine analogs (**161**-**168**) in our series inhibited the APP^+ signal in a live-cell imaging assay and did not induce depolarization in the Ca^{2+} assay, indicating that this series of compounds act as reuptake inhibitors at DAT. Similar to the *t*MP series, we also showed that the 3,4-disubstituted analog (i.e., **168**) increases the potency of the hybrid series as DAT reuptake inhibitors. A significant correlation (r = 0.91) was obtained between the binding affinity of the *t*MP series and the functional activity of the 2-benzoylpiperidine series. These findings suggest that the SAR of *t*MP might be applicable to novel synthetic cathinones (i.e., the 2-benzoylpiperidine series) that are yet to be seen on the market. Additionally, it also suggests that our hDAT models were reliable as we were able to successfully predict that the 2-benzoylpiperidines would be less potent than *t*MP in functional studies.

We also showed that the carbonyl oxygen atom of **161** is not important for the compound to act as a DAT reuptake inhibitor as our descarbonyl analog (2-benzylpiperidine, **169**) retained activity; however, the carbonyl oxygen atom helps to improve the potency at DAT as a reuptake inhibitor. Our homology model was also able to predict that the descarbonyl analog would be less potent than **161**, due to the loss of a hydrogen bonding feature

between the carbonyl oxygen atom and Ser422. This study has provided valuable insight and helped our understanding a complicated puzzle i.e., the SAR of synthetic cathinones as reuptake inhibitors.

The next question is whether these hybrid analogs behave similarly in in vivo studies and if they have abuse liability or potential therapeutic effects. Data from in vivo studies would help us correlate it with our in vitro data and provide additional support to our findings. It would also be interesting to know how the 2-benzoylpiperidine series behaves at NET and SERT, and also inform us about their selectivity profile among the three transporters. *t*MP is known to act as a NET reuptake inhibitor as well as a DAT reuptake inhibitor and therefore it would be fascinating to know if our series also has similar effects at NET. Additionally, it would be valuable to synthesize a similar series of benzoylpipridines with 2- and 3-substituents and conduct parallel SAR studies with the *t*MP series. In the *t*MP series, substitution at 2-position was not tolerated and substitution at the 3-position was found to result in compounds approximately equipotent to the 4-substituted analogs.[9] It would be interesting to see if the hybrid analogs with substituents at the 2- and 3-position follow the same trend or not. If so, we would be able to say, with greater confidence that the SAR of *t*MP is be applicable to synthetic cathinones.

VI. Experimental

A. Molecular modeling studies and HINT analysis

1. Homology modeling

Sequence of the template dDAT (PDB ID: 4XP4) was retrieved as FASTA files from the Protein Databank (PDB). Prior to the alignment the sequence was prepared be removal of water molecules, ligands and surfactants. Three-dimensional homology models of hDAT was prepared using MODELLER 9.10 (University of California San Francisco, San Francisco, CA) using dDAT as the template and the models were validated by docking cocaine.

2. Docking studies

The ligands were sketched in SybylX 2.1.1 (Tripos International) and energy minimized using Gasteiger-Hückel charges (dielectric constant = 4.0). Docking studies were conducted using GOLD suite 5.6.1 (Cambridge Crystallographic Data Centre, Cambridge, UK), and GOLD score was chosen as the scoring function. The binding pocket was defined as a spherical region of radius of 5 Å using Asp79 of hDAT. All the docking poses were clustered on the basis of similarity of poses within a RMSD of 1 Å. The clusters were visually inspected using SybylX 2.1.1 (Tripos International) and the

best fitting pose was merged with the model. The ligand-transporter complex were energy minimized using Tripos Force Field (Gasteiger- Hückel charges, dielectric constant = 4.0).

3. HINT analysis

The ligand-transporter complex was scored using HINT (Hydropathic INTeraction) in Sybyl 8.1 in order to quantify the interactions observed in the modeling studies. The logP of ligands were calculated using the calculate option, whereas hDAT was calculated using the dictionary option with the default settings. The atom-based breakdown of HINT score was analyzed to determine the contributions of favorable and unfavorable interactions of the individual atoms to the interactions with the amino acid residues at the binding region of hDAT. The favorable interactions comprised of hydrogen bond, acid/base, and hydrophobic interactions, whereas unfavorable interactions comprised of acid/acid, base/base, and hydrophobic/polar interactions.

B. Synthesis

Melting points were measured with a Thomas-Hoover or MEL TEMP (for compounds with mp >200 °C) apparatus using glass capillaries. Compounds were characterized by ^{1}H NMR, mass spectrometry (MS), and IR spectroscopy. ^{1}H NMR spectra were recorded using a Bruker AXR 400 MHz spectrometer using tetramethylsilane (TMS) as an internal standard. The spectra were reported by their peak position in parts per million (ppm) downfield from TMS, and their splitting pattern (s = singlet, d = doublet, t = triplet, q = quartet, dd = doublet of doublets, m = multiplet), coupling constant (J, Hz) and integration. IR spectra were recorded using a Thermo Nicolet iS10 FT-IR, and MS were recorded using a Waters Acquity tandem quadrupole (TQD) instrument with electrospray ionization. Reactions were routinely monitored by thin-layer chromatography (TLC) using silica gel GHLF plates (250 mm, 2.5 x 10 cm; Analtech Inc. Newark, DE), and flash chromatography was performed on a CombiFlash Companion/TS (Teledyne Isco Inc. Lincoln, NE). All final compounds were prepared as water-soluble hydrochloride salts. The purity of the novel compounds was determined by elemental analysis for C, H and N (Atlantic Micolab Inc.; Norcross, GA) and the results were within 0.4% of the calculated values. The $AlCl_3$ was freshly sublimed for every reaction.

2-Benzoylpiperidine Hydrochloride (161)

Jones reagent (1.78 mL, 4.47 mmol), prepared from chromium(VI) oxide (2.50 g) and concentrated H_2SO_4 (2.50 mL), and H_2O (7.50 mL) was added in a dropwise manner to a solution of phenyl(2-piperidinyl)methanol (**173**) in a mixture of acetone (10 mL) and H_2O (2 mL) at 0 °C. The reaction mixture was allowed to stir at 0 °C for 1 h and then at room temperature for 18 h. The reaction mixture was basified by addition of a saturated solution of $NaHCO_3$ (tp pH = ~8). The aqueous portion was extracted with EtOAc (3 x 30 mL) and the combined organic portion was dried (Na_2SO_4), filtered, and then evaporated to dryness under reduced pressure to yield a yellow solid. The solid was dissolved in Et_2O and HCl gas was allowed to slowly bubble through the solution yielding a white solid. The solid was collected by filtration and recrystallized from *i*-PrOH to yield 0.11 g (16%) of **161** as a white solid: mp 220-221 °C (lit.[146] mp 225-227 °C). IR (diamond, cm^{-1}): 1685 (C=O). ^1H NMR (DMSO-d_6) δ: 1.44-1.47 (m, 1H, CH), 1.50-1.77 (m, 4H, 2 X CH_2), 1.99-2.18 (m, 1H, CH), 2.34-2.40 (m, 1H, CH), 3.18-3.24 (m, 1H, CH), 4.92-5.12 (m, 1H, CH), 7.59 (t, 2H, *J* = 7.9 Hz, Ar-H), 7.72 (m, 1H, *J* = 8.5 Hz, Ar-H), 8.05 (dd, *J* = 7.0 Hz, 2H, ArH), 9.98 (br s, 2H, NH^+).

2-(4-Methylbenzoyl)piperidine Hydrochloride (162)

In a 2-neck flask, PCl_3 (1.31 g, 9.59 mmol) was added to a solution of *N*-Boc-*dl*-pipecolic acid (**174**) (2 g, 8.72 mmol) in anhydrous toluene (50 mL) under an N_2 atmosphere and the reaction mixture was allowed to stir for 2 h at 60 °C. Aluminum trichloride (3.48 g, 26.16 mmol) was added portionwise at 0 °C and the mixture was allowed to stir at room temperature overnight. The reaction mixture was quenched by careful pouring into ice-cold H_2O (50 mL) and extracted with EtOAc (50 mL). The aqueous portion was basified with NaOH (3 M, to pH 12), and extracted with EtOAc (3 x 50 mL). The combined organic portion was dried (Na_2SO_4), filtered, and the filtrate evaporated to dryness under reduced pressure to yield a yellow oil. The oily residue was dissolved in Et_2O and converted to its HCl salt by the addition of a saturated solution of HCl(g) in Et_2O. The solid material was collected by filtration and recrystallized from EtOH/Et_2O to give 0.49 g (23%) of compound **162** as a white solid: mp 258-261 °C. ^{1}H NMR (DMSO-d_6) δ: 1.29-1.55 (m, 1H, CH), 1.56-1.90 (m, 4H, 2 X CH_2), 1.95-2.20 (m, 1H, CH), 2.42 (s, 3H, CH_3), 2.79-3.10 (m, 1H, CH), 3.27-3.51 (m, 1H, CH), 4.79-5.27 (m, 1H, CH), 7.43 (d, 2H, J = 8.0 Hz, Ar-H), 7.96 (d, 2H, J = 8.2 Hz, Ar-H), 8.87 (br s, 1H, NH), 9.36 (br s, 1H, NH^+); IR (diamond, cm^{-1}): 1677 (C=O), 3453 (NH); Anal. Calcd ($C_{13}H_{17}NO \cdot HCl \cdot 0.1\ H_2O$) C, 64.64; H, 7.59; N, 5.79. Found C, 64.61; H, 7.60; N, 5.84.

2-(4-Ethylbenzoyl)piperidine Hydrochloride (163)

In a 2-neck flask, PCl_3 (0.50 g, 2.18 mmol) was added to a solution of *N*-Boc-*dl*-pipecolinic acid (0.32 g, 2.39 mmol) in anhydrous ethylbenzene (50 mL) under an N_2 atmosphere and the reaction mixture was allowed to stir for 2 h at 60 °C. Freshly sublimed $AlCl_3$ (0.87 g, 6.54 mmol) was added portionwise to the reaction mixture at 0 °C and the mixture was allowed to stir at room temperature overnight. The reaction mixture was quenched by careful pouring into ice-cold H_2O (50 mL) and extracted with EtOAc (50 mL). The aqueous portion was basified with NaOH (3 M, to pH 12), and extracted with EtOAc (3 x 50 mL). The combined organic portion was dried (Na_2SO_4), filtered, and then evaporated to dryness under reduced pressure to yield a yellow oil. The oily residue was dissolved in Et_2O and converted to its HCl salt by adding a saturated solution of HCl (g) in Et_2O. The solid obtained was collected by filtration and dried to give 0.35 g of a crude white solid that was recrystallized from *i*-PrOH to give 0.08 g (14%) of **163** as a white solid: mp 238-240 °C; ^{1}H NMR (DMSO-d_6) δ: 1.07-1.12 (m, 3H, CH_3), 1.20-1.23 (m, 2H, CH_2), 1.45-1.47 (m, 1H, CH), 1.49-1.77 (m, 4H, 2 X CH_2), 2.08-2.12 (m, 1H, CH), 2.96-2.99 (m, 2H, CH_2), 5.05-5.11 (m, 1H, CH), 7.46 (d, 2H, *J* = 8.6 Hz, Ar-H), 7.98 (d, 2H, *J* = 8.2 Hz, Ar-H), 8.87 (br s, 1H, NH), 9.37 (br s, 1H, NH^+); IR (diamond, cm^{-1}) 1668 (C=O), 3026 (NH); Anal. Calcd for ($C_{14}H_{19}NO \cdot HCl \cdot 0.1\ H_2O$) C, 66.26; H, 7.94; N, 5.52. Found: C, 65.07; H, 7.87; N, 5.63.

2-(4-Chlorobenzoyl)piperidine Hydrochloride (164)

2-(4-Chlorobenzoyl)piperidine-1-carbaldehyde (**176**) in EtOH (2 mL) and HCl (3 N, 2 mL) was heated at reflux for 3 h, cooled to room temperature, and the solution was evaporated to dryness under reduced pressure to give 0.26 g (21%) of a crude white solid which was recrystallized from *i*-PrOH to give 0.03 g (11%) of compound **164** as a white solid: mp 282-284 °C. ^{1}H NMR ($CDCl_3$) δ: 1.33-1.38 (m, 1H, CH), 1.89-2.07 (m, 4H, 2 X CH_2), 2.48-2.54 (m, 1H, CH), 3.06-3.17 (m, 1H, CH), 3.60-3.51 (m, 1H, CH), 4.88-4.78 (m, 1H, CH), 7.38 (d, 2H, *J* = 8.1 Hz, Ar-H), 7.79 (d, 2H, *J* = 8.1 Hz, Ar-H), 9.20 (br s, 1H, NH), 10.54 (br s, 1H, NH^+); IR (diamond, cm^{-1}): 1681 (C=O); Anal. Calcd for ($C_{12}H_{14}ClNO \cdot HCl$) C, 55.40; H, 5.81; N, 5.38. Found: C, 55.10; H, 5.91; N, 5.42.

2-(4-Bromobenzoyl)piperidine Hydrochloride (165)

2-(4-Bromobenzoyl)piperidine-1-carbaldehyde (**177**) was heated at reflux in EtOH (2 mL) and HCl (3 N, 2 mL) for 3 h, cooled to room temperature and the solution evaporated to dryness under reduced pressure to give a crude white solid which was recrystallized from *i*-PrOH to give 0.12 g (13%) of compound **165** as a white solid: mp 250-252 °C. ^{1}H NMR (DMSO-d_6) δ: 1.06-2.03 (m, 4H, 2 X CH_2), 2.18-2.39 (m, 2H, CH), 3.01-3.21 (m, 1H, CH), 3.43-3.60 (m, 1H, CH), 4.85-5.95 (m, 1H, CH), 7.74 (d, 2H, *J* = 7.0 Hz, Ar-H), 7.88 (d, 2H, *J* = 7.8 Hz, Ar-H), 8.76 (br s, 1H, NH), 9.45 (br s, 1H, NH^+); IR (diamond, cm^{-1}): 1678 (C=O), 3456 (NH); Anal. Calcd for ($C_{12}H_{14}BrNO \cdot HCl$) C, 47.31; H, 4.96; N, 4.59. Found: C, 47.52; H, 5.08; N, 4.60.

2-(4-Methoxybenzoyl)piperidine Hydrochloride (166)

In a 3-neck flask, a solution of *tert*-butyl 2-(methoxy(methyl)carbamoyl)piperidine-1-carboxylate (**178**) (0.80 g, 2.93 mmol) in anhydrous ether (10 mL) was brought to -23 °C under an N_2 atmosphere, and intermediate 4-(methoxyphenyl)lithium (**182**) was added dropwise via syringe over 15 min. The reaction mixture was allowed to stir at -23 °C for 3 h, warmed to room temperature, and quenched by carefully pouring into an ice-cold solution of 1M KH_2PO_4 (30 mL). The aqueous layer was extracted with EtOAc (3 x 30 mL) and the combined organic portion was dried (Na_2SO_4), filtered, and then evaporated to dryness under reduced pressure to yield a crude residue which was purified by column chromatography (silica gel; hexane/EtOAc; 10:0 to 2:8) to afford a yellow oil. The oily residue was stirred in methanolic HCl overnight and evaporated to dryness to yield a yellow solid which upon which upon recrystallization from *i*-PrOH yielded 0.03 g (3%) of compound **166** as a white solid: mp 218-220 °C. ^{1}H NMR (DMSO-d_6) δ: 1.03-1.05 (m, 1H, CH), 1.41-1.49 (m, 4H, 2 X CH_2), 1.78-1.76 (m, 1H, CH), 2.95-2.97 (m, 1H, CH), 3.81-3.89 (m, 1H, CH), 5.03-5.07 (m, 1H, CH), 7.12-7.14 (d, 2H, J = 6.7 Hz, Ar-H), 8.03-8.05 (d, 2H, J = 8.8 Hz, Ar-H), 9.01 (br s, 1H, NH), 9.37 (br s, 1H, NH^+); IR (diamond, cm^{-1}): 1677 (C=O); Anal. Calcd ($C_{13}H_{17}NO_2 \cdot HCl \cdot 0.2\ H_2O$) C, 61.05; H, 7.09; N, 5.48. Found: C, 59.81; H, 6.76; N, 5.34.

2-(4-Trifluoromethylbenzoyl)piperidine Hydrochloride (167)

In a 3-neck flask, a solution of *tert*-butyl 2-(methoxy(methyl)carbamoyl)piperidine-1-carboxylate (**178**) (0.39 g, 1.32 mmol) in anhydrous ether (5 mL) was brought to -23 °C under an N_2 atmosphere, and intermediate 4-(trifluoromethylphenyl)lithium (**183**) was added dropwise via syringe over 15 min. The reaction mixture was allowed to stir at -23 °C for 3 h, warmed to room temperature, and quenched by carefully pouring into an ice-cold solution of 1M KH_2PO_4 (20 mL). The aqueous layer was separated and extracted with EtOAc (3 x 30 mL) and the combined organic portion was dried (Na_2SO_4), filtered, and then evaporated to dryness under reduced pressure to yield a crude residue which was purified by column chromatography (silica gel; hexane/EtOAc; 10:0 to 2:8) to afford a yellow oil. The oily residue was stirred in methanolic HCl overnight and evaporated to dryness to yield a yellow solid which, upon recrystallization from *i*-PrOH yielded, 0.12 g (26%) of compound **167** as a white solid: mp 273-275 °C. ^{1}H NMR (DMSO-d_6) δ: 1.03-1.05 (m, 1H, CH), 1.48-1.51 (m, 4H, 2 X CH_2), 1.71-1.73 (m, 1H, CH), 1.81-2.12 (m, 1H, CH), 3.76-3.79 (m, 1H, CH), 5.19-5.22 (m, 1H, CH), 7.99-8.01 (d, 2H, J = 8.0 Hz, Ar-H), 8.25-8.27 (d, 2H, J = 8.2 Hz, Ar-H), 9.02 (br s, 1H, NH), 9.54 (br s, 1H, NH^+); IR (diamond, cm^{-1}): 1689 (C=O); Anal. Calcd ($C_{13}H_{14}F_3NO \cdot HCl$) C, 53.16; H, 5.15; N, 4.77. Found: C, 53.25; H, 5.22; N, 4.78.

2-(3,4-Dichlorobenzoyl)piperidine Hydrochloride (168)

In a 3-neck flask, a solution of *tert*-butyl 2-(methoxy(methyl)carbamoyl)piperidine-1-carboxylate (**178**) (0.34 g, 1.26 mmol) in anhydrous ether (5 mL) was brought to -23 °C under an N_2 atmosphere, and intermediate 3,4-(dichlorophenyl)lithium (**184**) was added dropwise via syringe over 15 min. The reaction mixture was allowed to stir at -23 °C for 3 h, warmed to room temperature, and quenched by carefully pouring in ice-cold solution of 1M KH_2PO_4 (20 mL). The aqueous layer was extracted with EtOAc (3 x 30 mL) and the combined organic portion was dried (Na_2SO_4), filtered, and then evaporated to dryness under reduced pressure to yield a crude residue which was purified by column chromatography (silica gel; hexane/EtOAc; 10:0 to 2:8) to afford a yellow oil. The oily residue was stirred in methanolic HCl overnight and evaporated to dryness to yield a yellow solid which upon recrystallization from *i*-PrOH yielded 0.02 g (13%) of compound **168** as a beige solid: mp 273-275 °C. ^{1}H NMR (DMSO-d_6) δ: 1.05-1.09 (m, 1H, CH), 1.50-1.55 (m, 4H, 2 X CH_2), 1.71-1.75 (m, 1H, CH), 1.89-2.10 (m, 1H, CH), 3.71-3.78 (m, 1H, CH), 5.25-5.28 (m, 1H, CH), 7.85-7.88 (d, 1H, J = 7.7 Hz, Ar-H), 7.91-7.95 (d, 1H, J = 7.9 Hz, Ar-H), 8.30 (s, 1H, Ar-H), 9.02 (br s, 1H, NH), 9.54 (br s, 1H, NH^+); IR (diamond, cm^{-1}): 1683 (C=O); HRMS (ESI-TOF) *m/z*: $[M + H]^+$ calcd for $C_{12}H_{14}Cl_2NO$, 258.0448; found, 258.0452.

2-Benzylpiperidine Hydrochloride (169)

To a solution of phenyl (2-piperidinyl)methanol (**173**) (0.88 g, 4.68 mmol) in AcOH (40 mL) and perchloric acid (2 mL), 5% Pt/C (0.35 g) was added. The mixture was treated with H_2 gas on a Parr hydrogenator at 50-55 psi for 72 h. The reaction mixture was filtered through Celite and evaporated to dryness to yield a yellow oil. The oily residue was basified with NaOH (3M, to pH ~ 12) and extracted with methylene chloride (3 x 50 mL). The combined organic portion was dried (Na_2SO_4) and evaporated to dryness under reduced pressure to yield a white solid. The solid was dissolved in Et_2O and HCl gas was allowed to slowly bubble through the solution yielding a white solid. The solid obtained was filtered and dried to give a solid which upon recrystallization from *i*-PrOH yielded 0.45 g (45%) of compound **169** as a white solid: mp 135-136 °C (lit.[126] mp 130-135 °C). ^{1}H NMR (DMSO-d_6) δ: 1.08-1.85 (m, 6H, 3 x CH_2), 2.36-2.83 (m, 4H, 2 X CH_2), 3.27-3.34 (m, 1H, CH), 7.14 (t, 2H, *J* = 6.0 Hz, Ar-H), 7.20 (m, 1H, *J* = 7.2 Hz, Ar-H), 7.37 (dd, *J* = 8.5 Hz, 2H, ArH). Note: This compound was different than that (i.e., **130** Table 12) previously reported.[125]

Piperidine-2-carbonyl chloride Hydrochloride (171)

Pipecolic acid (**170**) (1 g, 7.74 mmol) was added to a suspension of PCl_5 (1.62 g, 7.74 mmol) in anhydrous CH_2Cl_2 (20 mL) at 0 °C under an N_2 atmosphere. The reaction mixture was allowed to warm to room temperature and stirred for 3 h. The solvent was evaporated under reduced pressure and further dried under high vacuum to yield 1.02 g of compound **171** as a white solid: mp 130-132 °C (lit.[147] mp 130 °C). IR (diamond, cm^{-1}): 1770 (C=O).

Phenyl (2-piperidinyl)methanol (173)

Pt/C (5%, 0.32 g) was added to a solution of 2-benzoylpyridine (1 g, 5.45 mmol) in AcOH (50 mL). The mixture was treated with H_2 gas in a Parr hydrogenator at 30-40 psi for 6 h. The reaction mixture was filtered through Celite and the filtrate was evaporated to dryness to yield a yellow oil. The oily residue was basified with NaOH (3M, to pH ~ 12) and extracted with methylene chloride (3 x 50 mL). The combined organic portion was dried (Na_2SO_4), filtered, and the filtrate evaporated to dryness under reduced pressure to yield a white solid which upon recrystallization with *i*-PrOH yielded 0.83 g (80%) of compound **173** as a white solid: mp 135-136 °C (lit.[148] mp 137 °C); ^{1}H NMR (DMSO-d_6) δ: 1.40-1.48 (m, 1H, CH), 1.56-1.81 (m, 4H, 2 X CH_2), 1.91-2.23 (m, 2H, CH_2), 2.39-2.81 (m, 1H, CH), 3.27-3.34 (m, 1H, CH), 4.71-4.92 (m, 2H, CH_2), 7.49 (t, 2H, *J* = 8.1 Hz, Ar-H), 7.54 (m, 1H, *J* = 7.5 Hz, Ar-H), 8.1 (dd, *J* = 7.0 Hz, 2H, ArH); IR (diamond, cm^{-1}) 3267 (OH).

***N*-Formyl pipecolic acid (175)**

Acetic anhydride (5 mL) was added in a dropwise manner at 0 °C (ice-bath) to a stirred solution of pipecolic acid (1 g, 7.75 mmol) in HCOOH (10 mL). The reaction mixture was allowed to stir at room temperature for 1 h and quenched by careful addition of distilled H_2O (10 mL). The solvent was evaporated to dryness under reduced pressure to yield a crude white solid which upon recrystallization from 95% EtOH yielded 0.73 g (57%) of compound **175** as a white solid; mp 84-86 °C (lit.[149] mp 85-87 °C); IR (diamond, cm^{-1}) 1621 (C=O). Compound **175** was prepared according to the literature procedure as reported by Pizzorno and Albonico.[149]

2-(4-Chlorobenzoyl)piperidine-1-carbaldehyde (176)

In a 3-neck flask, PCl_3 (0.69 g, 5.03 mmol) was added to a solution of *N*-formyl pipecolic acid[149] (**175**) (0.71 g, 4.57 mmol) in anhydrous chlorobenzene (50 mL) under an N_2 atmosphere and the reaction mixture was allowed to stir for 2 h at 60 °C. Aluminum trichloride (1.82 g, 13.72 mmol) was added portionwise at 0 °C and the reaction mixture was allowed to stir at room temperature overnight. The reaction mixture was quenched by carefully pouring in ice-cold H_2O (50 mL) and washed with EtOAc. The aqueous portion was basified with NaOH (3 M, to pH 12) and extracted with CH_2Cl_2 (3 x 50 mL). The combined organic portion was washed with brine (30 mL), dried (Na_2SO_4), filtered, and then evaporated to dryness under reduced pressure to yield a crude residue which was purified by column chromatography (silica gel; hexane/EtOAc; 10:0 to 5:5) to afford 0.25 g (21%) of compound **176** as a yellow oil; ^{1}H NMR ($CDCl_3$) δ: 1.20-1.90 (m, 4H, 2 X CH_2), 1.94-2.07 (m, 2H, CH_2), 3.15-3.25 (m, 1H, CH), 3.59-3.70 (m, 1H, CH), 5.70-5.80 (m, 1H, CH), 7.61 (d, 2H, *J* = 2.0 Hz, Ar-H), 7.94 (d, 2H, *J* = 4.8 Hz, Ar-H), 8.1 (s, 1H, H); IR (diamond, cm^{-1}): 1660 (C=O).

2-(4-Bromobenzoyl)piperidine-1-carbaldehyde (177)

In a 3-neck flask, PCl_3 (0.61 g, 4.51 mmol) was added to a solution of *N*-formyl pipecolic acid[149] (**175**) (0.64 g, 4.10 mmol) in bromobenzene (50 mL) under an N_2 atmosphere and the reaction was stirred for 2 h at 60 °C. Aluminum trichloride (1.64 g, 12.30 mmol) was added portionwise to the reaction mixture at 0 °C and the reaction mixture was allowed to stir at room temperature overnight. The reaction mixture was quenched by careful pouring in ice-cold H_2O (50 mL) and washed with EtOAc (50 mL). The aqueous portion

was basified with NaOH (3 M, to pH 12), and extracted with CH_2Cl_2 (3 x 50 mL). The combined organic portion was washed with brine (30 mL), dried (Na_2SO_4), filtered and then evaporated to dryness under reduced pressure to yield compound **177** as a yellow oil. The formyl group of compound **177** was deprotected without further analysis.

***tert*-Butyl 2-(methoxy(methyl)carbamoyl)piperidine-1-carboxylate (178)**

In a 3-neck flask, *N,O*-dimethylhydroxylamine hydrochloride (0.50 g, 5.19 mmol) and TEA (1.55 g, 15.30 mmol) were added to a stirred solution of *N*-Boc-*dl*-pipecolinic acid (**174**) (1 g, 4.36 mmol) under an N_2 atmosphere. To this mixture BOP (2.10 g, 4.74 mmol) was added and the reaction mixture was allowed to stir for 6 h at room temperature. The reaction mixture was diluted with methelene chloride (50 mL) and extracted with 1M HCl (1 x 30 mL). The organic portion was washed with $NaHCO_3$, brine, and H_2O, dried (Na_2SO_4), filtered, and evaporated to dryness under reduced pressure and the crude residue was purified by column chromatography (silica gel; hexane/EtOAc; 10:0 to 7:3) to yield 0.90 g (82%) of **178** as white solid: mp 64-66 °C (lit mp[150] 66-68 °C). Compound **178** was prepared using the literature procedure as described by Thai et al.;[142] however, they reported **178** as a colorless oil.

4-(Methoxyphenyl)lithium (182)

In a 3-neck flask, 4-bromoanisole (0.54 g, 2.93 mmol) was allowed to stirred in anhydrous Et_2O (5 mL) at -78 °C under an N_2 atmosphere. To the reaction mixture, a 2.5 M solution of *n*-BuLi in hexane (2.33 mL, 5.84 mmol) was carefully added in a dropwise manner. The reaction mixture was warmed to -40 °C and allowed to stir for 3 h. The intermediate,

although unreported, was synthesized according to a literature procedure for a similar compound.[151] The intermediate, **182**, was used for the next step without characterization for the preparation of **166**.

4-(Trifluoremethylphenyl)lithium (183)

In a 3-neck flask, 4-bromotrifluoromethylbenzene (0.29 g, 1.32 mmol) was allowed to stir in anhydrous Et_2O (5 mL) at -78 °C under an N_2 atmosphere. To the reaction mixture, a 2.5 M solution of *n*-BuLi in hexane (1.05 mL, 2.64 mmol) was carefully added in a dropwise manner. The reaction mixture was warmed to -40 °C and stirred for 3 h. The intermediate, although unreported, was synthesized according to a literature procedure for a similar compound.[151] The intermediate, **183**, was used for the next step without characterization for the preparation of **167**.

3,4-(Dichlorophenyl)lithium (184)

In a 3-neck flask, 1-bromo-3,4-dichlorobenzene (0.34 g, 1.52 mmol) was allowed to stir in anhydrous Et_2O (5 mL) at -78 °C under an N_2 atmosphere. To the reaction mixture, a 2.5 M solution of *n*-BuLi in hexane (1.21 mL, 3.04 mmol) was carefully added in a dropwise manner. The reaction mixture was warmed to -40 °C and stirred for 3 h. The intermediate was synthesized according to a literature procedure.[151] The intermediate, **184**, was used for the next step without characterization for the preparation of **168**.

C. APP^+ uptake assay

1. Preparation of HEK293 cells

A stable cell line expressing the hDAT was developed previously in the laboratory as described by Cameron et al.[152] Cells were prepared in Dulbecco's modified Eagle's medium (DMEM) supplemented with 10% fetal bovine serum. The cells were plated on 96-well plates and were transfected with red fluorescent protein (DsRed, TaKaRa Bio USA, Mountain View, CA) which is a coding plasmid and helps to focus cells in the fluorescence microscope before the addition of APP^+. Doxycycline (1mg/mL) was added to the culturing media 3 days before the experiment to induce expression of DAT.

2. Solution for the experiment

Imaging solution (IS) was prepared and was used to dissolve all the analogs and as a vehicle. It consisted of NaCl (130 mM), KCl (4 mM), $CaCl_2$ (2 mM), $MgCl_2$ (1 mM), Hepes (10 mM), and glucose (10 mM). The pH of the IS was adjusted between 7.3-7.4 using a saturated solution of NaOH.

3. Drugs

Cocaine and *threo*-methylphenidate were purchased as their hydrochloride salts from Sigma-Aldrich, St. Louis, MO.

4. Live-cell imaging

The cells were placed on the stage of the epifluorescent microscope (Olympus IX70) equipped with a light source Polycrome V (Till Photonics, Gräfelfing, Germany), a Luca S digital camera (Andor Technology, Belfast, UK), and an automated perfusion system. The imaging system was coordinated using the Live Acquisition Software from Till Photonics. The entire experiment was done at room temperature. The DsRed signal of transfected cells were used to find the focal plane of the cell monolayer. The wavelength of 460 nm was used to detect the APP^+ for excitation and 540 nm for emission.

The experiment consisted of three phases over 70 seconds and was under constant perfusion. The cells were exposed with the IS for 10 seconds followed by the compound of interest for 30 seconds and finally compound of interest + APP^+ (3 μM) for 30 seconds. All the hybrid analogs were evaluated at six different concentrations in order to get a complete dose-response curve.

5. Analysis

The data obtained from the APP^+ were analyzed using Fiji ImageJ Version 2.0 and the dose-response curves were plotted using GraphPad Prism 8.0.

D. Intracellular Ca^{2+} determination

1. Preparation of HEK293 cells

A stable cell lines expressing hDAT was previously developed in the laboratory as described by Cameron et al.[152] and cells were plated in 96-well imaging plates. The HEK293 cells were cotransfected with voltage-gated Ca^{2+} with plasmids coding $\alpha_{1.2}$, β_3, $\alpha_2\delta$, and enhanced green fluorescent protein (EGFP) using FuGENE (Promega, Madison, WI).

2. Solution for the experiment

IS was prepared and was used to dissolve all the analogs and as a vehicle. It consisted of NaCl (130 mM), KCl (4 mM), $CaCl_2$ (2 mM), $MgCl_2$ (1 mM), Hepes (10 mM), and glucose (10 mM). The pH of the IS was adjusted between 7.3-7.4 using a saturated solution of NaOH.

3. Live-cell imaging

Ca^{2+}-sensitive dye Fura2 (Life Technologies) was dissolved in DMSO pluronic F-127 20% and diluted with IS to final concentration of 3 μM. HEK293 cells were loaded with Fura2 for 40 minutes at 37 °C and then washed twice with IS. The cells were then placed on the stage of the epifluorescence microscope. The setup is similar as described in APP+ assay. The measurements were done under constant perfusion at 34 °C using a ThermoClamp-1 heater (AutoMate Scientific, Berkeley, CA). The Fura2 signal was measured using the exciting wavelength of 340 and 380 nm and the emission wavelength used was 520 nm.

The experiment was performed in four phases over 110 seconds. First, the cells transfected with EGFP were identified and the baseline of Fura2 signal was recorded for 10 seconds using IS. Next the cells were exposed to DA (10 μM) for five seconds followed by 30 seconds of washing with IS. Third, a single concentration (10–times the IC_{50}) of our compound of interest was perfused for 30 seconds and lastly a mixture of compound and DA (10 μM) was applied for five seconds followed by a final wash with IS.

4. Analysis

All the signals were background subtracted and the graphs were plotted using GraphPad Prism 8.0.

Reference:

1. High-Risk Drug Use and New Psychoactive Substances. In European Monitoring Center for Drugs and Drug Addiction: Luxemburg. **2017**; pp 1–24.
2. Glennon, R. A.; Dukat, M. Structure-activity relationship of synthetic cathinones. *Curr. Top. Behav. Neurosci.* **2017**, *32*, 19–47.
3. Kalix, P. The pharmacology of khat. *Gen. Pharmacol.* **1984**, *15*, 179–187.
4. Barkley, R. A. A review of stimulant drug research with hyperactive children. *J. Child Psychol. Psychiatry* **1977**, *18*, 137–165.
5. Szporny, L.; Görög, P. Investigations into the correlations between monoamine oxidase inhibition and other effects due to methylphenydate and its stereoisomers. *Biochem. Pharmacol.* **1961**, *8*, 263–268.
6. Gatley, S. J.; Pan, D.; Chen, R.; Chaturvedi, G.; Ding, Y.-S. Affinties of methylphenidate derivatives for dopamine , norepinephrine and serotonin transporters. *Life Sci.* **1996**, *58*, 231–239.
7. Richelson, E.; Pfenning, M. Blockade by antidepressants and related compounds of biogenic amine uptake into rat brain synaptosomes: Most antidepressants selectively block norepinephrine uptake. *Eur. J. Pharmacol.* **1984**, *104*, 277–286.
8. Misra, M.; Shi, Q.; Ye, X.; Gruszecka-Kowalik, E.; Bu, W.; Liu, Z.; Schweri, M. M.; Deutsch, H. M.; Venanzi, C. A. Quantitative structure-activity relationship studies of threo-methylphenidate analogs. *Bioorg. Med. Chem.* **2010**, *18*, 7221–7238.
9. Deutsch, H. M.; Shi, Q.; Gruszecka-Kowalik, E.; Schwer, M. M. Synthesis and pharmacology of potential cocaine antagonists. 2. Structure-activity relationship studies of aromatic ring-substituted methylphenidate analogs. *J. Med. Chem.* **1996**,

39, 1201–1209.

10. Global Overview of Drug Demand and Supply. *Latest Trends, Cross-Cutting Issues*; World Drug Report. United Nations Office of Drug and Crime: Vienna. 2018, pp 1–64.
11. European Drug Report. In European Monitoring Centre for Drug and Drug Addiction: Luxemburg. 2018, pp 1–96.
12. *Executive Summary. Conclusions and Policy Implications*; World Drug Report. United Nations Office of Drug and Crime: Vienna. 2018, pp 1–34.
13. United Nations. *World Drug Report. Analysis of Drug Markets*; 2018.
14. Recommended methods for the identification and analysis od synthetic cathinones in seized materials; United Nations Office od Drug and Crime: Vienna. **2015**, pp 1–46.
15. Al-Hebshi, N. N.; Skaug, N. Khat (Catha Edulis) - An updated review. *Addict. Biol.* **2005**, *10*, 299–307.
16. Alles, G. A.; Fairchild, M. D.; Jensen, M. Chemical pharmacology of *Catha Edulis*. *J. Med. Chem.* **1961**, *3*, 323–352.
17. Brooke, C. Khat (*Catha Edulis*): Its production and trade in the Middle East. *Georg. J.* **1960**, *126*, 52-59.
18. Kennedy, J. G. In The flowers of paradise: The institutionalized use of the drug qat in North Yemen. Reidel Pub: Dordrechet, Holland; 1987.
19. Getasetegn, M. Chemical composition of *Catha edulis* (khat): A review. *Phytochem. Rev.* **2016**, *15*, 907–920.
20. Getahun, A.; Krikorian, A. D. Chat : Coffee's rival from Harar, Ethiopia. I Botany,

cultivation and use. *Econ. Bot.* **1973**, *27*, 353–377.

21. Kalix, P.; Braenden, O. Pharmacological aspect of the chewing of khat leaves. *Pharmacol. Rev.* **1985**, *37*, 149–164.
22. Al-Motarreb, A.; Baker, K.; Broadley, K. J. Khat: Pharmacological and medical aspects and its social use in Yemen. *Phytotherapy Research*. **2002**, *16*, 403–413.
23. Beitter, A. Pharmakognostisch-Chemische Untersuchung der Catha. *Pharm. Berl.* **1901**, *268*, 17–33.
24. Wolfes, O. Über Das Vorkommen von D-nor-iso-Ephedrin in *Catha Edulis*. *Arch. Pharm.* **1930**, *268*, 18–21.
25. Paris, M.; Moyse, M. Abyssinian tea (*Catha Edulis* Forssk, Celastraceae). A study of some samples of varying geographical origin. *Bull. Narc.* **1958**, *10*, 29–34.
26. Friebel, H.; Brilla, A. Über den zantralerregenden Wirkstoff der Frischen Blätter und zweigspitzen von *Catha Edulis* Forsk. *Naturwissenschaften* **1963**, *50*, 354–355.
27. Cais, M.; Ginsburg, D.; Mandelbaum, A. Constituents of *Catha Edulis*. Isolation and structure of cathine D. *Tetrahedron* **1975**, *31*, 2727–2731.
28. Kalix, P. Pharmacological properties of the stimulant khat. *Pharmacol. Ther.* **1990**, *48*, 397–416.
29. Gugelmann, R.; von Allmen, M.; Brenneisen, R.; Porzig, H. Quantitative differences in the pharmacological effects of (+)- and (-)-cathinone. *Experientia* **1985**, *41*, 1568–1571.
30. United Nation Document MNAR/7/1978: *Etudes sur la composition chimique du khat; la confuguration absolue de la cathinone,* 1978.
31. Luqman, W.; Danowski, T. S. The use of khat (*Catha Edulis*) in Yemen. Social and

medical observations. *Ann. Intern. Med.* **1976**, *85*, 246–249.

32. Yanagita, T. Studies on cathinones : Cardiovascular and behavioral effects in rats and self-administration experiment in rhesus monkeys. *NIDA Res.Monogr.* **1979**, *27*, 326–327.
33. Kohli, J. D.; Goldberg, L. I. Cardiovascular effects of (−)-cathinone in the anaesthetized dog: Comparison with (+)-amphetamine. *J. Pharm. Pharmacol.* **1982**, *34*, 338–340.
34. Nencini, P.; Ahmed, A. M. Naloxone-reversible antinociceptive activity of cathinone, the active principle of khat, in the mouse and rat. *Pharmacol. Res. Commun.* **1982**, *14*, 759–770.
35. Glennon, R. A.; Showalter, D. The effect of cathinone and several related derivatives on locomotor activity. *Res. Commun. Subst. Abuse* **1981**, *2*, 186–192.
36. Valterio, C.; Kalix, P. The effect of the alkaloid (-)cathinone on the motor activity in mice. *Arch. Int. Pharmacodyn. Ther.* **1982**, *255*, 196–203.
37. Kalix, P. Hyperthermic response to (-)cathinone, an alkaloid of *Catha Edulis* (khat). *J. Pharm. Pharmacol.* **1980**, *32*, 662–663.
38. Zelger, J. L.; Schorno, X.; Carlini, E. A. Behavioural effects of cathinone, an amine obtained from *Catha edulis* Forsk.: Comparisons with amphetamine, norpseudoephedrine, apomorphine and nomifensine. *Bull. Narc.* **1980**, *32*, 67–81.
39. Foltin, R. W.; Schuster, C. R. Interaction between the effects of intragastric meals and drugs on feeding in rhesus monkeys. *J. Pharmacol. Exp. Ther.* **1983**, *226*, 405–410.
40. Zelger, J. L.; Carlini, E. A. Anorexigenic effects of two amines obtained from *Catha*

edulis Forsk. (khat) in rats. *Pharmacol. Biochem. Behav.* **1980**, *12*, 701–705.

41. Jansson, T.; Kristiansson, B.; Qirbi, A. Effect of khat on uteroplacental blood flow in awake, chronically catheterized, late-pregnant guinea pigs. *J. Ethnopharmacol.* **1988**, *23*, 19–26.
42. WHO Advisory Group: Review of the pharmacology of khat. Bull. Narc. **1980**, *32*, 83-93.
43. Willner, P. Animal models of addiction. *Hum. Psychopharmacol.* **1997**, *12*, 59–68.
44. Glennon, R. A.; Schechter, M. D.; Rosecrans, J. A. Discriminative stimulus properties of of S(-)- and R(+)-cathinone, (+)-cathine and several structural modifications. *Pharmacol. Biochem. Behav.* **1984**, *21*, 1–3.
45. Schechter, M. D.; Glennon, R. A. Cathinone, cocaine and methamphetamine: similarity of behavioral effects. *Pharmacol. Biochem. Behav.* **1985**, *22*, 913–916.
46. Goudie, A. J.; Atkinson, J.; West, C. R. Discriminative properties of the psychostimulant dl-cathinone in a two lever operant task. Lack of evidence for dopaminergic mediation. *Neuropharmacology* **1986**, *25*, 85–94.
47. Glennon, R. A. Discriminative stimulus properties of phenylisopropylamine derivatives. *Drug Alcohol Depend.* **1986**, *17*, 119–134.
48. Johanson, C. E.; Schuster, C. R. A comparison of the behavioural effects of l- and dl-cathinone and d-amphetamine. *J. Pharmacol. Exp. Ther.* **1981**, *219*, 355–362.
49. Woolverton, W. L.; Johanson, C. E. Preference in rhesus monkeys given a choice between cocaine and d,l-cathinone. *J. Exp. Anal. Behav.* **1984**, *41*, 35–43.
50. Yanagita, T. intravenous self-administration of (-)-cathinone and 2-amino-1-(2,5-dimethoxy-4-methyl)phenylpropane in rhesus monkeys. *Drug Alcohol Depend.*

1986, *17*, 135–141.

51. Calcagnetti, D. J.; Schechter, M. D. Place preference for the psychostimulant cathinone is blocked by pretreatment with a dopamine release inhibitor. *Prog. Neuropsychopharmacol. Biol. Psychiatry* **1993**, *17*, 637–649.
52. Schechter, M. D. Effect of learned behavior upon conditioned place preference to cathinone. *Pharmacol. Biochem. Behav.* **1991**, *38*, 7–11.
53. Kalix, P. A constituent of khat leaves with amphetamine-like releasing properties. *Eur. J. Pharmacol.* **1980**, *68*, 213–215.
54. Zelger, J. L.; Carlini, E. A. Influence of cathinone (α-aminopropiophenone) and cathine (phenylpropanolamine) on circling behavior and on the uptake and release of [^{3}H]dopamine in striatal slices of rats. *Neuropharmacology* **1981**, *20*, 839–843.
55. Sloviter, R. S.; Drust, E. G.; Connor, J. D. Evidence that serotonin mediates some behavioral effects of amphetamine. *J. Pharmacol. Exp. Ther.* **1978**, *206*, 348–352.
56. Kalix, P. Effect of the alkaloid (-)cathinone on the release of radioactivity from rabbit atria prelabelled with ^{3}H-serotonin. *Neuropsychobiology* **1984**, *12*, 127–129.
57. Glennon, R. A.; Liebowitz, S. M. Serotonin receptor affinity of cathinone and related analogues. *J. Med. Chem.* **1982**, *25*, 393–397.
58. Kalix, P. Effect of the alkaloid (−)-cathinone on the release of radioactivity from rabbit striatal tissue prelabelled with ^{3}H-norepinephrine. *Life Sci.* **1983**, *32*, 801–807.
59. Kalix, P. A comparison of the catecholamine releasing effect of the khat alkaloids (-)-cathinone and (+)-norpseudoephedrine. *Drug Alcohol Depend.* **1983**, *11*, 395–401.
60. Kawaguchi, T.; Iizuka, H.; Yanagita, T. Pharmacological effects of active ingredients of khat. *Jpn. J. Pharmacol.* **1979**, *29*, 72P.

61. Kalix, P.; Glennon, R. A. Further evidence for an amphetamine-like mechanism of action of the alkaloid cathinone. *Biochem. Pharmacol.* **1986**, *35*, 3015–3019.

62. Huang, J. T.; Ho, B. T. Discriminative stimulus properties of d-amphetamine and related compounds in rats. *Pharmacol. Biochem. Behav.* **1974**, *2*, 669–673.

63. Glennon, R. A.; Yousif, M.; Naiman, N.; Kalix, P. Methcathinone: A new and potent amphetamine-like agent. *Pharmacol. Biochem. Behav.* **1987**, *26*, 547–551.

64. Eberhard, A. Ueber das Ephedrin und verwandte Verbindungen. *Arch. Pharm.* **1915**, *253*, 62–91.

65. Eberhard, A. Ueber die Synthese des inaktiven Ephedrins bez. Pseudoephedrins. *Arch. Pharm.* **1920**, *258*, 97–129.

66. Glennon, R. A. Bath salts, mephedrone, and methylenedioxypyrovalerone as emerging illicit drugs that will need targeted therapeutic intervention. *Adv. Pharmacol*. **2014**, *69*, 581–620.

67. Hyde, J. F.; Browning, E.; Adams, R. Synthetic homologs of d,l-ephedrine. *J. Am. Chem. Soc.* **1928**, *50*, 2287–2292.

68. Bockmuhl, G.; Gorr, G. Verfahren Zur Darstellung von Optisch Active 1-Aryl-2-Amino-1-propanolen. German Patent 639,126, 1936.

69. L'Italien, Y. J.; Park, H.; Rebstock, L. C. Methylaminopropiophenone compounds and methods for producing the same. US Patent 2,802,865. August 13, 1940.

70. van der Schoot, J. B.; Ariens, E. J.; van Rossum, J. M.; Hurkmans, J. A. T. M. Phenylisopropylamine derivatives, structure and action. *Arzneimittelforschung* **1962**, *12*, 902–907.

71. Simmons, S. J.; Leyrer-Jackson, J. M.; Oliver, C. F.; Hicks, C.; Muschamp, J. W.;

Rawls, S. M.; Olive, M. F. DARK Classics in Chemical Neuroscience: Cathinone-Derived Psychostimulants. *ACS Chem. Neurosci.* **2018**, *9*, 2379–2394.

72. Young, R.; Glennon, R. A. Cocaine-stimulus generalization to two new designer drugs: methcathinone and 4-methylaminorex. *Pharmacol. Biochem. Behav.* **1993**, *45*, 229–231.
73. Glennon, R. A.; Young, R.; Martin, B. R.; Dal Cason, T. A. Methcathinone ("cat"): An enantiomeric potency comparision. *Pharmacol. Biochem. Behav.* **1995**, *50*, 601–606.
74. Young, R.; Glennon, R. A. Discriminative stimulus effects of s(-)-methcathinone (cat): A potent stimulant drug of abuse. *Psychopharmacology* **1998**, *140*, 250–256.
75. Rothman, R. B. In vitro characterization of ephedrine-related stereoisomers at biogenic amine transporters and the receptorome reveals selective actions as norepinephrine transporter substrates. *J. Pharmacol. Exp. Ther.* **2003**, *307*, 138–145.
76. Cozzi, N. V.; Sievert, M. K.; Shulgin, A. T.; Jacob, P.; Ruoho, A. E. Inhibition of plasma membrane monoamine transporters by β-ketoamphetamines. *Eur. J. Pharmacol.* **1999**, *381*, 63–69.
77. Dal Cason, T. A.; Young, R.; Glennon, R. A. Cathinone : an investigation of several n-alkyl and methylenedioxy-substituted analogs. *Pharmacol. Biochem. Behav.* **1997**, *58*, 1109–1116.
78. Yu, H.; Rothman, R. B.; Dersch, C. M.; Partilla, J. S.; Rice, K. C. Uptake and release effects of diethylpropion and its metabolites with biogenic amine transporters. *Bioorg. Med. Chem.* **2000**, *8*, 2689–2692.

79. Foley, K. F.; Cozzi, N. V. Novel aminopropiophenones as potential antidepressants. *Drug Dev. Res.* **2003**, *60*, 252–260.

80. Iverson, L. E. *Consideration of the cathinones. Advisory council on the misuse of drugs. A Report Submitted to the House Secretary of the UK*, 2010; pp 1-50.

81. Schedules of Controlled Substances: Temporary placement of three synthetic cathinones into Schedule I. *Fed. Regist.* **2011**, *76*, 65371–65375.

82. Synthetic Drug Abuse Prevention Act (2012). Section 1152. Addition of synthetic drugs to Schedule I of the Controlled Substances Act. pp 138–140.

83. Schedules of Controlled Substance: Placement of methylone into Schedule I. *Fed. Regist.* **2013**, *78*, 21818–21825.

84. Rothman, R. B.; Baumann, M. H.; Dersch, C. M.; Romero, D. V.; Rice, K. C.; Carroll, F. I.; Partilla, J. S. Amphetamine-type central nervous system stimulants release norepinephrine more potently than they release dopamine and serotonin. *Synapse* **2001**, *39*, 32–41.

85. Cameron, K.; Kolanos, R.; Verkariya, R.; De Felice, L.; Glennon, R. A. Mephedrone and methylenedioxypyrovalerone (MDPV), major constituents of “bath salts,” produce opposite effects at the human dopamine transporter. *Psychopharmacology* **2013**, 493–499.

86. Cameron, K. N.; Kolanos, R.; Solis, E. Jr.; Glennon, R. A.; De Felice, L. J. Bath salts components mephedrone and methylenedioxypyrovalerone (MDPV) act synergistically at the human dopamine transporter. *Br. J. Pharmacol.* **2013**, *168*, 1750–1757.

87. Baumann, M. H.; Partilla, J. S.; Lehner, K. R.; Thorndike, E. B.; Hoffman, A. F.; Holy,

M.; Rothman, R. B.; Goldberg, S. R.; Lupica, C. R.; Sitte, H. H.; Brandt, S. D.; Tella, S. R.; Cozzi, N. V.; Schindler, C E. Powerful cocaine-like actions of 3,4-methylenedioxypyrovalerone (MDPV), a principal constituent of psychoactive 'bath salts ' products. *Neuropsychopharmacology* **2012**, *38*, 552–562.

88. Simmler, L. D.; Buser, T. A.; Donzelli, M.; Schramm, Y.; Dieu, L. H.; Huwyler, J.; Chaboz, S.; Hoener, M. C.; Liechti, M. E. Pharmacological characterization of designer cathinones in vitro. *Br. J. Pharmacol.* **2013**, *168*, 458–470.
89. Del Bello, F.; Sakloth, F.; Partilla, J. S.; Baumann, M. H.; Glennon, R. A. Ethylenedioxy homologs of N-methyl-(3,4-methylenedioxyphenyl)-2-aminopropane (MDMA) and its corresponding cathinone analog methylenedioxymethcathinone: Interactions with transporters for serotonin, dopamine, and norepinephrine. *Bioorg. Med. Chem.* **2015**, *23*, 5574–5579.
90. Bonano, J. S.; Banks, M. L.; Kolanos, R.; Sakloth, F.; Barnier, M. L.; Glennon, R. A.; Cozzi, N. V.; Partilla, J. S.; Baumann, M. H.; Negus, S. S. Quantitative structure-activity relationship analysis of the pharmacology of para-substituted methcathinone analogues. *Br. J. Pharmacol.* **2015**, *172*, 2433–2444.
91. Walther, D.; Shalabi, A. R.; Baumann, M. H.; Glennon, R. A. Systematic structure-activity studies on selected 2-, 3-, and 4-monosubstituted synthetic methcathinone analogs as monoamine transporter releasing agents. *ACS Chem. Neurosci.* **2019**, *10*, 740–745.
92. Sakloth, F.; Kolanos, R.; Mosier, P. D.; Bonano, J. S.; Banks, M. L.; Partilla, J. S.; Baumann, M. H.; Negus, S. S.; Glennon, R. A. Steric parameters, molecular modeling and hydropathic interaction analysis of the pharmacology of para-

substituted methcathinone analogues. *Br. J. Pharmacol.* **2015**, *172*, 2210–2218.

93. Shalabi, A. R.; Walther, D.; Baumann, M. H.; Glennon, R. A. Deconstructed analogues of bupropion reveal structural requirements for transporter inhibition versus substrate-induced neurotransmitter release. *ACS Chem. Neurosci.* **2017**, *8*, 1397–1403.
94. Odoardi, S.; Romolo, F. S.; Strano-Rossi, S. A snapshot on NPS in Italy: Distribution of drugs in seized materials analysed in an italian forensic laboratory in the period 2013-2015. *Forensic Sci. Int.* **2016**, *256*, 116–120.
95. Blough, B. E.; Decker, A. M.; Landavazo, A.; Namjoshi, O. A.; Partilla, J. S.; Baumann, M. H.; Rothman, R. B. The dopamine, serotonin and norepinephrine releasing activities of a series of methcathinone analogs in male rat brain synaptosomes. *Psychopharmacology* **2019**, *236*, 915–924.
96. Kolanos, R.; Solis, E. Jr.; Sakloth, F.; De Felice, L. J.; Glennon, R. A. “Deconstruction” of the abused synthetic cathinone methylenedioxypyrovalerone (MDPV) and an examination of effects at the human dopamine transporter. *ACS Chem. Neurosci.* **2013**, *4*, 1524–1529.
97. Kolanos, R.; Partilla, J. S.; Baumann, M. H.; Hutsell, B. A.; Banks, M. L.; Negus, S. S.; Glennon, R. A. Stereoselective actions of methylenedioxypyrovalerone (MDPV) to inhibit dopamine and norepinephrine transporters and facilitate intracranial self-stimulation in rats. *ACS Chem. Neurosci.* **2015**, *6*, 771–777.
98. Wander, A. α-Pyrrolidino Valerophenones. British Patent GB927475, May 29, 1963.
99. Kolesnikova, T. O.; Khatsko, S. L.; Demin, K. A.; Shevyrin, V. A.; Kaluef, A. V. DARK classics in chemical neuroscience: α-pyrrolidinovalerophenone (“Flakka”). *ACS*

Chem. Neurosci. **2019**, *10*, 168–174.

100. *α-PVP. EMCDDA–Europol Joint Report on a New Psychoactive Substance: 1-Phenyl-2-(1-Pyrrolidinyl)- 1-Pentanone*. In European Monitoring Center for Drugs and Drug Addiction: Luxemburg. 2015; pp 1-26.
101. *Report on the Risk Assessment of 1-phenyl-2-pPyrrolidin-1-yl)pentan-1one (α-pyrrolidinovalerophenone, α-PVP) in the Framework of the Council Decision on New Psychoactive Substances.* In European Monitoring Center for Drugs and Drug Addiction: Luxemburg. 2016; pp 1-48.
102. Scocard, A.; Cottencin, O.; Karila, L. Neuropharmacology MDPV and α-pvp use in humans: The twisted sisters. **2018**, *134*, 65–72.
103. Palamar, J. J.; Rutherford, C.; Keyes, K. M. "Flakka" use among high school seniors in the United States. *Drug Alcohol Depend.* **2019**, *196,* 86-90.
104. U.S. Department of Justice, Drug Enforcement Administration. Lists of: Scheduling Actions Controlled Substances Regulated Chemicals. **2018**; pp 1-89.
105. Marusich, J. A.; Antonazzo, K. R.; Wiley, J. L.; Blough, B. E.; Partilla, J. S.; Baumann, M. H. Pharmacology of novel synthetic stimulants structurally related to the "bath salts" constituent 3,4-methylenedioxypyrovalerone (MDPV). *Neuropharmacology* **2014**, *87*, 206–213.
106. Kolanos, R.; Sakloth, F.; Jain, A. D.; Partilla, J. S.; Baumann, M. H.; Glennon, R. A. Structural modification of the designer stimulant α-pyrrolidinovalerophenone (α-PVP) influences potency at dopamine transporters. *ACS Chem. Neurosci.* **2015**, *6*, 1726–1731.
107. Nelson, K. H.; López-Arnau, R.; Hempel, B. J.; To, P.; Manke, H. N.; Crissman, M.

E.; Clasen, M. M.; Rice, K. C.; Riley, A. L. Stereoselective effects of the second-generation synthetic cathinone α-pyrrolidinopentiophenone (α-PVP): assessments of conditioned taste avoidance in rats. *Psychopharmacology* **2019**, *236*, 1067-1077.

108. Panizzon, L. La preparazione di piridil- e piperidil-arilacetonitrili e di alcuni prodotti di trasformazione (Parte I). *Helv. Chim. Acta* **1944**, *27*, 1748–1756.
109. Heal, D. J.; Pierce, D. M. Methylphenidate and its isomers their role in the treatment of attention-deficit hyperactivity disorder using a transdermal delivery system. *CNS Drugs* **2006**, *20*, 713–738.
110. Challman, T. D.; Lipsky, J. J. Methylphenidate: Its pharmacology and uses. *Mayo Clin. Proc.* **2009**, *75*, 711–721.
111. Wenthur, C. J. Classics in chemical neuroscience: Methylphenidate. *ACS Chem. Neurosci.* **2016**, *7*, 1030–1040.
112. Ding, Y. S.; Fowler, J. S.; Volkow, N. D.; Dewey, S. L.; Wang, G. J.; Logan, J.; Gatley, S. J.; Pappas, N. Chiral drugs: comparison of the pharmacokinetics of [^{11}C]d-threo and l-threo-methylphenidate in the human and baboon brain. *Psychopharmacology* **1997**, *131*, 71–78.
113. Wargin, W.; Patrick, K.; Kilts, C.; Gualtieri, C.; Ellington, K.; Mueller, R. A.; Kreamer, G.; Breese, G. R. Pharmacokinetics of methyiphenidate. *J. Pharmacol. Exp. Ther.* **1983**, *226*, 382–386.
114. Srinivas, N. R.; Hubbard, J. W.; Midha, K. K. Enantioselective gas chromatographic assay with electron-capture detection for dl-ritalinic acid in plasma. *J. Chromatogr. B Biomed. Sci. Appl.* **1990**, *530*, 327–336.
115. Faraj, B. A.; Israili, Z. H.; Perel, J. M.; Jenkins, M. L.; Holtzman, S. G.; Cucinell, S.

A.; Dayton, P. G. Metabolism and disposition of methylphenidate-^{14}C: Studies in man and animals. *J. Pharmacol. Exp. Ther.* **1974**, *191*, 535–547.

116. Srinivas, N. R.; Hubbard, J. W.; Korchinski, E. D.; Midha, K. K. Stereoselective urinary pharmacokinetics of dl-threo-methylphenidate and its major metabolite in humans. *J. Pharm. Sci.* **1992**, *81*, 747–749.
117. Patrick, K. S.; Kilts, C. D.; Breese, G. R. Synthesis and pharmacology of hydroxylated metabolites of methylphenidate. *J. Med. Chem.* **1981**, *24*, 1237–1240.
118. Sun, Z.; Murry, D. J.; Sanghani, S. P.; Davis, W. I.; Kedishvili, N. Y.; Zou, Q.; Hurley, T. D.; Bosron, W. F. Methylphenidate is stereoselectively hydrolyzed by human carboxylesterase CES1A1. *J. Pharmacol. Exp. Ther.* **2004**, *310*, 469–476.
119. Andersen, P. H. The dopamine uptake inhibitor GBR 12909: Selectivity and molecular mechanism of action. *Eur. J. Pharmacol.* **1989**, *166*, 493–504.
120. Patrick, S.; Breese, R.; Park, T.; Carolina, N.; Hill, C.; Caroline, N. Pharmacology of the enantiomers of threo-methylphenidate. *Pharmacology* **1987**, *241*, 152–158.
121. Kuczenski, R.; Segal, D. S. Effects of methylphenidate on extracellular dopamine, serotonin, and norepinephrine: comparison with amphetamine. *J. Neurochem.* **1997**, *68*, 2032–2037.
122. Pan, D.; Gatley, S. J.; Dewey, S. L.; Chen, R.; Alexoff, D. A.; Ding, Y.; Fowler, J. S. Binding of bromine-substituted analogs of methylphenidate to monoamine transporters. *Eur. J. Pharmacol.* **1994**, *264*, 177–182.
123. Portoghese, P. S.; Malspeis, L. Relative hydrolytic rates of certain alkyl (b) dl-α-(2-piperidyl)-phenylacetates. *J. Pharm. Sci.* **2016**, *50*, 494–501.
124. Ferris, R. M.; Tang, F. L. M.; Maxwell, R. A. A comparison of the capacities of

isomers of amphetamine, deoxypipradrol and methylphenidate to inhibit the uptake of tritiated catecholamines into rat cerebral cortex slices, synaptosomal preparations of rat cerebral cortex, hypothalamus and striatum and adrenergic nerves of rabbit aorta. *J. Pharmacol. Exp. Ther.* **1972**, *181*, 407–416.

125. Kim, D. Il; Deutsch, H. M.; Ye, X.; Schweri, M. M. Synthesis and pharmacology of site-specific cocaine abuse treatment agents: restricted rotation analogues of methylphenidate. *J. Med. Chem.* **2007**, *50*, 2718–2731.
126. Yamashita, S.; Kurono, N.; Senboku, H.; Tokuda, M.; Orito, K. Synthesis of phenanthro[9,10-b]indolizidin-9-ones, phenanthro[9,10-b] quinolizidin-9-one, and related benzolactams by $Pd(OAc)_2$-catalyzed direct aromatic carbonylation. *European J. Org. Chem.* **2009**, 8, 1173–1180.
127. Freifelder, M.; Robinson, R. M.; Stone, G. R. Hydrogenation of substituted pyridines with rhodium on carbon catalyst. *J. Org. Chem.* **1962**, *27*, 284–286.
128. Deutsch, H. M.; Ye, X.; Shi, Q.; Liu, Z.; Schweri, M. M. Synthesis and pharmacology of site specific cocaine abuse treatment agents: a new synthetic methodology for methylphenidate analogs based on the blaise reaction. *Eur. J. Med. Chem.* **2001**, *36*, 303–311.
129. Froimowitz, M.; Patrick, K. S.; Cody, V. conformational analysis of methylphenidate and its structural relationship to other dopamine reuptake blockers such as CFT. *Pharm. Res.* **1995**, *12*, 1430–1434.
130. Froimowitz, M.; Wu, K. M.; George, C.; VanDerveer, D.; Shi, Q.; Deutsch, H. M. Crystal structures of analogs of threo-methylphenidate. *Struct. Chem.* **1998**, *9*, 295–303.

131. Sakloth, F. Psychoactive Synthetic Cathinones (or Bath Salts): Investigation of Mechanism of Action. Ph.D. Dissertation, Virginia Commonwealth University, Richmond, VA, 2015.

132. Wang, K. H.; Penmatsa, A.; Gouaux, E. Neurotransmitter and psychostimulant recognition by the dopamine transporter. *Nature* **2015**, *521*, 322–327.

133. Larkin, M. A.; Blackshields, G.; Brown, N. P.; Chenna, R.; Mcgettigan, P. A.; McWilliam, H.; Valentin, F.; Wallace, I. M.; Wilm, A.; Lopez, R.; Thompson, J. D.; Gibson, T. J.; Higginsm D. G. Clustal W and Clustal X Version 2.0. *Bioinformatics* **2007**, *23*, 2947–2948.

134. Jones, G.; Willett, P.; Glen, R. C.; Leach, A. R.; Taylor, R. Development and validation of a genetic algorithm for flexible docking. *J. Mol. Biol.* **1997**, *267*, 727–748.

135. Hollingsworth, S. A.; Karplus, P. A. A fresh look at the ramachandran plot and the occurrence of standard structures in proteins. *Biomol. Concepts* **2010**, *1*, 271–283.

136. Ramachandran, G. N.; Ramakrishnan, C.; Sasisekharan, V. Stereochemistry of polypeptide chain configurations. *J. Mol. Biol.* **1963**, *7*, 95–99.

137. Schmitt, K. C.; Reith, M. E. A. The atypical stimulant and nootropic modafinil interacts with the dopamine transporter in a different manner than classical cocaine-like inhibitors. *PLoS One* **2011**, *6*, 1-13.

138. Kellogg, G. E.; Semus, S. F.; Abraham, D. J. HINT: A new method of empirical hydrophobic field calculation for CoMFA. *J. Comput. Aided. Mol. Des.* **1991**, *5* , 545–552.

139. Kellogg, G. E.; Abraham, D. J. Hydrophobicity: Is $LogP_{o/w}$ more than the sum of its

parts? *Eur. J. Med. Chem.* **2000**, *35*, 651–661.

140. Fries, D. S. Opioid Analgesics. In Lempke, T. L.; Williams, D. A.; Roche, V. F.; Zito, S. W. (Eds.), *Foye's principles of medicinal chemistry* (pp. 652–678) (6th ed.) Baltimore, MD: Lippincott, Williams & Wilkins, 2008.
141. Greene, T. W.; Wuts, P. G. M. In Protective Groups in Organic Synthesis; 2nd ed. Wiley: New York; 1991.
142. Thai, D. L.; Sapko, M. T.; Reiter, C. T.; Bierer, D. E.; Perel, J. M. Asymmetric synthesis and pharmacology of methylphenidate and its para- substituted derivatives. *J. Med. Chem.* **1998**, *41*, 591–601.
143. Ruchala, I.; Cabra, V.; Solis, E.; Glennon, R. A.; De Felice, L. J.; Eltit, J. M. Electrical coupling between the human serotonin transporter and voltage-gated Ca^{2+} channels. *Cell Calcium* **2014**, *56*, 25–33.
144. Moerke, M. J.; Ananthan, S.; Banks, M. L.; Eltit, J. M.; Freitas, K. C.; Johnson, A. R.; Saini, S. K.; Steele, T. W. E.; Negus, S. S. Interactions between cocaine and the putative allosteric dopamine transporter ligand SRI-31142. *J. Pharmacol. Exp. Ther.* **2018**, *367*, 222–233.
145. Steele, T. W. E.; Eltit, J. M. Using Ca^{2+}-channel biosensors to profile amphetamines and cathinones at monoamine transporters: Electro-engineering cells to detect potential new psychoactive substances. *Psychopharmacology* **2019**, *236*, 973-988.
146. Guzman, A.; Quintero, C.; Muchowski, J. M. Alkylation of α-tert-butoxycarbonylamino letone enolate anions. A useful synthesis of α-alkyl-α-amino ketones, 2-acylpyrrolidines, and 2-acylpiperidines. *Can. J. Chem.* **2006**, *69*, 2059–2063.

147. Rangisetty, J. B.; Pullagurla, M. R.; Muthiah, R. J. J.; Jobdevairakkam, C. N. Process of making optically pure l-pipecolic acid and process of making anesthetics and intermediates therefrom, US Patent 2006/0276654 A1. December 7, 2006.

148. Li, C.; Ji, Y.; Cao, Q.; Li, J.; Li, B. Concise and facile synthesis of (R,R)-dexmethylphenidate hydrochloride and its three stereoisomers. *Synth. Commun.* **2017**, *47*, 1301–1306.

149. Pizzorno, M. T.; Albonico, S. M. Novel synthesis of 5,6,7,8-tetrahydroindolizines. *J. Org. Chem.* **1977**, *42*, 909–910.

150. Gál, K.; Wéber, C.; Wágner, G. A.; Bobok, A. A.; Nyéki, G.; Vastag, M.; Keserü, G.; Háda, V. Tetrazole derivatives as modulators of metabotropic glutamate, US Patent 2007/039782 A1. October 5, 2005.

151. Minami, Y.; Noguchi, Y.; Hiyama, T. Synthesis of benzosiloles by intramolecular anti-hydroarylation via ortho-C-H activation of aryloxyethynyl silanes. *J. Am. Chem. Soc.* **2017**, *139*, 14013–14016.

152. Cameron, K. N.; Solis, E.; Ruchala, I.; De Felice, L. J.; Eltit, J. M. Amphetamine activates calcium channels through dopamine transporter-mediated depolarization. *Cell Calcium* **2015**, *58*, 457–466.

VITA

Barkha J. Yadav was born on April 16, 1991 to Jitendra and Usha Yadav in Mumbai, India. She received her Bachelors of Pharmacy degree from Dr. Bhanuben Nanavati College of Pharmacy, Mumbai University in July 2013. She then received a Masters degree in Pharmaceutical Analysis from the University of Strathclyde, Glasgow, Scotland, UK in 2014 following which she enrolled in the doctoral program in the Department of Medicinal Chemistry, School of Pharmacy, Virginia Commonwealth University, Richmond, VA, USA.